PUBLICATIONS
OF
DEBRECEN
HELIOPHYSICAL OBSERVATORY
OF THE
HUNGARIAN ACADEMY OF SCIENCES

ПУБЛИКАЦИИ
ДЕБРЕЦЕНСКОЙ
ГЕЛИОФИЗИЧЕСКОЙ ОБСЕРВАТОРИИ
ВЕНГЕРСКОЙ АКАДЕМИИ НАУК

A MAGYAR TUDOMÁNYOS AKADÉMIA
DEBRECENI
NAPFIZIKAI OBSZERVATÓRIUMÁNAK
KÖZLEMÉNYEI

VOLUME 2

6th Regional Consultation on Solar Physics
Gyula, Hungary
1971

PUBLICATIONS
OF
DEBRECEN
HELIOPHYSICAL OBSERVATORY
OF THE
HUNGARIAN ACADEMY OF SCIENCES

ПУБЛИКАЦИИ
ДЕБРЕЦЕНСКОЙ
ГЕЛИОФИЗИЧЕСКОЙ ОБСЕРВАТОРИИ
ВЕНГЕРСКОЙ АКАДЕМИИ НАУК

A MAGYAR TUDOMÁNYOS AKADÉMIA
DEBRECENI
NAPFIZIKAI OBSZERVATÓRIUMÁNAK
KÖZLEMÉNYEI

VOLUME 2

Proceedings of the
6th Regional Consultation on Solar Physics
held in Gyula, Hungary,
September 1971

EDITOR: LORÁNT DEZSŐ
DIRECTOR, HELIOPHYSICAL OBSERVATORY OF
THE HUNGARIAN ACADEMY OF SCIENCES
H-4010 D E B R E C E N
HUNGARY

(Publ.Debrecen Obs.,Volume 2)

C O N T E N T S

P R E F A C E

The 6th Regional Consultation on Solar Physics was held in Gyula, Hungary, from 6 to 11 September 1971, under the joint sponsorship of the Hungarian Academy of Sciences and the Hungarian Government Committee of Space Research and organized by the Debrecen Heliophysical Observatory of the Hungarian Academy of Sciences.

The general topic of the Consultation was Solar Flares and Magnetic Fields. Special emphasis has been laid on ground--based observations relating to Intercosmos programmes.

This Consultation should be regarded as a member of the series, initiated by Czechoslovak and Polish solar astronomers, that includes the meetings which were held in *1*. Tatranská Lomnica, Czechoslovakia (1961), *2*. Kalatowki, Poland (1962), *3*. Tatranská Lomnica, Czechoslovakia (1964), *4*. Sopot, Poland (1966) and *5*. Potsdam, GDR (1968). Papers presented at these Consultations have been published successively in *1*. Contr. Wrocław Astr.Obs. No.14 (1964); *2*. Bull.Astr.Inst.Czech.,Vol.14. No.3.(1964); *3*. Czechoslovak Acad.Sci.,Publ. of the Astr.Inst. No.51. (1965); *4*. Contr.Wrocław Astr.Obs. No.17. (1969); *5*. Geod.Geophys.Veröff.Akad.Berlin R II,H.13 (1969).

Some of the papers read at the Consultation (by A.Böhme, J. Hanasz, G. Mariş, S. Pintér, E. Tifrea and B. Valnicek) are not included in this volume, and in some cases only the abstract is published here, because the full text is to be found elsewhere.

We would like to express our appreciation to Drs.V.Bumba, T. Fortini, J. Hanasz, F. W. Jäger, M. Kopecký, B. Rompolt and B. Valniček for being the chairmen of sessions and for their many stimulating discussions.

L. Dezső

L I S T O F P A R T I C I P A N T S

AUSTRIA

Astr.Inst.Graz Univ.,Solar Observatory
K A N Z E L H Ö H E

PETTAUER Thomas

CZECHOSLOVAKIA

Astronomical Institute,Czechoslovak Acad.Sci.
O N D Ř E J O V

AMBROŽ Pavel

BUMBA Vaclav

HANA Vladislav

KOPECKÝ Miloslav

KŘIVSKÝ Ladislav

LETFUS Vojtech

RUZIČKOVA-TOPOLOVA Blazena

SUDA Jan

TLAMICHA Antonin

VALNIČEK Boris

Astronomical Institute,Slovak Acad.Sci.
T A T R A N S K Á L O M N I C A

RUŠIN Vojtech

RYBANSKÝ Milan

SÝKORA Julius

Geophys.Institute, Slovak Acad.Sci.
H U R B A N O V O

PINTÉR Stephen

Observatory,
H U R B A N O V O

KNOŠKA Stephen

GERMAN D.R.

Central Institute for Solar-Terrestrial Physics, GDR Acad.Sci.

BÖHME Annelies *POTSDAM*

JÄGER Friedrich *POTSDAM, Solar Observatory,Einstein-Tower*

KRÜGER Albrecht *BERLIN-ADLERSHOF*

HUNGARY

Konkoly Observatory,Hungarian Acad.Sci.
B U D A P E S T

BARCZA Szabolcs

CSADA Imre

Laboratory of Cosmic Rays, Central Research Institute for Physics, Hungarian Acad.Sci.
B U D A P E S T

KÓTA József

VARGA András

Astronomy Department, Eötvös Univ.
B U D A P E S T

MARIK Miklós

Heliophysical Observatory,Hungarian Acad.Sci.
D E B R E C E N

DEZSŐ Loránt

GERLEI Ottó

GUMAN István

GYERTYÁNOS Gyöngyi

KÁLMÁN Béla

KOVÁCS Ágnes

MÁRKI-ZAY Lajos

ITALY

Astronomical Observatory of Rome
R O M A

FORTINI Teresa

NORWAY

Institute of Theoretical Astrophysics,
University of Oslo,
O S L O

ENGVOLD Oddbjörn

POLAND

Astronomical Observatory,Wroclaw Univ. and
Astronomical Institute,Polish Acad.Sci.
W R O C L A W

GARCZYNSKA Irena

PACIOREK Jana

ROMPOLT Bogdan

STANKIEWICZ Adolf

Astronomical Institute,Torun Univ. and
Polish Acad.Sci.
T O R U N

HANASZ Jan

WELNOWSKI Henryk

ROUMANIA

Astronomical Observatory,Roumanian Acad.Sci.
B U C U R E S T I

MARIŞ Georgeta

NICOLESCU Simona

ŢIFREA Emilia

YUGOSLAVIA

Astronomical Observatory,
B E O G R A D

KUBIČELA Aleksandar

PUBLICATIONS OF DEBRECEN HELIOPHYSICAL OBSERVATORY
Vol. 2 No. 1 1971

LARGE-SCALE REGULARITIES IN SOLAR MAGNETIC FIELD DISTRIBUTION AND OCCURRENCE OF LARGE FLARES

V. BUMBA
Astronomical Institute of the Czechoslovak Acad.Sci.,Observatory Ondřejov

Abstract:

Some observational facts about the relation of the position of very large flares accompanied by cosmic ray and PCA events during the declining part of the 19th cycle to the large-scale patterns formed by solar magnetic fields are presented. At the same time the correlation of periods of enhanced geomagnetic activity with the longitudinal distribution of large-scale regular features of solar magnetic field is discussed.

1. Introduction

In the present note we should like to collect some observational facts about the close relation of the position of very large flares (flares with cosmic ray and PCA events) to the regularities in the large-scale distribution of solar magnetic fields we found earlier (Bumba and Howard, 1965; Ambroz et al., 1971).

As the basic observational material the Atlas of Mt. Wilson Solar Magnetic Fields 1959 - 1966 (Howard et al., 1967) was used, individual synoptic magnetic charts of which were integrated by overlapping two sequentional maps to avoid the inhomogenities of some of the charts. Opposite polarities were studied separately, as well as unseparated. The list of type IV bursts connected with the cosmic ray and PCA events (Švestka and Olmr, 1966) was taken as a catalogue of great flares.

2. Results

There are certain differenc es in the appearance of the large-scale distribution of both the opposite polarities of solar magnetic fields, although they are mutually very closely related in all kinds of distributions. For example, the minus polarity rows and streams (Bumba, Howard, 1969) in the equatorial parts of synoptic charts mounted subsequently during the declining part of the previous cycle of activity and an increasing part of the present cycle are narrower and more concentrated in comparison to those of the plus polarity which are broader and more diffuse (Ambrož et al., 1971).

Although both polarities very often form in practically opposite heliographic longitudes a very complex magnetic situation composed from a large Unipolar Magnetic Region (UMR), a "ghost" UMR and a "mirror image" of the UMR developed from a complex of activity, as was the case during the second half of the previous cycle (Bumba, Howard, 1965), the polarities of the same complex magnetic situation,studied separately, show a tendency to form certain huge regular structures developing in their streams, the morphology of which is akin to a very large cellular feature sometimes nearly 180° long (not counting the tail) - we call them "supergiant" structures (Ambrož et al., 1971). They can be observed better in the negative polarity magnetic fields, and they have their own internal structure (30°-35°; 60°) *(Figure 1)*.

The minus polarity "supergiant" structures generally coincide with the new formations of solar activity (heliographic longitudes with prevailing, newly formed active regions), this means with the younger magnetic fields, on the other hand, the plus polarity streams formed from prevailing older fields seem to be in close relation with geomagnetic disturbances, or rather with solar wind (Ambrož et al., 1971; Bumba, 1972 a, b).

2.1. CORRELATION OF PARTICLE-EMITTING FLARES WITH NEGATIVE LARGE-SCALE REGULAR FEATURES

In the list of large flares published by Švestka and Olmr (1966) there are about 46 flares in 22 active regions observed during the period of time covered by the Atlas of solar magnetic synoptic charts (Howard et al., 1967). Because of the bad quality of the maps, 4 flares in 3 active regions could not be correlated. Of the remaining flares about 32, possibly 40 in all,possibly 17 active regions brightened in a very specific minus polarity configuration. In *Figure 2* we can see examples of this very complex magnetic situation: the negative polarity "supergiant" structure is drop-shaped with its tail located in higher latitudes of the northern hemisphere. The drop, evolved over several rotations with its head to the West is about 90°-100° long. The centre of gravity of the largest solar activity and the location of the greatest probability of occurrence of particle emitting flares is located in the eastern part of the pattern, just below the root of the tail. The head of the drop-shaped pattern, formed from older activity regions, is more stable and regular than its left (eastern) part, where the activity changes more rapidly.

Studying the plus polarity distribution during the investigated situation, we may find a certain regularity too. It is, above all, represented by a similar feature forming a "mirror" image to that of the minus polarity with its tail stretched out to the higher latitudes of the southern hemisphere and with its body filled in the drop of the minus polarity [illegible]

Only the visibility of the plus polarity structures is less pronounced in comparison with the minus polarity fields. (Examples see also in *Figure 2.*)

2.2 CORRELATION OF PARTICLE EMITTING FLARES WITH NEGATIVE POLARITY INTERPLANETARY MAGNETIC FIELDS

Another very preliminary statistical result speaks in favour of the close relation of large particle emitting flares with solar regions covered by the prevailing minus polarity. If we correlate the occurrence of large flares collected by Křivský (1969) as the Supplement II to the list of particle emitting flares concerning the first half of the present cycle with the yet published (Wilcox and Colburn, 1970; Severny et al., 1970) interplanetary magnetic field polarity data we may see that again during the first half of the present cycle the greatest flares are more often related to the negative polarity on the Sun as well as in interplanetary space. From 13 flares 8, possibly 9, correlate with the negative polarity interplanetary magnetic field; 1, possibly 2 with the positive polarity and 3, possibly 2 with zero magnetic field in the interplanetary space (Bumba, 1972a).

2.3 CORRELATION OF HELIOGRAPHIC LONGITUDES WHICH CONTAIN PREVAILING POSITIVE POLARITY WITH GEOMAGNETIC DISTURBANCES

If we compare the daily geomagnetic disturbances shifted for four days to take into account the particles travelling time with the magnetic synoptic charts, we find a fairly good correlation of the daily geomagnetic character figures C 9, published by the Geophysikalisches Institut Göttingen with the positive polarity magnetic large-scale features. This correlation is practically always pronounced when the geomagnetic disturbances on Göttingen charts display the long-lasting strips of enhanced geomagnetic activity with 27 days recurrence, as is usually observed to the end of each solar cycle.

This was the case at the end of the 18th cycle in 1953 when we can use Babcock's results (Babcock and Babcock,1955). The same has been shown for the declining phase of the 19th cycle (Ambrož et al., 1970). During the growth of the 20th cycle such sequences of enhanced geomagnetic activity can very rarely be followed. But when they are observed, they again tend to correlate mostly with the positive polarity large--scale fields on the Sun (Bumba, 1972b).

2.4 CORRELATION OF GEOMAGNETIC DISTURBANCES WITH THE POSITIVE POLARITY FIELD IN INTERPLANETARY SPACE

Taking the estimations of the polarity of the interplanetary magnetic field published by Wilcox and Colburn (1970) we can construct a histogram of the distribution of geomagnetic character figures dependent on the polarity of the interplanetary magnetic field during the phase of growth of the present 20th cycle of solar activity (Bumba, 1972b). From this histogram we may conclude that also in interplanetary space the geomagnetic disturbances tend to be related more to the positive polarity than to the opposite one, although in the data the positive and negative values are, in practice, equally frequent.

One more piece of information may be obtained from a histogram demonstrating the occurrence frequency of positive as well as negative polarity in the interplanetary space (Bumba, 1972b): the largest secondary maximum of the histogram giving for the most frequent time-interval of the sector of one polarity of about 6 days - which makes approximately 80° on the Sun - is again in close correlation with the dimensions of the large-scale structures of the field of one polarity on the Sun.

3. Discussion

In conclusion to the observational facts demonstrated above we may see that there are large-scale features of opposite polarity magnetic fields on the Sun frequently developed in separated heliographic longitudes. To the negative polarity fields new and great activity formations including large flares are bound and they tend to be the source of the sudden commencement of geomagnetic disturbances. The positive polarity structure usually with less and older activity or rests of old activity correlate with recurrent geomagnetically enhanced periods of time which means that they are sources of the quiet solar wind. The predominance of one polarity in a large area of solar surface can by no means be explained as an absence of the opposite polarity. Both polarities form a very complex and complicated situation and much more investigation is needed for understanding the geometry, the rules and physics of this behaviour of solar magnetic fields.

The results presented may have some importance for the observation of sunlike stars: they mean that if the Sun is observed as a star during the period when the integrated magnetic fields have the negative sign the enhancement of some spectral lines due to the greater activity, as well as enhanced X- and radio-emission, may be expected. On the other hand the Sun being positive is the source of an undisturbed solar wind.

R e f e r e n c e s

Ambrož,P., Bumba,V., Howard,R., Sýkora,J.: 1971, *IAU Symposium No.* 43, *696*.

Babcock,H.W., Babcock,H.d.: 1955, *Astrophys. J.*121, *349*.

Bumba,V.: 1972a, in C.P. Sonett et al (ed.), *Solar Wind, 31* NASA SP-308.

Bumba,V.: 1972b, in C.P. Sonett et al (ed.), *Solar Wind, 151* NASA SP-308.

Bumba,V., Howard,R.: 1965, *Astrophys. J.* 141, *1502*.

Bumba,V., Howard,R.: 1969, *Solar Phys.* 7, *28*.

Howard,R., Bumba,V., Smith,S.F.: 1967, *Carnegie Inst. of Washington Publ. No.* 626.

Křivský,L.: 1969, *Bull. Astr. Inst. Czech.* 20, *293*.

Severny,A.B., Wilcox,J.M., Scherrer,P.M., Colburn,D.S.: 1970, *Solar Phys.* 15, *3*.

Švestka,Ž., Olmr,J.: 1966, *Bull. Astr. Inst. Czech.* 17, *4*.

Wilcox,J.M., Colburn,D.S.: 1969, *J. Geophys. Res.*, 75, *6366*.

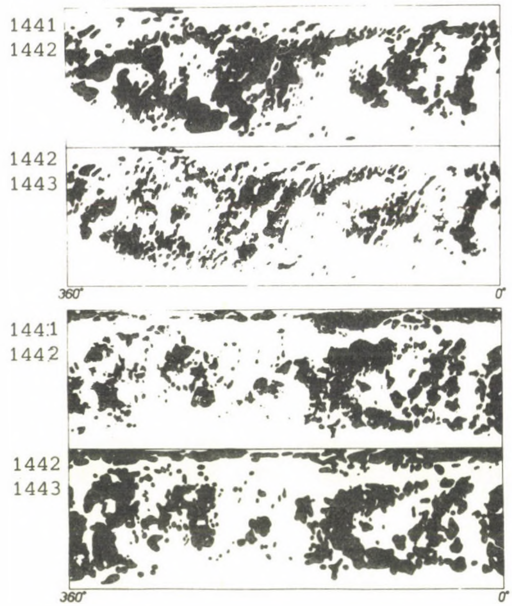

Figure 1. The "supergiant" structures during the period of their best visibility on magnetic synoptic chart rotations Nos.1441 - 1443 drawn in separated polarities (plus at the top, minus at the lower half of the figure).For integration two consecutive maps,one of which is repeated are overlapped.

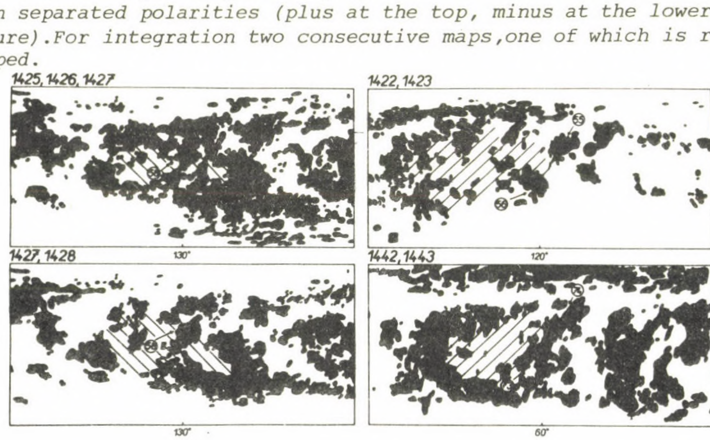

Figure 2. Examples of complex magnetic situation in the negative (to the right) and positive (to the left) polarity large-scale distribution in which large particle-emitting flares have developed (the positions of flares are indicated by an arrow and number of the active region). Again for integration two consecutive maps are overlapped.

ROLE OF THE CONVECTIVE NETWORK IN THE DEVELOPMENT OF SUNSPOTS, SUNSPOT GROUPS AND FLARES

V. B U M B A, J. S U D A
Astronomical Institute of the Czechoslovak Acad.Sci., Observatory Ondřejov

P. R A N Z I N G E R
Astronomical and Geophysical Obs.,Univ. of Ljubljana, Ljubljana

Abstract:
Using the high-resolution photographs of sunspot groups the regularities in spot distribution are studied. It is shown that the supergranular network controls development of practically all activity phenomena in the solar atmosphere.

1. Introduction

During recent years it has been demonstrated that the development of active regions is closely related to the supergranular network: plages, faculae and small spots develop in the crossings of adjacent cells, the development of plages proceeds in the form of an extension of the emission pattern around a supergranule (Bumba, Howard, 1965a), and the fully developed spots fill in the supergranules (Bumba, 1965; Ichsanov, 1967; Dmitrieva et al. 1968). During the summer of 1969 we succeeded in obtaining relatively numerous and good photographic material concerning the fine-scale structure of the photospheric features, primarily of groups of sunspots. On the basis of these observations it is possible to try to build up a more general picture of the relationship between individual sunspots and their groups and to the convectional network during the process of spot and group formation and to obtain some information about the trends prevailing in the dynamics of the studied relations. In this connection it seems to be meaningful to mention the older results concerning the analogy between the flare and active region development.

2. Observational data

In 1969 with the aid of an excellent double-lens objective (diameter 20.5 cm; equivalent focus 27.8 m) made about one hundred years ago by the famous optician A. Clark using a relatively narrow band-pass of a metallic interference filter (about 100 A around λ5890 A) and with the help of a ciné camera, about 200 000 pictures of about 50 sunspot groups were obtained. Although the efficiency of the cinematographic method is only a few percent, enough observations were available for evaluation.This material was supplemented by a few thousand pictures of about 20 spot groups, obtained during 1963 with the same refractor and a photographic camera.

The method of evaluating the obtained photographs is the simplest: the study and comparison of a series of consecutively mounted positives, made with different exposures to display the details from the darkest part of the umbra to the penumbra, and the spot surrounding the photosphere in their evolution and examination of hundreds of drawings made with the use of a magnifying device.

3. Results

From the study of all spot groups in different stages of development, some of them having been followed for many days, it is clear that at all stages of development in the form of the sunspot groups, in the position and internal distribution of the spots in the group, and in the size and form of the spots, simple as well as complex, the convective supergranular network plays the determining role.

3.1 THE FORM OF GROUPS DURING THE PHASE OF GROWTH

In our material there are about 15 groups photographed during the first few days after their appearance. In most cases during the first one to three days the centres of gravity of two clusters of small pores and spots without a penumbra, developing in regions of opposite polarities usually in the West-East direction, are at a distance of about 31 000 km (*Fig. 1*) which is usually transformed by greater groups during the subsequent days into a distance of about 54 000 km (*Fig.1.*). During the first hours of development the group has the form of a triangle, the spot, forming the end of the arm of the triangle, being about 25 - 30 000 km distant mostly from the leading part to the North or South of the centre of the group and having the same polarity as the leading spots. A larger value of the flux from the magnetic field concetrated in the trailing spots of the group (Bumba, Howard, 1965a) is often observed during the first day or two of the growth of the group. Later the spots form an ellipse with an inclined dividing line of polarities, mostly going from the North-East to the South--West.

During the transformation of the smaller ellipse into the larger, one may observe the successive transition of one form into the other one with clusters of small spots remaining at the end of the smaller ellipse so that the largest ellipse is practically composed of two smaller elements with dimensions of about 24 000 km and 30 000 km (*Fig. 1.*). It seems that the transformation of one feature, indicated by the organization of spots into the other, is made mainly by the development of new small spots in the vicinity of older spots at the periphery of the features, and by the later disappearance of older spots so that the resulting effect looks like a real shift of spots meanly in the eastward or westward direction. But this problem is still to be examined in greater detail.

3.2 THE FORM OF SPOT GROUPS DURING THE MAXIMUM AND POST-MAXIMUM PHASE OF GROWTH

The same regularities of spots distribution in groups may be found during the whole life of the group, sometimes in very convincing examples. By studying carefully the geometry and distances of the spot distribution in all groups, having a sufficient number of spots in our material, we may see that there exist two main structural elements of elliptical form with the dimensions of their main axes as mentioned above, and some smaller, as well as larger, less frequent structures which seem to build up the whole sunspot group. Their number depends upon the importance of the group, and always one smaller and one larger feature creates the biggest one.

During the declining phase, when the group loses its bipolar character, the remaining spots in the clusters are still organized in elliptical patterns with concentrations of spots at opposite ends of these patterns usually at a distance of about 20 000 km.

3.3 THE FORM AND SIZE OF SPOTS

To find the regularities in the forms and sizes of the individual sunspots we superimposed all sunspot drawings with the aid of sheets of tracing paper. This method, using the drawings made from photographs taken near the centre of the Sun or made to follow the direction of that diameter of the spot which is parallel to the solar limb and, therefore,without geometrical shortening, indicated that the dimensions of the studied sunspots do not cover a continuous interval of dimensions between the smallest and biggest spot but that they are grouped around certain values. The most frequent sizes are those with an unshortened diameter of the whole spot (umbra plus penumbra) around 27 000 km, 36 000 km and 46 000 km. There are some spots grouped around 20 000 km on one side of the scale of diameter values and around 57 000 km on the other side of the scale. Let us call the obtained discrete values of dimensions, pertinent to the length of spot diameters, dimensional types a, b, c, d and e (*Fig.2*; a is the smallest and e the largest).

The composition of larger spots from smaller types is often visible, and also the transition of one type into the other without the shift of the individual components may be seen during one or two days (*Fig.2.*). There are also certain regularities in the organization and form of individual nuclei of the umbra in all mentioned types of dimensions. It may be noted that the sizes of dimensional types b, c and d coincide with the three values of quantized sunspot areas, published several years ago (Bumba, 1965).

The organization of smaller parts in the bigger complex spot is analogous to that of ellipses in sunspot groups shown above. Even when the whole area of a complex formation is not filled in by an umbra and penumbra, the outer boundary of the feature occupied by pieces of that umbra and penumbra can have the form of practically all dimensional types. This is usually the case in the following region, but many times also in the leading region of a large sunspot stream.

3.4 THE DEVELOPMENT OF SOLAR FLARES WITHIN THE SUPERGRANULAR NETWORK

It was shown some time ago (Bumba, Howard, 1965b) that the development of flares, at least those observed in ionized calcium lines, is also closely related to the supergranular network, forming a striking morphological analogy to the development of active regions, only the rate of flare--development is several hundreds times greater than that of active regions.

Experienced observers know the striking similarity of the forms and distribution of bright features in various flares, not to mention the recurrent flares, which are certainly of the same nature as those observed by spot distribution.

4. Discussion of results

The displayed and quoted observational facts demonstrate that the supergranular network - which is, as is now accepted, the result of convection in the solar photosphere - controls the two processes which feed the solar atmosphere with the largest amount of energy: the slow development of active regions (of the order of 10^5 -10^6 sec) in which the magnetic energy is probably built up and the fast development of flares (of the order of 10^3 sec) is probably consuming a portion of this magnetic energy. We must not forget that the feet of the filaments and prominences are anchored in the supergranular network with the same characteristic distances, too (Sykora, 1968), so that all photospheric and choromospheric activity phenomena are at least bound to the network.

Taking into account the results of some stellar research (Wilson, 1963; Wilson, 1964) the intensity of the ionized calcium emission which is closely related on the Sun to the same supergranular network and magnetic field distribution, is not only a measure of chromospheric as well as flare--activity (Wilson, 1971) and an indicator of stellar age on a large number of sunlike stars, but, as we may see from the Wilson-Bappu relation (Wilson and Bappu, 1957), it is in close connection with the production of energy in the stellar interior. This means the supergranular network or the convection must be cosmologically important and we may not be very far from reality if we accept that the magnetic energy of sunspots and faculae in an active region is in some way the transformed and accumulated energy of convection in the region occupied by spots.

R e f e r e n c e s

Bumba,V.: 1965, in R. Lüst (ed.) *IAU Symposium No.* 22, *192.*

Bumba,V., Howard,R.: 1965a, *Astrophys. J.* 141,*1492.*

Bumba,V., Howard,R.: 1965b, *Astrophys. J.* 142, *796.*

Dmitrieva,M.G., Kopecký,M., Kuklin,G.V.: 1968, in K.O. Kiepenheuer (ed.), *IAU Symposium No.* 35, *174.*

Ichsanov,R.: 1967, *Soln. Dannye No.* 7.

Sýkora,J.: 1968, *Bull. Astr. Inst. Czech.* 19, *37.*

Wilson,O.C.: 1963, *Astrophys. J.* 138, *832.*

Wilson,O.C.: 1964, *Publ. Astr. Soc. Pacific* 76, *28.*

Wilson,O.C.: 1971, *private communication.*

Wilson,O.C., Bappu,M.K.:1957, *Astrophys. J.* 125,*661.*

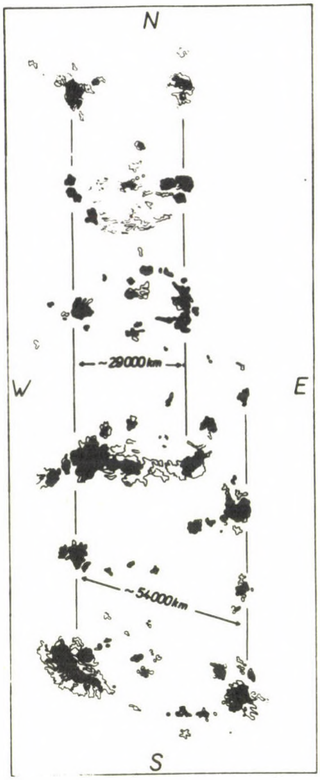

Figure 1.

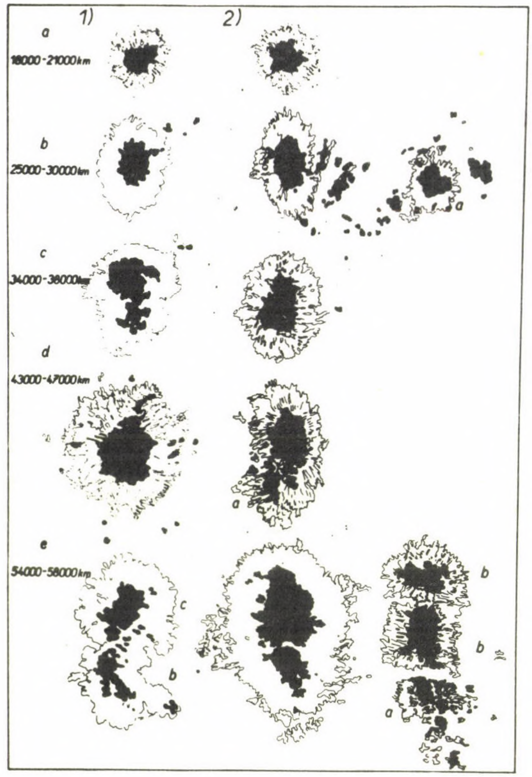

Figure 2.

Figure 1. *Different sunspot groups during the first days of their development. The characteristic values of distances are indicated.*

Figure 2. *Examples of sunspot dimensional types a, b, c, d and e with indicated intervals of diameter values. The composition of larger spots from smaller types may be seen.*

LARGE-SCALE DISTRIBUTION OF MAGNETIC REGIONS, CA II PLAGES, FILAMENTS AND SUNSPOTS ON THE SOLAR SURFACE

P. AMBROŽ

Astronomical Institute of the Czechoslovak Acad.Sci.,Observatory Ondřejov

Abstract:

The paper compares the longitudinal distribution of the maximum tidal effects of planets on the solar surface with the distribution of the occurrence of Ca II flocculae, filaments and sunspots for cycle 19. A simple equation is derived for the description of the planetary effect. The time fluctuation of solar activity with the mean duration of 260 days are analysed. In confrontation with synoptic charts of the magnetic field a close relation was found between these fluctuations and the development of complex activity.

1. Introduction

The purpose of the presented paper is to discuss and summarize a complex of several studies concentrated on the analysis of the large-scale morphological properties of the distribution of different forms of activity on the solar surface. It is assumed that these studies could be useful in working out the method of forecasting solar activity.

As the fundamental hypothetical model for forecasting the generation and development of the activity the fact, studied in the past by a number of authors, was adopted according to which there exists a causal relation between the gravitational effect of the planets on the Sun and the morphology of the generation and occurence of solar activity.

2. The planetary tidal forces

Theoretically one can form a most comprehensive idea of the effects of tidal forces of planets on the solar surface. Therefore the total values of the tidal forces of the six planets closest to the Sun (as far as Saturn) were computed. The studied interval covers the whole of cycle 19 and a ten day interval was taken between the computed values.

The total tidal force displays periodic fluctuations of magnitude and the vector of the instantaneous maximum magnitude rotates with respect to the Carrington heliographic network.

n The author is of the opinion that relative maxima of the tidal force may play a significant role with a view to the force effect of the planets, since at these times a discontinuity in the effects of the tidal force on the solar surface may occur. The points at which the tidal force reaches maximum on the Sun are not distributed over the solar surface at random, but the relation between the time and the average position of the planetary effect is linear and can be expressed by straight lines:

$$Y = 1.56\ X - 2041.35 \qquad (1)$$

and the second straight line is situated 180° away on the opposite hemisphere of the Sun, where Carrington's revolutions are substituted for X, and Y gives the average heliographic longitude of the region of the planetary effect.

The computed force is only the vertical component of the total vector of the tidal force and has an immediate relation

37

to the deformation of the solar surface. Trellis (1966a) showed that this statical deformation is very small. Due to the very small slope of line (1) and to the comparatively high frequency of the maxima of the pulses (the fundamental period of the pulses is around 27 days) we are justified in assuming that the deformation of the solar sphere may attain incomparably higher values as a result of the resonance of tidal pulses with the deformations of the surface.

Besides, there also exists a horizontal component of the tidal force which mostly takes part in the horizontal motions of the solar mass. Hydrodynamic and magnetohydrodinamic effects of this force on the Sun have not been studied yet. It is necessary to stress that the total tidal effect acts on most of the total solar mass since the considered forces per unit mass have comparatively small values, which from the point of view of energy is in no way negligible. Trellis (1966b) maintains that the lower estimate of the energy which is released during the tidal action of planets on the Sun is about 10^{35} erg per day.

Since one cannot say anything concrete about the direct mechanism of the planetary effect on the forming of solar activity inspite of all these deliberations, and since one in fact assumes it as a result of a number of statistical papers, we have attempted to find an appropriate relation between the structure of the action of the planetary tidal force and the morphology of the distribution of the activity.

3. Longitudinal distribution of solar activity

Recently Dodson and Hedeman (1968a,b) showed an interesting fact in that antipode active regions and rapid manifestations of activity such as flares and prominences occur in some cases. We attempted to investigate whether this phenomenon is general in the distribution of several manifestations of activity, using the data from cycle 19.

Figure 1 shows three diagrams of the dependence on time of the longitudinal distribution of the activity in the equatorial zone $\pm$ 20° for (a) Ca II plages, (b) filaments, and (c) sunspots. The pictures were formed by different methods. In case (a) it was the surface integration of the distribution and magnitude of Ca II plages over a circle of radius 34°. In cases (b) and (c) groups were formed always of six synoptic charts and maps from each group were mutually superimposed. In all three cases a regular longitudinal distribution can be seen in two longitudinal zones 180° away.

The summarizing *Figure 2* can be used to compare the positions of the longitudinal minima of the activities of the individual forms of its manifestation, and the run of lines (1) of the planetary effect has also been included. For forecasting purposes this figure can be used to substantiate the statement that most of the activity in cycle 19 is concentrated in the regions between the lines of the planetary effect, i.e., with their axes on the straight lines.

4. Fluctuations of solar activity indices with mean period 260 days

Figure 1a, which shows the isodensity diagram of occurrence of Ca II plages reflects the fact that the density of the plages as a function of time fluctuates markedly. A comparison of the percentage representation of the individual levels of activity was made for each rotation in the whole of the equatorial zone.

Figure 3 shows that the activity shows irregular pulsations with a duration of 8 - 10 rotations. We carried out a comparison of these pulsations with the fluctuations of the total area of sunspots and prominences on the disc and with the fluctuations of the relative number. The three latter indices were processed by computer. Two sets of values of one parameter, smoothed by gliding averages over 13 and 5 rotations, were formed from the fundamental set of average areas and relative numbers. The first set denote A_{13} and the second set A_5. The fluctuations are then the deviations $B = A_5 - A_{13}$. All four curves in *Fig. 3* show very good agreement for different phases of the solar cycle with respect to the manifestation of the mentioned index in the equatorial zone.

Short-period fluctuations have already been studied by several authors: Bezrukova (1958), Vitinskij (1961), Dodson and Hedeman (1971). The principal feature of these fluctuations is that they do not have the character of harmonic oscillations and that they display sudden changes of phase. A histogram of the occurrence frequency of the duration of positive and negative amplitudes of fluctuation pulses was compiled to cover the period 1940 - 1969. Two maxima were found, i.e.,two most frequent durations of pulses on the zero axis, around 120 - 140 and around 180 - 200 days. The result is illustrated in *Fig. 4*. As can be seen the double length of the second interval is almost precisely one year. Recently, Švestka (1968) pointed out this nature of annual variations of activity in connection with their exploitation for long-term prognoses. It is necessary to stress that this is not a question of regular oscillations, but of fluctuations of a random nature, the duration of which, as will be shown below, is conditioned by a complicated development of the activity complex.

5. Formation and some morphological properties of magnetic supercells

The longitudinal and temporal inhomogeneity in the distribution and occurrence of activity was also studied using detailed data covering rotations 1431 - 1447. For the analysis the following were used:

a) Atlas of Solar Magnetic Fields - Howard, et al. (1967)

b) Cartes Synoptiques de la Chromosphere Solaire - Meudon

c) Heliographische Karten der Photosphäre - Zürich

As mentioned in the paper of Ambrož et al. (1971) the dynamic development of the activity of the individual polarities leads to the fact that, in one of its phases the development of magnetic regions is formed to the system of vast, closed supergiant-structures, which cover as much as 180° in heliographic longitude and about 110° in latitude. The supergiant regular structures of positive and negative polarity are in general mutually cylindrically symmetrical with respect to the axis of solar rotation, and at the time the supergiant regular structures of both polarities become most outstanding as shown in *Fig. 5*. It seems that the magnetic structures are mutually point symmetrical in the plane of the synoptic map (period of rotations 1440 - 1443). The point of symmetry being at a heliographic longitude of about 175°± 15°. The average heliographic longitude of the planetary effect for considered time interval according to Eq. (1) is 208°. Recently, Fung et al. (1971) published a paper in which the possibility of an external planetary effect was rejected in the first instance because of the insufficient correlation of the same actual indices of activity for the northern and southern hemispheres. However, from the above it is clear that there exist macrostructural similarities on the solar surface which are not, however, directly accompanied by similarities of the manifestations of activity. But this fact is apparently the limitation of the applicability of the ideas on planetary effects. It now seems improbable that a concrete relation would exist between the instantaneous positions of planets and the occurrence of sunspots, prominences and flares. It is much more probable, if the effect of planetary forces is really manifested, that this would be in a form of variations of some partial parameter in the magnetohydrodynamic equations, which describe the motion of mass on the solar surface.

Considerable attention has been devoted to the development of the individual magnetic regions, separately for the positive and negative polarity, as well as for their sum. This was done numerically and percentage values were determined of the total area of magnetic regions which exceed the level of 3 gauss on the surface of the synoptic charts. Besides, the similarity in the distribution of the magnetic field between the northern and southern hemispheres was also investigated.

The resultant graph is compared in *Fig. 6* with the average area of spots per one rotation. It was found that for the interval of maximum symmetry, i.e. for rotation 1442, the activity increases markedly, which is shown by the area of the spots as well as the total area of the magnetic field. In this interval the maximum of the fluctuations also occurs. According to the run of the average total area of spots per one rotation, when these fluctuations become outstanding, the previous maximum occurred during rotation 1430 and the subsequent during rotation 1452. If one investigates the total area of the individual polarities on the synoptic chart separately, it is clear that during the interval of rotations 1431-1439 it was expressively predominant and that it developed plus polarity, whereas during rotations 1440-1445 this role was taken over by the minus polarity. A similar trend can be observed in the graphs of the similarity of northern and southern polarity. The similarities were computed always for two mutually corresponding areas of $5 \times 5°$ in terms of heliographic coordinates on both hemispheres.

This fact is connected with the distribution of polarities into individual longitudinal zones of preferred activity occurrence. The positive polarity is concentrated mostly into the region of longitudes 210 - 310°, whereas the negative polarity into the opposite region, around 50 - 150°. This means that during the first period the magnetic activity concentrated mostly around longitude 260° and in the second period around longitude 100°.

6. Fluctuations and the development of activity complexes

The activity shifts from one active longitudinal zone to another. The development of magnetic regions is accompanied by the development of the complex of activity, with which one also observes shifts from one longitudinal zone of the preferred activity occurrence to another. It seems that the fluctuations, discussed above, represent the development of the individual activity complexes. Their mean lifetimes also correspond to 260 days, i.e. 9,6 rotations, and this is a period close to the typical lifetime of an activity complex.

The substance of the fluctuations, however, also allows one to understand partly the irregularities in the duration and shape of the fluctuations. These irregularities may be caused by the disruption of the regularity of the development of the activity complex on the one hand, and by interaction or the simultaneous development of several such complexes on the other.

Under these circumstances one may expect that the statistical study of the fluctuations with a time of duration of 8 - 12 rotations will not be very useful for forecasting purposes. On the other hand, the detailed study of the dynamics of the development of the activity complex is much more hopeful. It seems that the development of the activity complex is conditioned by a number of magnetic and non-magnetic forces of solar origin, which enter the system of magnetohydrodynamic equations describing the motion of the volume elements of mass in the solar atmosphere formally. Apart from this, with a view to the results discussed at the beginning of this paper, external forces due to planets also act on the solar atmosphere, which probably take part in the longitudinal distribution of activity.

R e f e r e n c e s

Ambrož,P., Bumba,V., Howard,R., Sýkora,J.: 1971,in R.Howard, (ed.), *IAU Symposium No.* 43, *696.*

Bezrukova,A.J.: 1958, *Izv. GAO (Pulkovo) 16.* 159, *77.*

Dodson,H.W., Hedeman,E.R.: 1968a, *IQSY Annals* 4, *3.*

Dodson,H.W., Hedeman,E.R.: 1968b, in K.O.Kiepenheuer,(ed.) *IAU Symposium No.* 35,*56.*

Dodson,H.W., Hedeman,E.R.: 1972, in *Astrophys. and Space Sci.Library* Vol. 29, *Part I, 151.*

Fung,P.C.W., Sturrock,P.A., Switzer,P., Van Hoven,C.: 1971, *Solar Phys.* *18*,90 —,90

Trellis,M.M.: 1966a, *Compt.Rend. Acad. Sci. (Paris)* 262, *221.*

Trellis,M.M.: 1966b, *Compt.Rend. Acad. Sci. (Paris)* 262, *376.*

Vitinskij,J.I.: 1961, *Izv. GAO (Pulkovo) No.* 167, *121.*

Švestka, Z: 1968, Solar Phys., 4, 18.

45

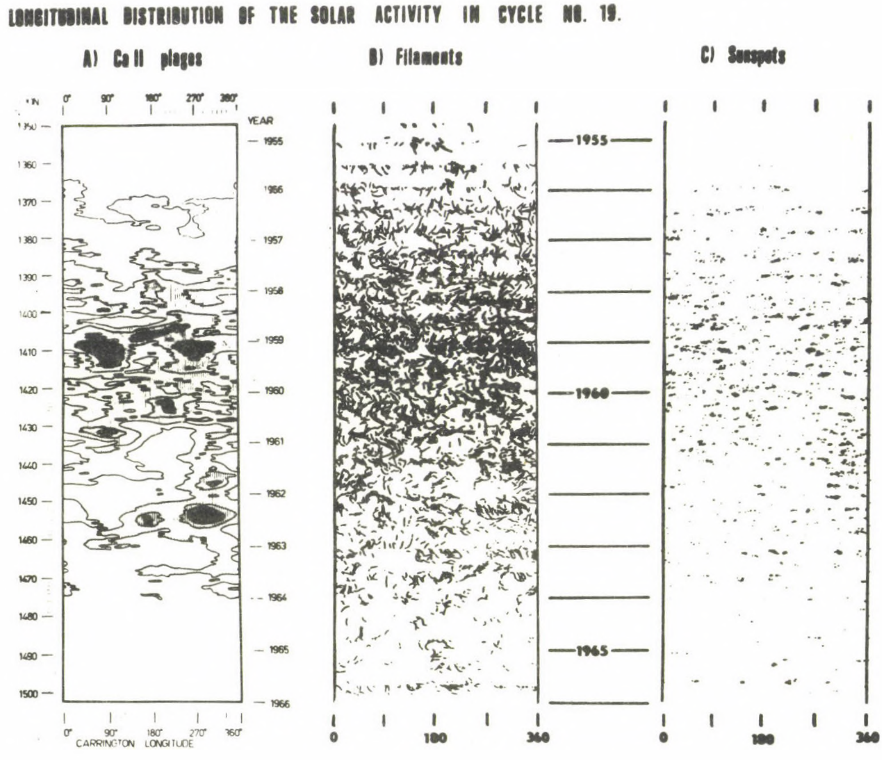

Figure 1. *Diagrams of the longitudonal distribution time dependence for different forms of activity in the equatorial zone $\pm$ 20°: (A) Ca II plages, (B) filaments, (C) sunspots.*

Figure 2. *Comparison of the longitudinal minima positions for individual forms of activity with the run of dashed lines of the planetary effect. Below right equation for one line is written.*

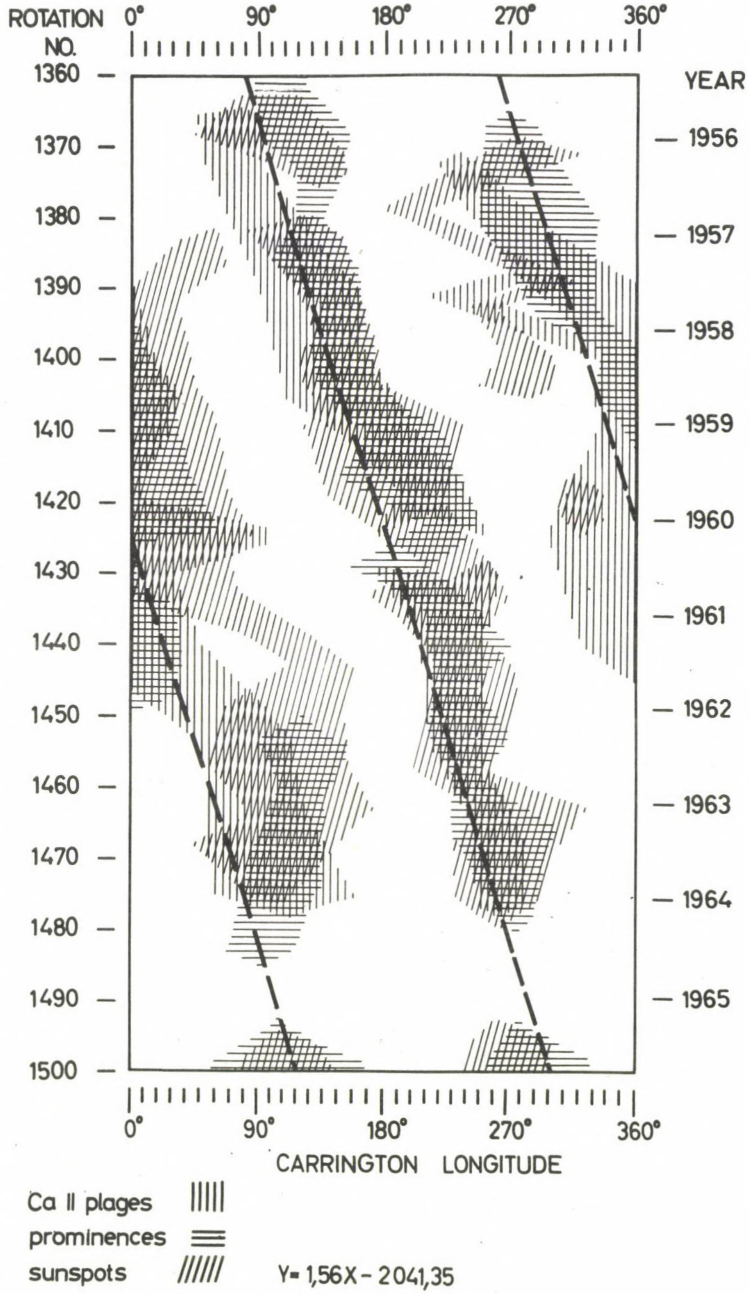
ROTATION NO.
0°
90°
180°
270°
360°
1360
1370
1380
1390
1400
1410
1420
1430
1440
1450
1460
1470
1480
1490
1500
YEAR
1956
1957
1958
1959
1960
1961
1962
1963
1964
1965
CARRINGTON LONGITUDE
Ca II plages
prominences
sunspots
Y= 1,56X - 2041,35

Figure 2.

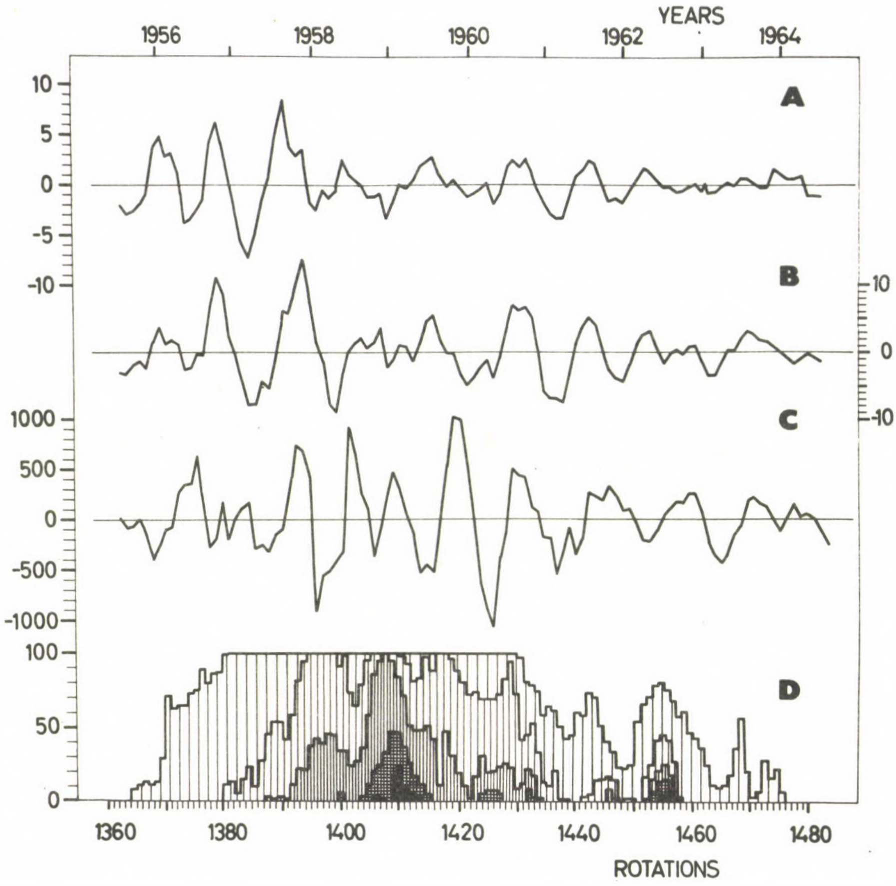

Figure 3. *Comparison of fluctuations having duration of 8 - 10 rotations for (A) sunspot areas, (B) sunspot relative numbers, (C) prominence areas and (D) surface-density of Ca II plages.*

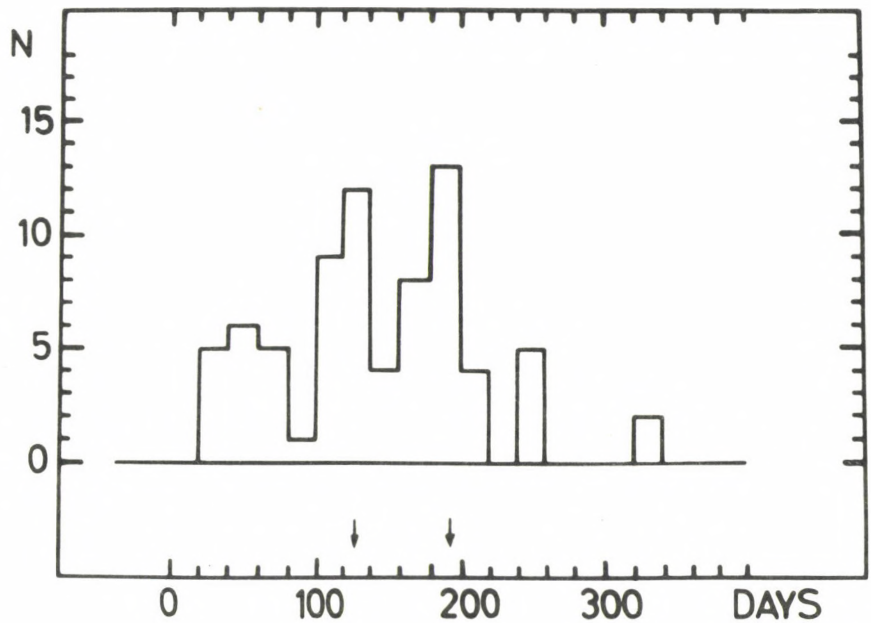

Figure 4. *A histogram of the occurence frequency for the duration of positive and negative amplitudes of fluctuation pulses for the period 1940 - 1969.*

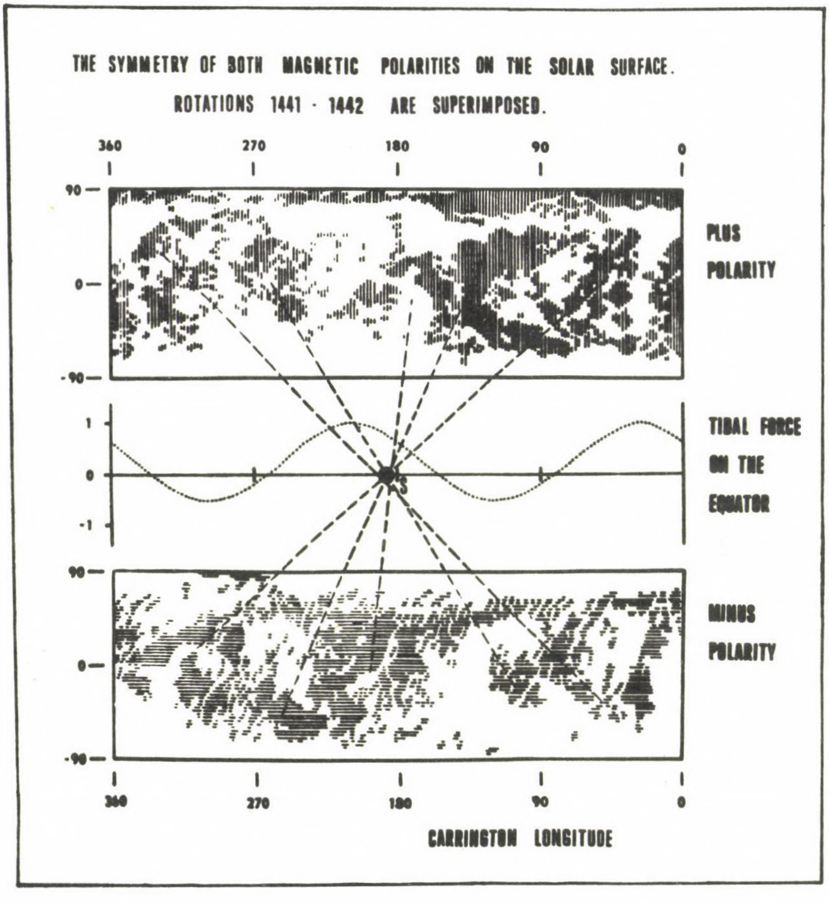

Figure 5. Demonstration of the point symmetry of magnetic synoptic charts for both magnetic field polarities.

Figure 6. Comparison of the (A) total area average of sunspots per one rotation with the (B) total area of both polarities of the magnetic field from synoptic charts and with the (C) similarity of northern and southern hemisphere during rotation numbers 1431 - 1447. (Dashed line represents the positive polarity, dotted line the negative polarity and the sum of both values is drawn by the full line).

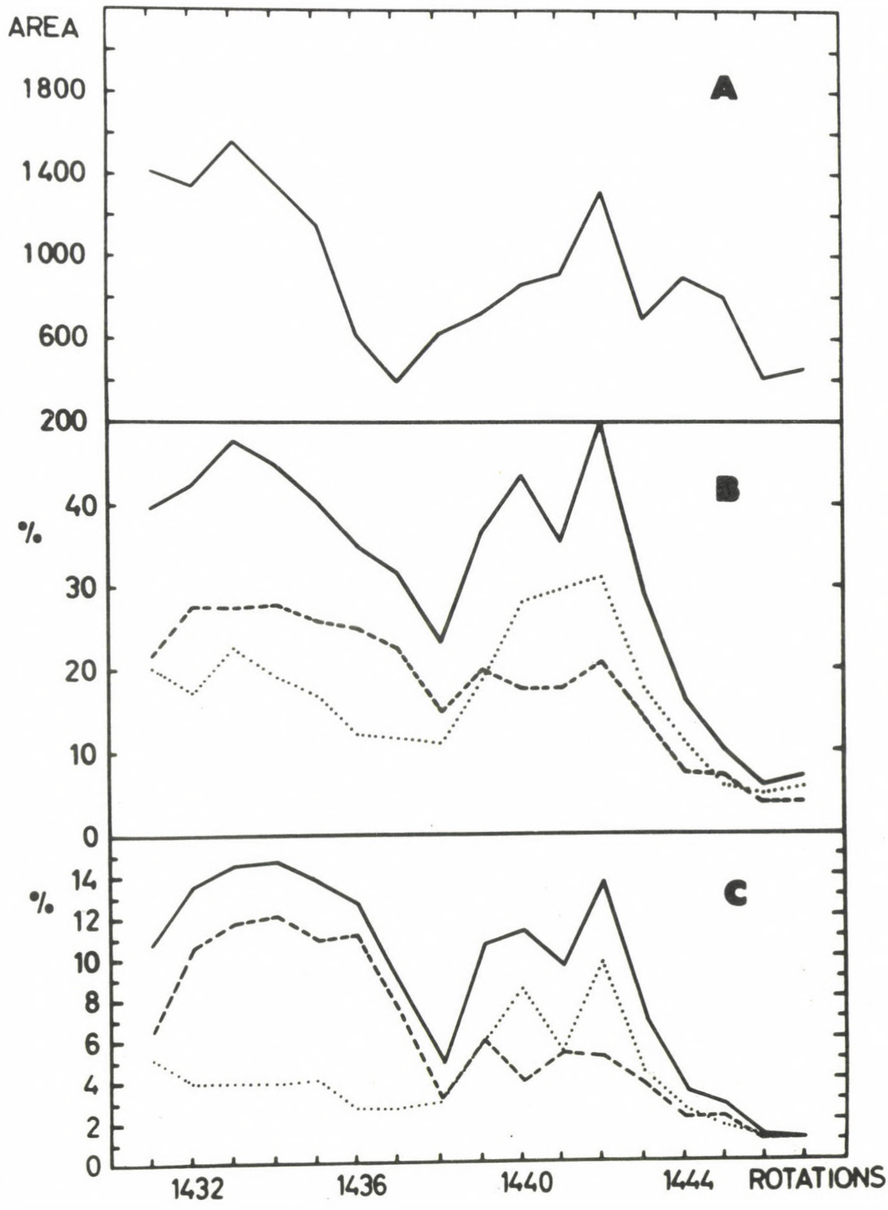
AREA
1800
1400
1000
600
200
A
40
%
30
20
10
0
B
14
%
12
10
8
6
4
2
0
C
1432
1436
1440
1444
ROTATIONS

Figure 6.

PUBLICATIONS OF DEBRECEN HELIOPHYSICAL OBSERVATORY

MEAN EMISSION MEASURES AND MEAN ELECTRON TEMPERATURES OF THE SOLAR CORONA DERIVED FROM STANDARD MEASUREMENTS OF SOLAR X-RAY FLUXES

V. L E T F U S

Astronomical Institute of the Czechoslovak Acad. Sci.,Observatory Ondřejov

Abstract:

An attempt has been made to derive the mean electron temperature and the emission measure of active coronal features from the solar X-ray emission data. Daily averages in the ranges 0 - 8 Å and 8 - 20 Å in the period from December 1965 to November 1968, published from the satellites SOLRAD 8 and 9, have been investigated using theoretical X-ray spectrum of an isothermal source.

On an average the temperature ranges from about 2.5×10^6 to 3×10^6 °K with a trend of very slow increase for almost the whole period investigated. The emission measure increases in the beginning part of the given period, reaches its maximum in the first months of 1967 and then slowly decreases. Comparing the course of the emission measure with the 10 cm radio flux, one can find certain similarities with corresponding maxima and minima. A similar positive-correlation effect occurs also for the temperature course but only for several, shorter periods.

It is known from the X-ray images of the Sun made by pinhole cameras and grazing incidence telescopes, that the soft X-ray emission shorter than 20 Å originates only in the coronal condensations over the active regions. Thus the X-ray levels monitored by satellites give the radiation from the coronal condensations on the visible hemisphere of the Sun. Flux data from the two wavelength ranges are available, we can derive from their ratio the temperature and then, knowing the temperature, from the same fluxes also the corresponding emission measure. The only assumption is the knowledge of the theoretical spectrum of the coronal plasma as a function of the electron temperature.

We have used for our investigation daily average emission levels in the bands 1 to 8 Å and 8 to 20 Å, from the experiments of the Naval Research Laboratory, Washington. The period investigated, from June 1966 to November 1968, must be divided into three intervals. The photometric measurements were made in the first period from June 1966 to July 1967 with SOLRAD 8, in the second one from August 1967 to March 1968 with the OGO-IV and in the last interval from March 1968 to November 1968 with the SOLRAD 9 satellites (see Kreplin 1970).

The conversion of the photometer signal into the flux values is made currently by a simple supposition, that the Sun radiates in this spectral region as a black body with the temperature of 2×10^6 °K.For this spectral distribution the conversion factors of each photometer were calculated and they were used to multiply the detector's output to obtain the "conventional flux" levels. It is clear that the resulting flux data are not the true fluxes, but only signal values multiplied by a constant factor.

The daily average X-ray flux levels, converted by such a manner, are published in Solar Geophysical Data, Boulder. These averages were calculated by averaging all of the flux values from the real-time telemetry data, recorded during 5 to 10 minute passes by the system of NASA STADAN stations, and discarding obvious flare points. Such processing mostly gives sufficiently representative daily "quiet" levels, but for some days the discarding of X-ray bursts,namely their tail parts, when the burst activity is high and the Sun is not controlled permanently, could not be fully effective. Here we can expect that the data used will not be entirely free from errors.

The output of the ionization chambre is given by the expression

$$(1) \qquad I(T_e, y) = a\, e\, \omega \int_0^\infty \varepsilon(\lambda) F(\lambda, T_e, y)\, d\lambda$$

and that of the Geiger-Müller counter

$$(2) \qquad C(T_e, y) = (a/hc) \int_0^\infty \lambda \varepsilon(\lambda) F(\lambda, T_e, y)\, d\lambda$$

Here $F(\lambda, T_e, y)$ is the differential flux in the spectrum of coronal plasma, which is a function of the wavelength λ the electron temperature T_e and the emission measure

$$(3) \qquad y = \int^V n_e^2\, dV$$

where n_e is the electron concetration and V the emission volume; $\varepsilon(\lambda)$ is the spectral efficiency, a the window area, ω the number of ion pairs produced by energy of 1 erg and e the electric charge in Coulombs. For the counter it is supposed that one photon produces one count.

The conversion of the output into the flux is given by the conversion function

$$(4) \qquad \gamma_I(T_e) = F(\lambda_1, \lambda_2, T_e, y)/I(T_e, y)$$

$$(5) \qquad \gamma_C(T_e) = F(\lambda_1, \lambda_2, T_e, y)/C(T_e, y)$$

where

$$(6) \qquad F(\lambda_1, \lambda_2, T_e, y) = \int_{\lambda_1}^{\lambda_2} F(\lambda, T_e, y)\, d\lambda$$

The differential flux $F(\lambda, T_e, y)$ is supposed to be a linear function of the emission measure y and thus the conversion function γ is dependent only on the temperature. The limits of integration λ_1 and λ_2 in eq. (6) must correspond with the effective limits of the spectral efficiency to obtain minimum variability of the conversion function with temperature. Substituting for $F(\lambda, T_e, y)$ the Planck function at 2×10^{6}°K, we obtain the constant conversion factors used for the published data (Kreplin 1961, 1970).

The output's ratio of two photometers which are sensitive in two different spectral intervals and the corresponding flux ratio respectively are a function of the plasma temperature only. It could be used to determine the temperature from observations. The true spectral distribution of the Sun's radiation is not exactly known in such a case, here we have to use the theoretical spectrum of the coronal plasma to calculate the necessary relations, deduced from the equations (1) and (2) resp. We used one of the theoretical spectra, calculated by Beigman and Vainshtein (1969), Tab. 4g), which differences originate in the different abundances of elements. In the above mentioned work the differential fluxes are calculated for the emission measure $y_o = 3.2 \times 10^{49}$ cm^{-1} and distance of 1 a.e. With the known temperature deduced from the output ratio the theoretical integrated fluxes $F(\lambda_1, \lambda_2, T_e, y_o)$ and the real conversion functions can be calculated. Then the emission measure will be derived from the comparison of theoretical and observed fluxes; later they are corrected by the known conversion function. An isothermal model of the source has been used to simplify the calculations.

The results are given in *Figs. 1* to *3*. On the top of each figure the electron temperature is presented (in million degrees). In the middle there is the emission measure on the logarithmic scale and at the bottom the radio flux on 10 cm from Ottawa. The interruptions on the first two curves are due to the lack of data at enormously great aspect angles, caused by the precession of the spin oriented SOLRAD 8 sat.

The one or few days fluctuations on the temperature curve can be ascribed partly to the true variations of temperature, which can probably be connected to the complexity in the configurations of magnetic fields of some active regions (Chambe 1969, Ivanov et al. 1970, Parkinson and Pounds 1971), partly to the errors of not discarded flare points by averaging, giving the "noise". The last mentioned is more probable here and it is evidently seen on the graphs as substantial peak deviations from the mean level. Both effects must be considered also for the variations of temperature within range of few weeks. Probably in this case the first effect is more dominant. Here these variabilities did not have to be investigated. Considering the time run of the temperature as a whole and neglecting the fluctuations, we obtain an interesting result, that the mean level of temperature is nearly constant. During the whole period under consideration the temperature ranges between 2.5×10^6 and 3×10^6°K and here it has a very slow monotone increase.

The variation of the emission measure is considerably different from that of the electron temperature. Here it is to see a typical 27 days variation due to the solar rotation, which correlates well in their maxima and minima with the S-component of the 10 cm solar radio flux. Also the close similarity in the variations of the longer periods is clearly seen.

An exclusion from the main character of the time runs of temperature and emission measure have been found for the end of 1967 and the first months of 1968 during the very high activity period of the Sun. The typical 27 days variation is suppressed here for the emission measure curve and it appears conspicuously on the temperature curve.

To extend the investigated period and to verify the results obtained above, we completed the used NRL data by one set of data, monitored by a single telemetry-receiving station of Arcetri Observatory (Landini et al. 1969). Daily averages are presented from the passes of SOLRAD 8 over the station in the period December 1965 to November 1967. By averaging the observed levels and discarding the flare points the authors used only those flux levels from separate passes, that did not exceed 25 per cent of the minimum value F_m of the given day. It is evident that the average will be erroneous, when F_m is affected by a flare effect. Thus we may expect a low number of observations during one day, characteristic for a single station, that the dispersion of data will be greater than in the preceeding case. The fluxes for the wavelength interval from 0 to 8 Å were derived from the GM counter and only when the flux levels fell under the threshold of the counter sensitivity ($F_{min} \approx 7\times10^{-5}$erg cm^{-2}) the telemetry data from ionization chambers were used. The results are given in *Figs 4* and *5*. The results themselves and also the comparison with the preceeding results for the interval when they overlap confirm only the conclusions given above.

We can conclude that the observed 27 days variation of the X-ray fluxes is due to the variation of the emission measure, which is connected with the number and the importance of the coronal condensations. It explains also the high correlation coefficients of X-ray fluxes and solar radio radiation, found by Wende (1969) and Pintér and Olmr (1970).

The temperature derived here is higher as used for the calculation of the conventional constant conversion factors. In some sense striking is the conclusion that the temperature obtained from the averaged fluxes integrated over the whole Sun's disc is nearly constant during the whole studied interval. This fact is important and evidently bears upon the energy balance in coronal condensations. It means that the energy heating the coronal condensations will be in equilibrium with the energy losses in radiation in the short wavelength range of the spectrum of the coronal condensations. The slow increase of temperature may be connected with the general conditions in the whole solar corona during the ascending part of the solar cycle.

R e f e r e n c e s

Beigman,I.L., Vainshtein,L.A.: 1969, *Lebedev Phys.Inst. (Moscow) Prepr. No.* 94/1969.

Chambe,G.: 1969, *Solar Phys.* 8,*369.*

Ivanov,V.D., Letfus,V., Mandel'stam,S.L., Tindo,I.P.: 1970, *Lebedev Phys. Inst. (Moscow) Prepr. No.* 54/1970.

Kreplin,R.W.: 1961, *Ann. Geophys.* 17, *151.*

Kreplin,R.W.: 1970, *Ann. Geophys.* 26, *567.*

Landini,M., Monsignori Fossi,B., Russo,D., Tagliaferri,G.L.: 1969, *Oss. Mem. Astrofis. Arcetri, Fasc.* 91.

Parkinson,J.H., Pounds, K.A.: 1971, *Solar Phys.* 17, *146.*

Pintér,S., Olmr,H.: 1970, *Bull. Astr. Inst. Czech*21, *373.*

Wende,C.D.: 1969, *J.Geophys. Res.* 74,*4649.*

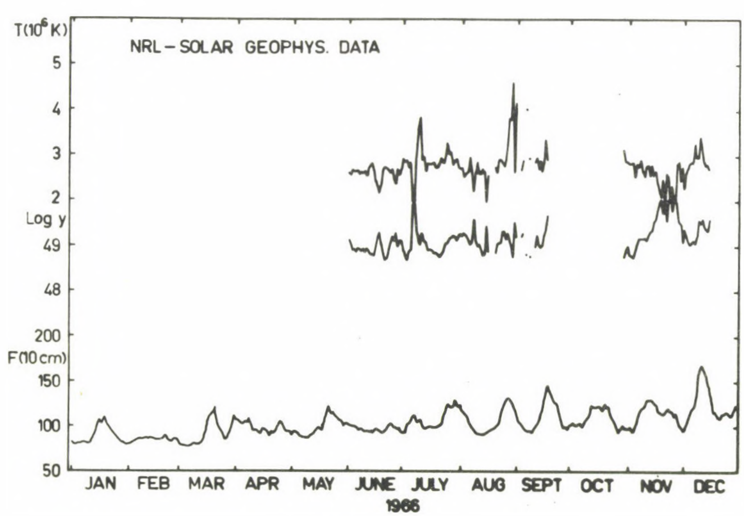

Figure 1.

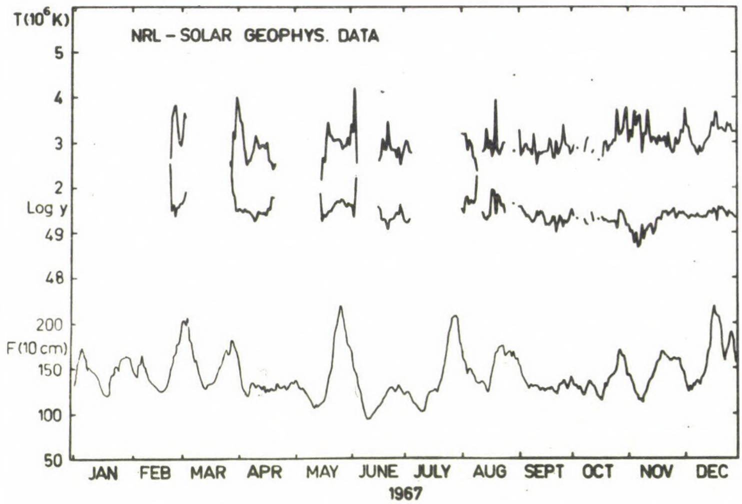

Figure 2.

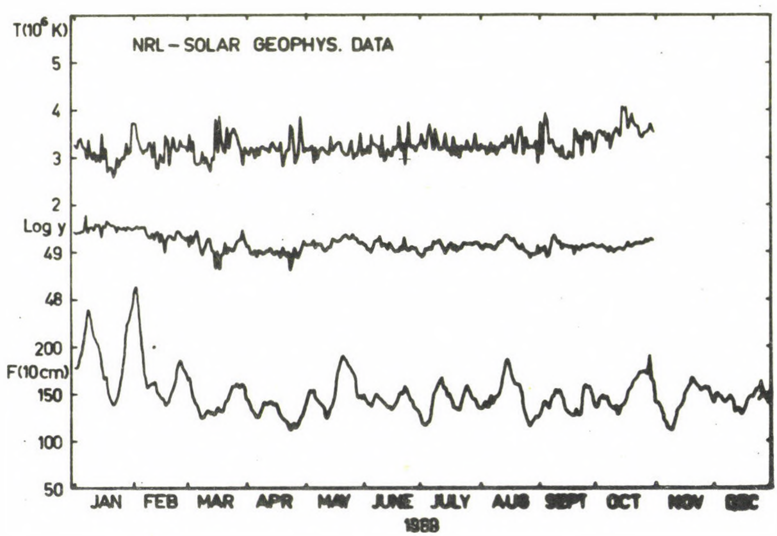

Figure 3.

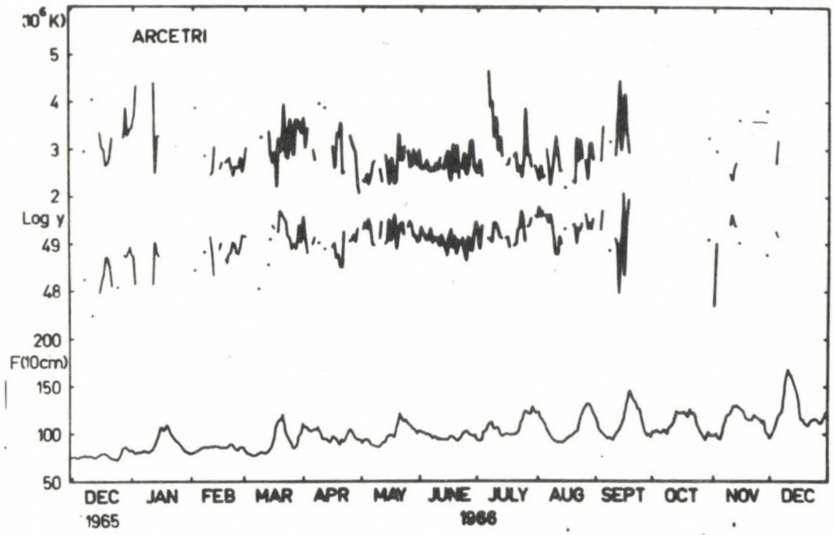

Figure 4.

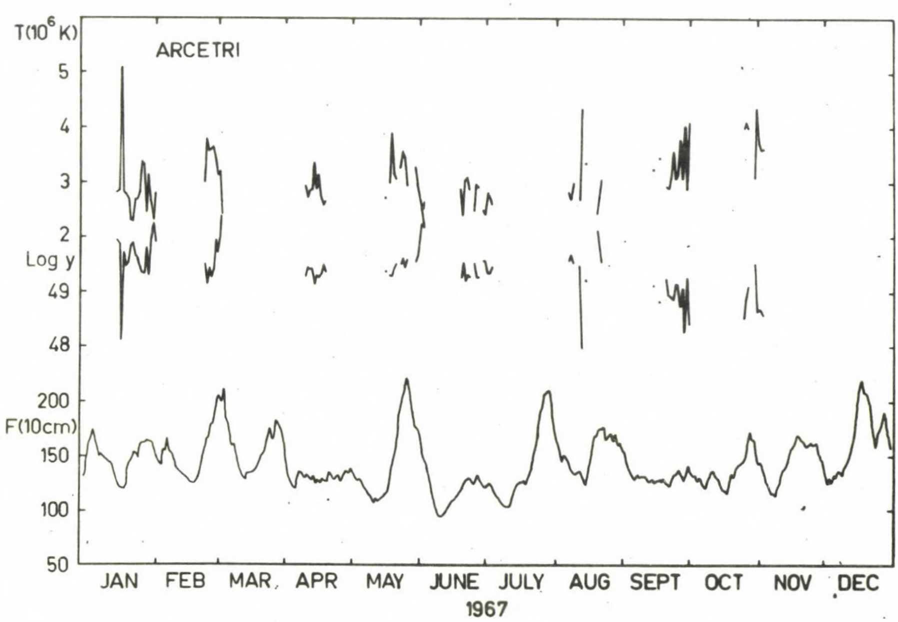

Figure 5.

PUBLICATIONS OF DEBRECEN HELIOPHYSICAL OBSERVATORY

CORRELATION OF SOLAR DM-BURSTINESS AND SOLAR MODULATION EFFECTS ON COSMIC RAYS

L. KŘIVSKÝ, V. LETFUS

Astronomical Institute of the Czechoslovak Acad.Sci.,Observatory Ondřejov

Abstract:

The autocorrelation between solar dm-burstiness and cosmic rays obtained by means of neutron monitors in Ottawa for the whole period from 1967 to 1969 and for a period of one year and a shorter period, respectively, was investigated. The cross-correlation between dm-burstiness and the cosmic rays was investigated for the period 1967 - 1969 and for periods of one year and half a year.

1. Introduction

The dm-burstiness is constructed from the observatories of Ondřejov (Czechoslovakia, 56 cm = 536 MHz) and Bedford (Mass., USA, 50 cm = 606 MHz) in order to obtain the maximum possible control of the radio activity during 24 hours. For our purpose we have prepared the tables of daily values of simple sums of bursts Σx_i (without respect to intensity and duration) and, using them, we have constructed a curve of a five term weighted moving average according to the formula

$$\Sigma x_i = \frac{\Sigma x_{i-2} + 2\Sigma x_{i-1} + 3\Sigma x_i + 2\Sigma x_{i+1} + \Sigma x_{i+2}}{9}$$

2. Autocorrelation of Solar Burstiness (λ 56 cm, 50 cm)

Figure 1 shows the autocorrelation computed from intervals of half a year, a whole year, and the whole investigated period of 1967 - 1969. Curves for the half-year period indicated that the expected recurrence, compatible with solar rotation, is only roughly displayed by the half years in 1967; as regards the other curves, the occurrence of subsidiary maxima is without apparent physically founded regularity and the individual autocorrelation curves are not mutually similar. This can also be seen with the annual curves. On the three--year curve, covering 1967 - 1969, the maxima on the 23rd and 25th days are more significant, which follows from the superposition of shorter intervals. Clearly, this result cannot be physically interpreted in a logical manner and is an expression of the random statistics of the phenomenon.

3. Cosmic Rays Autocorrelation - Ottawa

Figure 1 shows the autocorrelations of the diurnal cosmic rays values computed for semi-annual and annual intervals and for the whole investigated period of 1967 - 1969. The semi--annual curves indicate that the 27-day periodicity of event repetition is more or less established; in comparison to radio burstiness it seems that this is a result of the more permanent property of active regions and the solar rotation. This rotational effect is more marked in the 1st and 2nd halves of 1967, less so in the 2nd half of 1968 and 2nd half of 1969. As regards the annual curves the rotational recurrence is preserved, being most outstanding in 1967. As regards the autocorrelation curve covering the three years (1967-1969), the rotational period is preserved, but it is not very expressive. Clearly, the more long-term repetition of the effects on cosmic rays is an expression of the more permanent existence of certain active regions on the Sun regardless of the current activity of all active regions, illustrated, e.g., by the burstiness in the dm-range.

4. Cross-correlation of Solar Burstiness and Cosmic Rays

Figure 2 shows cross-correlations for semi-annual, annual intervals and for the period of 1967 - 1969.

Curves a - c show the values for 1967. The semi-annual intervals (curves a,b) and the curve for the whole year (c) indicate that the largest negative correlation occurs in the interval between the 6th and 10th day, the centre being the 7th day. The correlation during these days is about -0.3 (not particularly significant). This result agrees with the result obtained for the period from the end of 1969 over the 1st half of 1970 (Křivský et al. 1971).

Curves d - f show the cross-correlations for 1968. The semi-annual curves (d,e) show that in the 1st half of the year it is a matter of random fluctuations, which cannot be interpreted physically (small negative correlations present on the 0th and 1st days, larger correlation > -0.3 occurs on the 20th and 21st days). In the 2nd half of 1968 the situation is more promising; the negative correlation > 0.3 on the 2nd to 4th days. On the annual curve there is a very weak correlation on the 1st - 3rd days; clearly, this is a result of the non--uniformity of the variations in both halves of the year.

Curves g - i show the cross-correlations for 1969. The semi-annual curves (g,h) show that there is no marked correlation which could be physically interpreted in a logical manner. The same holds for the curve for the whole of 1969. No more regular relation of the two parameters investigated could be observed during this year.

Curve j shows the run of the cross-correlation for the period of the three years. It can be seen that a more permanent correlation of the parameters cannot be substantiated during the period of the few years around maximum solar activity which differ considerably with a view to the frequency of the activity on the Sun and its duration (or recurrence).

Figure 3 shows the daily data of radio burstiness and cosmic rays (Ottawa) by individual year. The burstiness curves are shifted in time to the right by the number of days given, as corresponds to the largest negative correlation found by cross-correlation for the individual years. The burstiness scale, contrary to the usual, is reversed.

5. Discussion of the Results

1) Radio burstiness displays recurrence in connection with the rotation of the Sun only over shorter periods of about ½ a year, and in a smaller number of semi-annual cases.

2) Cosmic rays, through their effects, display a much larger capacity for recurrence in connection with the rotation of the Sun. Clearly, this is the result of a special long--range nature of certain active regions on the Sun, which are capable of preserving a character of the emission of particles and fields into interplanetary space over a longer period (more than one rotation), which is able to evoke Forbush effects.

3) It seems that provided the negative correlation in the r.h.s. of the cross-correlation graphs shows more significant values (at least around -0.3), this correlation is concentrated in the interval between the 3rd and 7th days.

4) The occurrence of the weakly significant negative correlation between the 3rd and 7th days is observed in intervals when cosmic rays, in the first instance, and partly at least radio burstiness display a recurrent nature in connection with the 27-day solar rotation simultaneously.

5) It may be assumed that if there is permanent activity in several regions on the Sun (i.e., for several rotations of the Sun) and when no other short-lived activity is superimposed on it, a certain typical propagation velocity of the agent causing the Forbush effects of cosmic rays is established: the time-phase shift is about 3 - 7 days if the maxima of burstiness are identical in time with the minima of cosmic

rays. Relations of this type were found in the following time intervals: Jan. - Dec. 1967, Jul. - Dec. 1968, Nov. 1969 - Jun. 1970 (*Fig.4*).

6) The negative correlation of radio burstiness and cosmic rays around the 6th day found earlier (Křivský et al. 1971 *Fig.4*) has thus only been proved in some, roughly semi-annual intervals and it does not have a persistent nature. This makes it difficult to use this result for forecasting; this connection could be used for forecasting over a limited number of months if the "onset" of this correlation had already been observed.

7) The investigation of the individual active flare events on the Sun and the determination of their typical properties in connection with the situation of the fields in interplanetary space could lead to finding better relations between solar activity and Forbush effects than is the case with the radio dm-burstiness investigated (Dvoryashin, 1962; Gopasyuk, Křivský, 1967). One cannot exclude the possibility that the mutual relations (found in certain intervals) occur (even over longer intervals) when there are fewer active regions on the Sun and when some of them have a recurrent nature of longer duration.

R e f e r e n c e s

Dvoryashin,A.S.: 1962, *Izv. Krym. Astr. Obs.* 28, *293.*
Gopasyuk,S., Křivský,L.: 1967, *Bull. Astr. Inst. Czech.* 18, *125.*
Křivský,L., Olmr,J., Fischer,S., Chaloupka,P., Krajčovič,S., Pintér,S.: 1971, *WDC-A Rep. UAG-* 12, III, *337.*

66

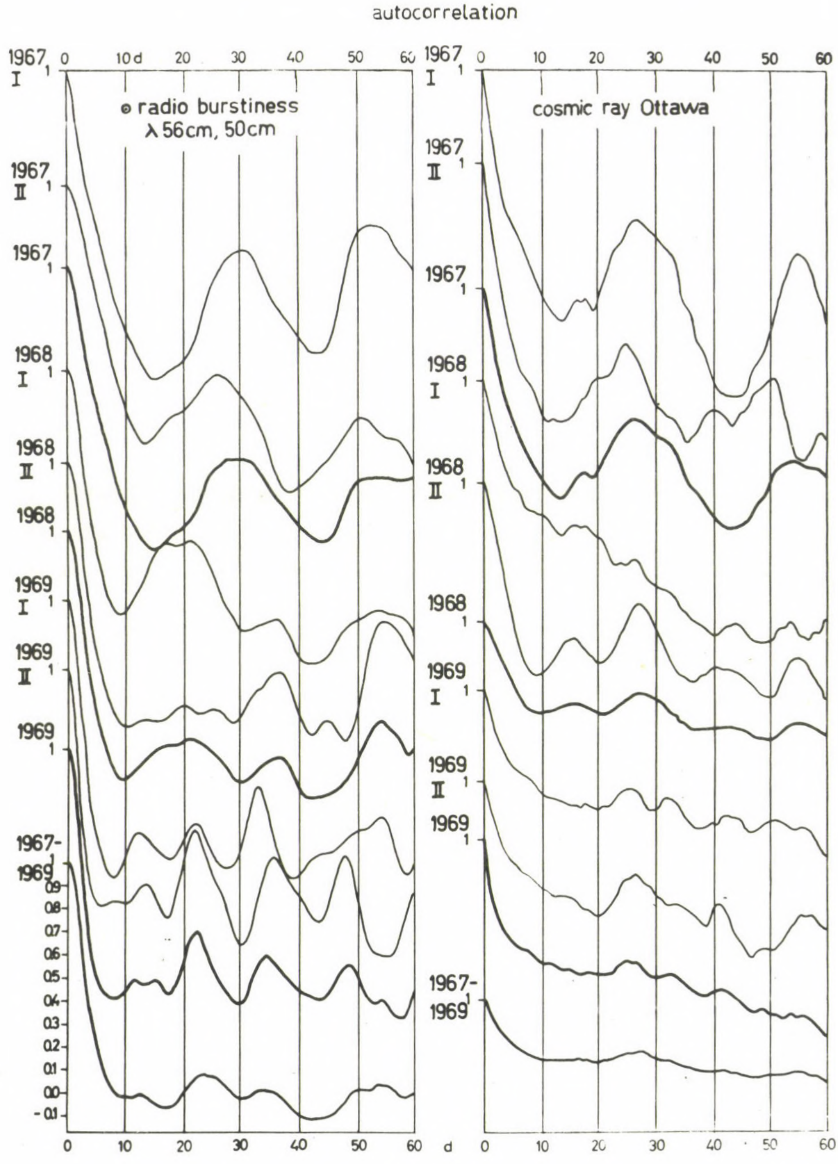
autocorrelation
radio burstiness
λ 56cm, 50cm
cosmic ray Ottawa
1967 I
1967 II
1967
1968 I
1968 II
1968
1969 I
1969 II
1969
1967-1969
0 10d 20 30 40 50 60
0 10 20 30 40 50 60 d
0.9
0.8
0.7
0.6
0.5
0.4
0.3
0.2
0.1
0.0
-0.1

Figure 1.

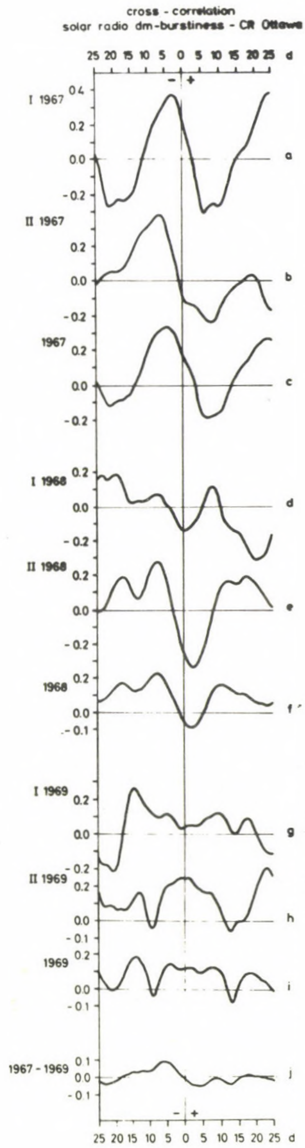

Figure 2.

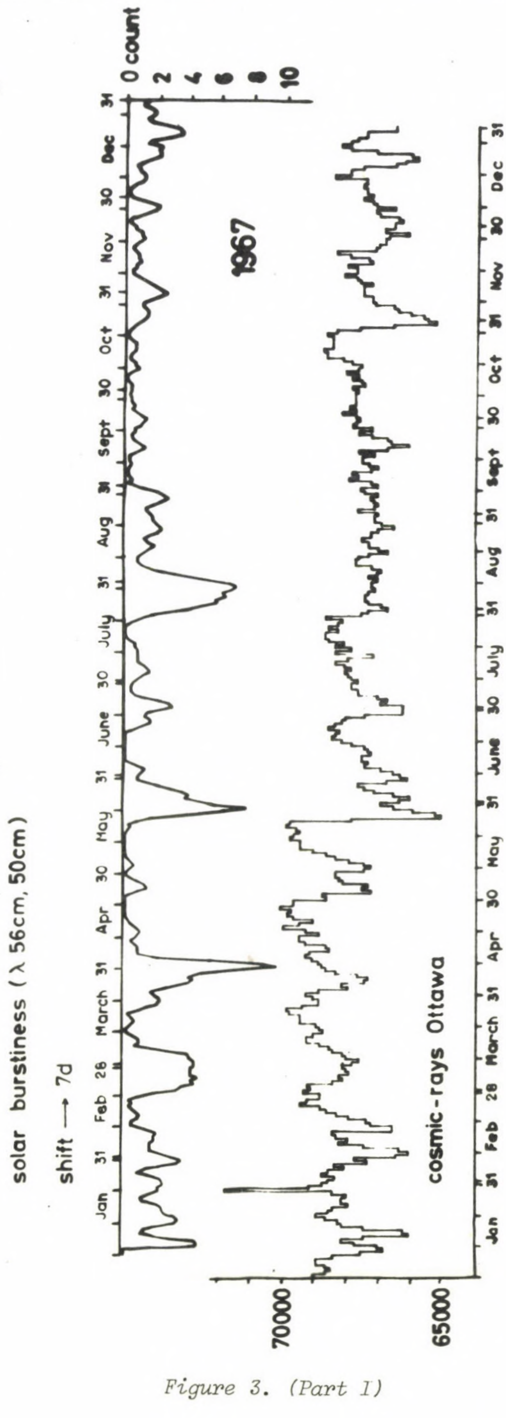

Figure 3. (Part I)

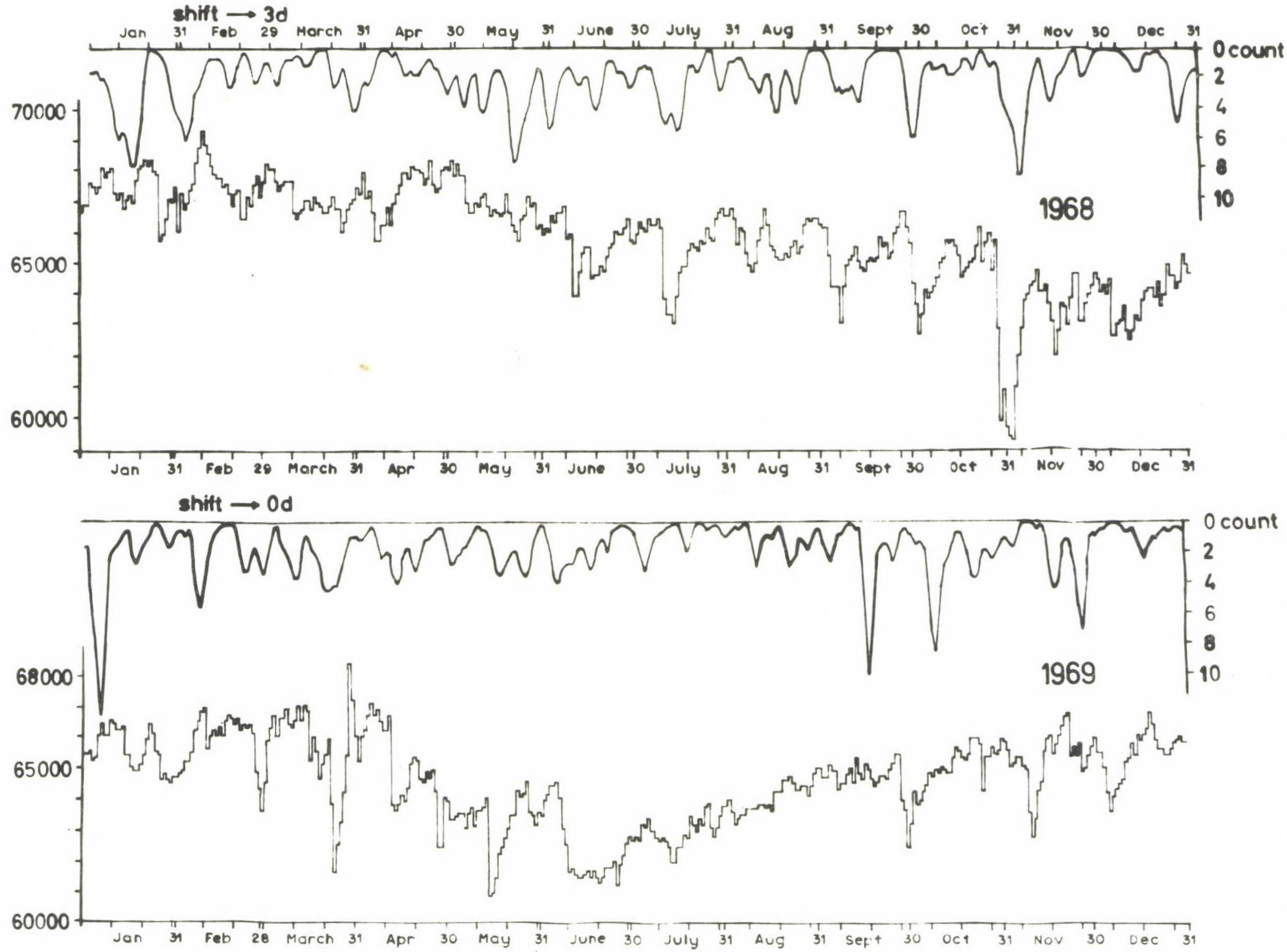

Figure 3. (Part II-III)

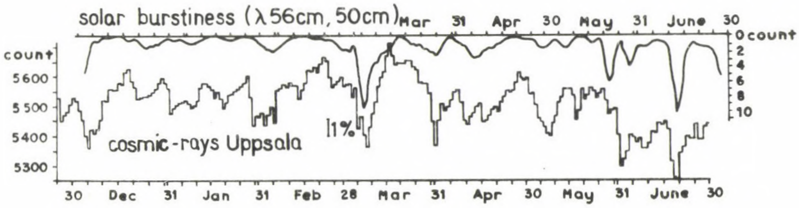
solar burstiness (λ56cm, 50cm)
Mar 31 Apr 30 May 31 June 30
0 count
2
4
6
8
10
count
5600
5500
5400
5300
cosmic-rays Uppsala
1%
30 Dec 31 Jan 31 Feb 28 Mar 31 Apr 30 May 31 June 30

Figure 4.

PUBLICATIONS OF DEBRECEN HELIOPHYSICAL OBSERVATORY

A REVIEW OF ELECTRICAL CONDUCTIVITIES IN THE PHOTOSPHERES OF THE SUN AND THE STARS

M. K O P E C K Ý

Astronomical Institute of the Czechoslovak Acad. Sci., Observatory Ondřejov

P. K O T R Č

Faculty of Sciences, The Purkyně University, Brno

Abstract:

The paper gives a summary of the values of the electrical conductivity at various optical and geometric depths of photospheric layers in the active centre on the Sun and at various optical depths of some types of stars. The electrical conductivity as a function of optical depth in a spot and in the solar photosphere is compared with the electrical conductivity as a function of optical depth in the photosphere of stars of similar spectral types.

1. Introduction

One of the important magnetohydrodynamic parameters is the electrical conductivity of plasma. Recently, the electrical conductivity σ has been determined in various formations of active regions on the Sun, in the photospheres of stars of F, G and K spectral types, and in the photospheres of early--type stars.

The purpose of this short contribution is to present a comprehensive review of the values of the electrical conductivity at various optical and geometrical depths of the photospheres of the stars and the Sun, based on our earlier computations.

As regards the photospheric layers of the Sun and the stars of F, G and K spectral types, the photospheric plasma is little ionized. In these cases it nearly always holds that

$$\log \frac{n_e}{n_n} < -2 \qquad (1)$$

where n_e is the number of electrons and n_n is the number of neutral particles per cm^3 . Therefore, for computing the electrical conductivity σ in these cases the following approximate relation was used (Kopecký 1966; Kopecký and Kuklin, 1969):

$$\log \sigma = 15.00 + 0.93 \log (n_e/n_n) \qquad (2)$$

As regards the photospheres of early-type stars, however condition (1) remains mostly unsatisfied. That is why in these cases the electrical conductivity was computed with the help of Kuklin's formula (1966):

$$\sigma = \frac{3e^2}{8\sqrt{\pi}(2kT)^{\frac{1}{2}}} \; \frac{n_1 \sum_{i=1}^{2} r_{i3}^2 m_{i3}^{\frac{1}{2}}}{n_1 m_{12}^{\frac{1}{2}} r_{12}^2 \sum_{i=1}^{2} r_{i3}^2 m_{i3}^{\frac{1}{2}} + n_3 \prod_{i=1}^{2} r_{i3}^2 m_{i3}^{\frac{1}{2}}} \qquad (3)$$

where

$$r_{12}^2 = \frac{8,1343}{T^2} \cdot 10^{-7} \left[8,1861 + 3 \log T - \log n_1\right] \qquad (4)$$

and e is the charge of the electron, k the Boltzmann constant, and T the electron temperature. In order to distinguish between the quantities corresponding to the individual plasma components the indices 1 ,2 and 3 were used to denote quantities associated with electrons, ions and neutral atoms,respectively. n_i is the number of particles of the i-th plasma component per cm^3,m_{ik} is the reduced mass of the particles of the i-th and k-th plasma components, and r_{ik}^2 is the effective collision cross-section of the particles of the i-th and k-th components of the plasma.

2. Review of the Values of Electrical Conductivities

A review of the values of the electrical conductivities σ in the photospheres of the stars and the Sun, obtained from Eqs. (2) and (3), is given in *TABLE I* to *IV*.

TABLE I gives the values of $\log \sigma$ at various optical depths τ for different homogeneous models of the solar photosphere, spots and faculae as determined with the help of Eq. (1) in the papers of Kopecký (1970a) and Kopecký and Soytürk (1971).

TABLE II gives the values of $\log\sigma$ at various optical depths of the photospheres of stars of the F, G and K spectral types. These electrical conductivities were computed with the help of Eq. (2) in the paper of Kopecký (1970b) from the models of stellar photospheres of de Jager and Neven (1967). Moreover, stars with $\log g = 4$ (where g is the gravitational acceleration on the surface of the star) represent stars in the main sequence and in *TABLE I* they are denoted as dwarf-stars, and stars with $\log g = 2$ represent giant-stars.

The electrical conductivities in the photospheres of the early-type stars, the review of which is given in *TABLE III*, were computed by means of Eq. (3) in the paper of Kopecký and Kotrč (1973) using models of atmospheres of early-type stars of Mihalas (1965). *TABLE III* is only valid for stars in the main sequence, i.e., for stars with $\log g = 4$.

Whereas *TABLES I - III* give the electrical conductivity as a function of optical depth, *TABLE IV* gives the electrical conductivity as a function of the geometrical depth h in the photospheric layers of various phenomena in the active region on the Sun. These are approximate values based on various models of spots, the photosphere and facula, as treated in Kopecký's paper (1971).

TABLES I - IV indicate that the electrical conductivities in the photospheric layers of the Sun and the stars are within the range of 10^{10} to 10^{14}, which depends on the effective temperature of the star and the optical depth in the first place, and as regards the Sun also on the phenomenon studied. The difference of 4 orders of magnitude, by which the electrical conductivities in various photospheric layers may differ, is relatively quite considerable, in any case large enough to affect the variety of magnetohydrodynamic processes taking place in these layers.

3. Comparison of the Electrical Conductivity on the Sun and Stars

The computations of the electrical conductivity, carried out earlier, give a possibility of comparing the electrical conductivity as a function of optical depth τ on the Sun and on stars similar to the Sun.

Figure 1 shows a comparison for the photosphere, the full line representing $\log \sigma$ in the photosphere of the stars in the main sequence of GO and G9 spectral types according to the models of de Jager and Neven, the dashed line referring to the same in the photosphere of the Sun according to four different models. Since the Sun is of a Gl to G2 spectral type, drawing om *Fig. 1* one may conclude that the variation of the electrical conductivity in the photosphere of the Sun roughly corresponds to the variation of the electrical conductivity in the photospheres of stars similar to the Sun.

On the other hand, the electrical conductivity in the spot umbra displays practically no agreement with the electrical conductivity in stellar photospheres. This can be seen in *Fig. 2*, where the full line represents $\log \sigma$ in the photospheres of the stars of the main sequence of G9 and K2 spectral types, the dotted line in giant-stars of G9 and K2 spectral types, and the dashed line in three different models of solar spot umbra. It can be seen from *Fig. 2* that the electrical conductivity in the different models of the umbra differs substantially in value (much more than with the models of the solar photosphere), moreover, the overall nature of the variation of log σ in the sunspots also differs from log σ in the stellar photospheres; with increasing optical depth the electrical conductivity in the spots increases more slowly than in the photospheres of the Sun and the stars.

R e f e r e n c e s

de Jager, C., Neven, L.: 1967, *Bull. Astr. Inst. Netherl. Suppl. Ser.* 2, *No. 4*.

Kopecký, M.: 1966, *Bull. Astr. Inst. Czech.* 17, *270*.

Kopecký, M.: 1970a, *Bull. Astr. Inst. Czech.* 21, *238*.

Kopecký, M.: 1970b, *Bull. Astr. Inst. Czech.* 21, *231*.

Kopecký, M.: 1971, *Bull. Astr. Inst. Czech.* 22, *343*.

Kopecký, M., Kotrc, P.: 1973, *Bull. Astr. Inst. Czech.* 24.

Kopecký, M., Kuklin, G.V.: 1969, *Solar Phys.* 6, *241*.

Kopecký, M., Soytürk, E.: 1971, *Bull. Astr. Inst. Czech.* 22, *154*.

Kuklin, G.V.: 1966, *Rezultaty nabljudenij i issledovanij v MGSS v Sibiri i na Dalnem Vostoke*, vyp. 1, *17*.

Mihalas, D.: 1965, *Astrophys. J. Suppl. Ser.* 9, *321*.

TABLE I.

Values of log σ in photospheric layers of the Sun

Object	Model	Optical depth τ			
		0,01	0,10	1,00	2,00
Sunspot's umbra	Michard	10,63	10,84	11,17	11,30
	Fricke-Elsässer	9,99	10,14	10,54	10,76
	Mattig	10,14	10,36	10,73	10,84
Sunspot's penumbra	Moe-Maltby	10,87	10,98	11,52	11,85
Faculae	Chapman	-	11,76	11,71	12,18
Photosphere of the Sun	Michard	11,12	11,21	12,01	12,46
	Elste-Bubke	10,91	11,08	12,01	12,52
	Mattig	10,87	11,09	11,79	12,34
	Bilderberg	10,95	11,06	11,88	12,27

TABLE II.

Values of log σ in photospheric layers of stars of spectral types F, G and K.

Object	T_{eff}	Optical depth τ			
		0,01	0,10	1,00	2,00
dwarf-stars	4 760°	10,13	10,42	11,07	11,55
	5 350°	10,55	10,83	11,58	12,23
	5 940°	10,89	11,12	12,29	12,86
	7 130°	11,34	12,06	13,35	-
giant-stars	4 760°	10,39	10,69	11,35	11,91
	5 350°	10,88	11,08	12,14	12,61
	5 940°	11,06	11,46	12,76	13,40
	7 130°	11,93	12,71	14,01	-

TABLE III.

The values of log σ in photospheres of early type stars with log g = 4.

T_{eff}	τ			
	0,01	0,10	1,00	2,00
7 200°	11,95	11,97	12,80	13,12
7 760°	12,40	12,41	13,06	13,28
8 410°	12,72	12,77	13,24	13,38
9 170°	12,93	13,02	13,34	13,43
10 100°	13,06	13,17	13,39	13,46
11 210°	13,14	13,24	13,42	13,48
12 610°	13,22	13,33	13,52	13,59
14 000°	13,26	13,38	13,56	13,63
15 740°	13,32	13,42	13,61	13,67
18 000°	13,38	13,48	13,67	13,73
24 000°	13,52	13,62	13,80	13,87
28 000°	13,61	13,72	13,90	13,96

TABLE IV.

The approximative values of σ in different geometrical depths h in different phenomena of solar active region.

h (km)	spot					photosphere	faculae
	homogeneous			inhomogeneous			
	umbra		penumbra	elements			
	transparent	dense		hot	cold		
0	10^{10}	10^{10}	$7x10^{10}$	10^{11}	$8x10^{9}$	10^{11}	$5x10^{11}$
150	10^{10}	$2x10^{10}$	10^{11}	$2x10^{11}$	$9x10^{9}$	$2x10^{11}$	$2x10^{11}$
300	10^{10}	$7x10^{10}$	$7x10^{11}$	$3x10^{12}$	$3x10^{10}$	$3x10^{12}$	10^{12}
3000	$6x10^{10}$	–	–	–	–	–	–

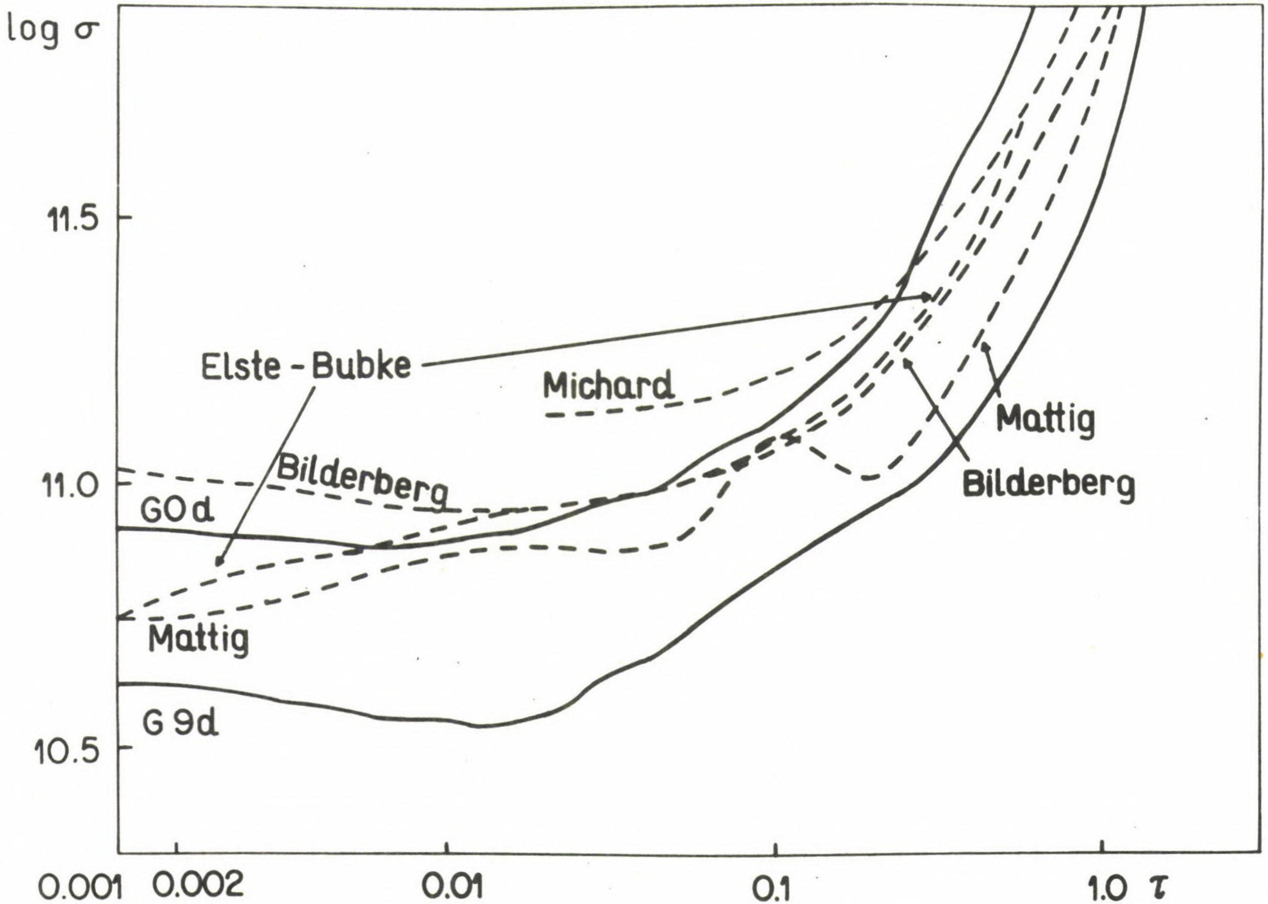
log σ
11.5
11.0
10.5
G0d
G 9d
Mattig
Bilderberg
Elste - Bubke
Michard
Mattig
Bilderberg
0.001
0.002
0.01
0.1
1.0
τ

Figure 1.

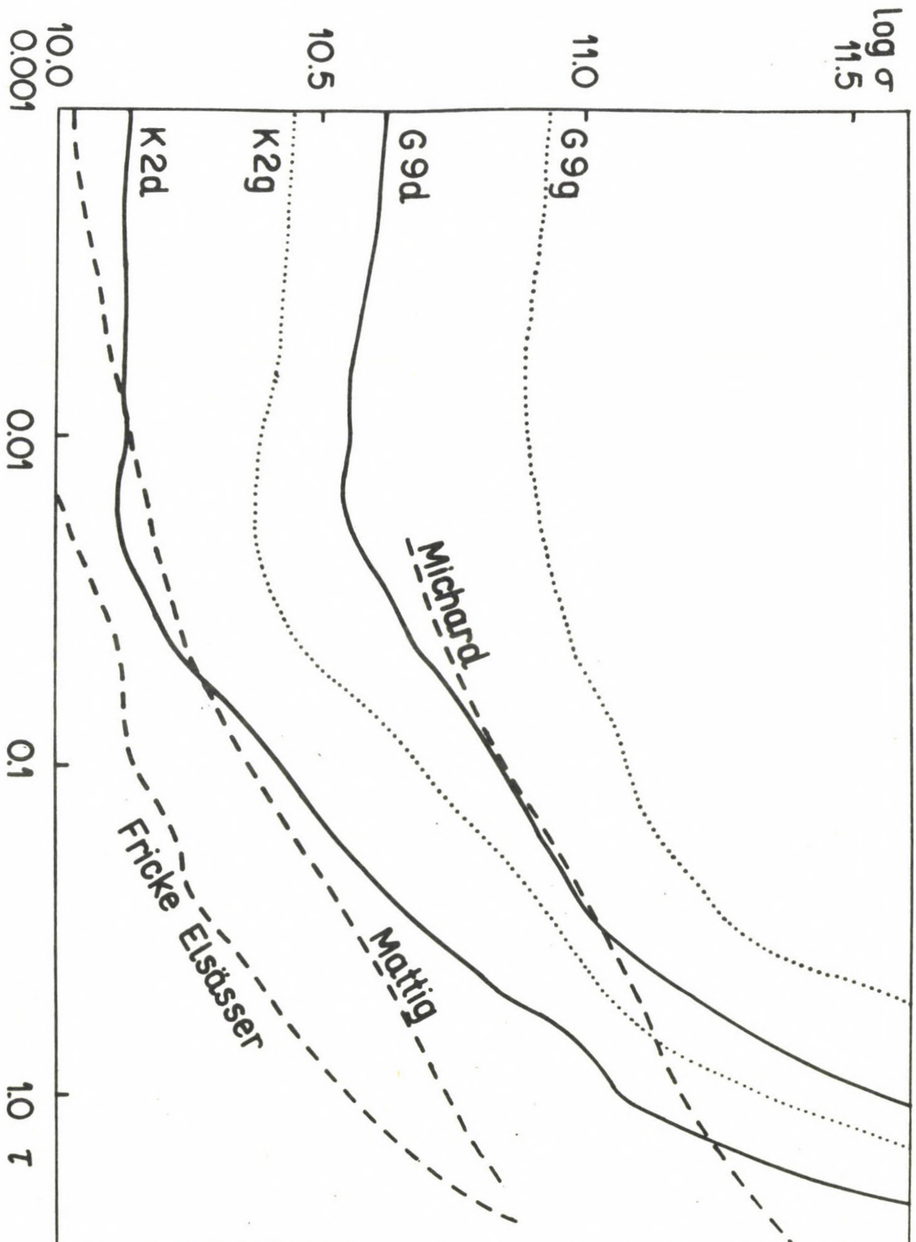

log σ
11.5
11.0
10.5
10.0
0.001
0.01
0.1
1.0
τ
G9g
G9d
K2g
K2d
Michard
Mattig
Fricke Elsässer

Figure 2.

PUBLICATIONS OF DEBRECEN HELIOPHYSICAL OBSERVATORY
Vol. 2 No. 2 1971

HIGH RESOLUTION SPECTRUM $\lambda\lambda$ 6610 - 6770 A OF A LARGE SUNSPOT

O. E N G V O L D
Institute of Theoretical Astrophysics, University of Oslo,Blindern, Oslo

During the spring of 1969 we obtained spectra of a large sunspot during excellent visibility at Oslo Solar Observatory. One of the wavelength regions covered was $\lambda\lambda$ 6610 - 6770 A, which is now reduced and corrected for parasitic light from penumbra and photosphere. We shall not go into detail how these corrections were made. This information will be given in the Institute of Theoretical Astrophysics Report series where this work will be published. We give a few relevant data of the sunspot and the instruments in the following table.

Roma number of the sunspot	5367
Heliographic angle of the spot	28°
Magnetic field strength	3300 gauss
$I_{umbra}/I_{photosphere}$ (at λ 6700A)	0.108
Spectral resolution	$\sim 3.10^5$
Linear dispersion on the film	~ 8.5 mm/A
Exposure time	1 - 3 sec

5

I must comment on the uncertainty in our corrected spectra. Where we observe lines stronger than about 5 mA in the spectrum of the parasitic light the uncertainty is increased. Where this is the case the spectrum is drawn with a broken line (see *Fig. 1 - 4*).

The following figures show the corrected spectrum in a few selected wavelength regions. We notice how the character of the spectrum is entirely different around 6620 A as compared to 6760 A. It turns out that the numerous strong and weak lines in this spectrum may be identified as those of the triplet γ-system of TiO. The next two figures show two of the bandheads of this triplet spectrum at λ 6681 A and λ 6714 A.

A laboratory TiO spectrum was produced from an arc between Ti-electrodes in air and recorded with the same spectrograph as the spectrum of sunspot. It appears that more than 90 % of the lines of the sunspot spectrum also appear in the spectrum of the Ti-arc.

In *Fig. 4* we also notice the strong LiI doublet (λ 6708A). We have recently used this spectrum to derive the solar Li abundance.

Figure 1. The spectrum of sunspot.

Figure 2. The spectrum of sunspot.

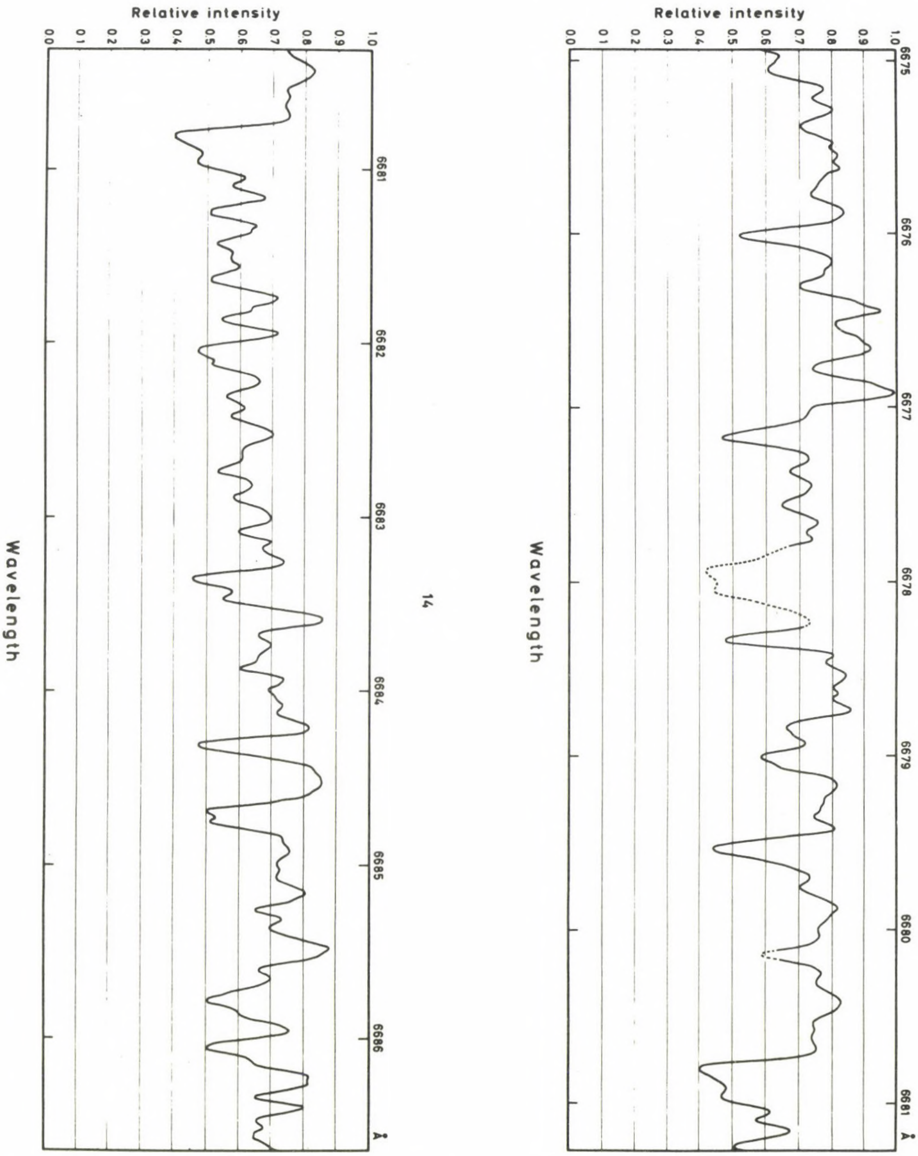

Figure 3. The spectrum of sunspot.
Notice the $R_2(J)$ (1,0) band head of the TiO γ-system at λ 6681 A.

Figure 4. The spectrum of sunspot.
The $R_1(J)$ (1,0) band head of TiO is seen at λ 6714.5 A.
Notice the LiI doublet line at λ6708 A.

PUBLICATIONS OF DEBRECEN HELIOPHYSICAL OBSERVATORY
Vol. 2 No. 3 1971

"QUANTISATION" OF SUNSPOT MAGNETIC FIELDS

Š. K N O Š K A
Observatory, Hurbanovo

Abstract:
The existence of discrete maximum intensity values in sunspots during the day of penumbra development is demonstrated.

1. Introduction

It has been shown by several authors (Bumba, 1965; Ichsanov, 1967; Dmitrieva et al., 1968) that the areas of fully developed sunspots, because of the close relation of spots to the convectional supergranular network in the solar atmosphere, have discrete values comparable with the dimensions of supergranules as they fill in the individual supergranular cells. On the other hand, Steshenko (1967) and Bumba (1967a) demonstrated that the intensity of the magnetic field of the smallest spots and pores also display discrete values equal to 1000 - 1200 gauss. There are other indications of the "quantization" of the magnetic flux in the solar atmosphere (Livingston, Harwey, 1969; Howard, Stenflo, 1972). All this led us to investigate whether the magnetic field intensity values in all sunspots do not have certain discrete values, too, or whether they may change their values continuously. And because it is known (Bumba, 1967b) that the formation of the penumbra is a very important moment in the life-time of a spot, practically finishing its phase of growth, we accepted the intensity values measured one day before the penumbra was formed and the intensity values obtained the first day with the penumbra as the basic observational material.

2. Observational material

As a source of these data the photographic measurements of magnetic field intensity in individual spots in all sunspot groups, compiled and published by the Pulkovo observatory in the USSR as a supplement to the journal Solneshnyje dannye, was used for the time interval August 1962 to December 1970. From all daily maps published, 202 sunspot groups with observed penumbra development at least for one spot, many times for two or more spots, were found. This means that for the spot with a penumbra development there existed measurements of the maximum intensity value at least for one day before and the day of the penumbra formation, and the spot was far enough from the limb (minimum about 20°) to be identified without difficulty. The maximum intensity value for another 152 sunspot groups were taken, which developed no penumbra at all, and were observed at least for three consecutive days. The measured maximum values of the magnetic field intensity were recorded separately for the studied leading and following sunspots, as well as for the northern and southern solar hemispheres.

3. Results

The main results of our investigation may at once be seen in *Figure 1:*

1) The histogram of the maximum magnetic field intensity values, obtained the day the penumbra was formed, for all the 368 sunspots from the available material on the right-hand side of the figure, is very narrow and has an outstanding maximum equal to 2000 gauss, the axis of symmetry of which gives a most probable value of 2100 gauss.

2) The histogram of the maximum magnetic field intensity values, measured one day before the penumbra developed, for 287 spots on the left-hand side of the picture, demonstrated that the field intensity of the spots with the penumbra yet developed does not exceed the value of about 1500 to 1800 gauss. The first, well separated maximum of this curve around 1200 gauss is in good agreement with the results of Steshenko (1967) and Bumba (1967a) mentioned above, showing that the smallest spots display the discrete value of intensity. The asymmetrical tail of the curve, proceeding to even smaller intensities, speaks in favour of the statistical nature of these measurements, which are very difficult for small spots. The reason for the different number of spots in cases 1) and 2) is the fact that many times the published observations have estimated intensity values only for one day of the two critical days.

3) The third curve in *Figure 2* demonstrates the histogram of maximum intensities for the spots which did not develope a penumbra at all. It coincides well with the second curve discussed above.

4. Discussion

The interpretation of the obtained results seems to be simple: not only do the smallest pores and spots have a critical step-value of their maximum magnetic field intensity (1000-1200 gauss), but also the maximum intensity of the larger spots, just completing their formation by the development of the penumbra, has its critical step-value around 2100-200 gauss which must be reached by a relatively large change of intensity, amounting to about 500 - 600 gauss. Taking into account that the area of such sunspots has a certain critical "quantized" value, which for the most frequent smallest spots with a penumbra is about 190 millionths of the visible disk of the Sun (about 6.10^{18} cm^2) (Bumba, 1965), we may estimate the basic magnetic flux for these sunspots as being about 12.10^{21} Maxwells, which is in good agreement with the results published earlier (Bumba, 1961; Sheeley, 1966). In other words the spot, without reaching a certain critical magnetic field intensity, area, and a certain magnetic flux value, cannot develop a penumbra. As regards the real intensity values, the difference between the measurements made at different observatories by different methods must be considered.

There are many interesting questions connected with the prepenumbral stage of the spots and dealing with the further development of sunspots when the penumbra has already been formed. To solve these problem, more detailed investigations must be made.

Acknowledgement

The author is indebted to Dr. V. Bumba for suggesting this work and for helpful discussions.

R e f e r e n c e s

Bumba,V.: 1961, *Bull. Astr. Inst. Czech.* 12, *82.*
Bumba,V.: 1965, in R. Lüst (ed.), *IAU Symposium No.* 22, *192.*
Bumba,V.: 1967a, *Solar Phys.* 1, *371.*
k Bumba,V.: 1967b, in P.A. Sturrock (ed.), *Plasma Astrophysics,* (Int. School Fermi) *77.*

Dmitrieva,M.G., Kopecký,M., Kuklin,G.V.: 1968, in K.O. Kiepenheuer (ed.) *IAU Symposium No.* 35, *174.*

Howard,R., Stenflo,J.O.: 1972, *Solar Phys.* 20.

Ichsanov,R.:1967, *Soln. Dannye No.* 7.

Livingston,W., Harvey,J.: 1969, *Solar Phys.* 10, *294.*

Sheeley,N.R., Jr.: 1966, *Astrophys. J.* 144, *723.*

Steshenko,N.: 1967, *Izv. Krym. Astr. Obs.* 37, *21.*

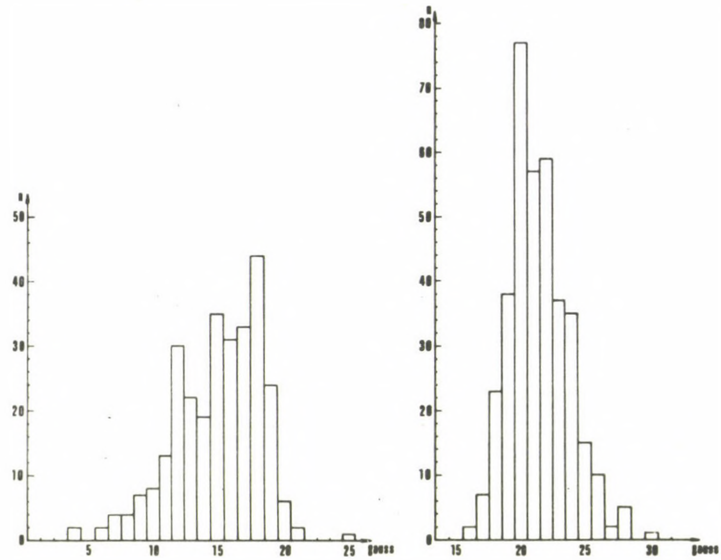

Figure 1. *Left-hand side: the histogram of the maximum magnetic field intensity values, one day before the penumbra developed.*

Right-hand side: the histogram of the maximum magnetic field intensity values, obtained the day the penumbra was formed.

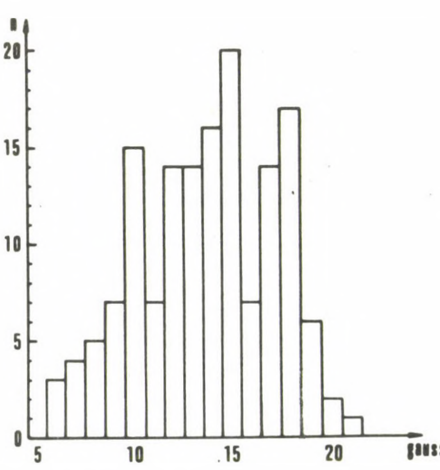

Figure 2. *The histogram of maximum magnetic field intensity values for the spots which did not develop a penumbra at all.*

PUBLICATIONS OF DEBRECEN HELIOPHYSICAL OBSERVATORY
Vol. 2 No.4 1971

OBSERVATIONS OF SOME CHARACTERISTIC TYPES OF SUNSPOT MOTIONS

L. D E Z S Ő, O. G E R L E I,
G Y. G Y E R T Y Á N O S, B. K Á L M Á N, Á. K O V Á C S
Heliophysical Observatory of the Hungarian Acad.Sci., Debrecen

Abstract:
On the basis of more than 400 heliograms, observed in Debrecen, in the ultraviolet continuum for higher contrast, the motions of sunspot umbrae were studied. Different types of various curvilinear and rotational movements are exhibited both with respect to some significant spots and within the Carrington system of coordinates.

Some years ago at the Debrecen Observatory we took initial steps in studying the proper motions of sunspots, on the basis of our photographic observations of the solar photosphere. By extending our plan of research we joined in the participation of the program "Rapid Variations of the Solar Magnetic Fields", a cooperative investigation of the solar observatories of socialist countries. Here and in another paper (1) we are giving some of our first results of measurements relating to this subject matter. In the following we present some examples of motions of sunspot umbrae observed during the summers of 1967, 1968 and 1969.

* * *

The observations used were obtained with a 5" photoheliograph of 2 m focal length; the diameter of the Sun's image at the secondary focus, i.e. on the original photographs, is about 10 cm. At the principal focus of the photoheliograph two spider-lines are fixed by which the zero of position angles can be determined. (To do this, zero photographs were usually taken each day by means of plates which have been exposed twice with an interval of about 110 seconds.)

All observations were taken through an ultraviolet metal interference filter of 120 A half-width. The filter has its maximal transparency at 3750 A. The photographs were taken generally on films of high contrast, principally on estar based Kodalith. Nevertheless, in 1967 and 1968 the majority of the photomaterials were Agfa and Gevaert diapositiv plates. In 1967 the objective was generally stopped down to 4 cm, but in 1968 and 1969 the free aperture was 10 cm or greater.

More than half of the observations were made by one of us (Á.K.), the rest by Erzsébet Horváth and I. Ökrös. To be able to follow and measure spot motions we tried to take long series of observations of good seeing at intervals of about 10 minutes.

The direct measurings of the spots positions were made with an Abbe comparator in an arbitrary x-y coordinate system. The data obtained were transformed to Carrington coordinates, i.e. heliographic longitude *(L)* and heliographic latitude *(B)*. We should like to emphasize that we always measured only umbra-position, i.e. the geometric center of the umbra. In some cases we determined also the area of the umbrae in millionths of the solar hemisphere.

* * *

The *Figures 1, 4, 6, 7, 9, 10, 12, 14* and *15* present the results of our coordinate measurements of the most important umbrae which we could identify unambiguously through a series of consecutive heliograms, i.e. a reasonably long enough period of time. In these Figures it is possible to read off the heliographic longitude and latitude differences to an accuracy of 0.1 degree and in consequence the spot motions are quite clearly seen.

Each separate umbra is denoted by a number or letter or a resonable combination of these signs. Occasionally almost detached umbrae, if they could not be followed long enough separately, were given common denotation. The denotations of umbrae also indicate the magnetic polarities, according to (2) and (3). The preceding polarity *(p)* is marked with numbers, the following one *(f)* with letters.

Figures 1, 3, 5, 11 and *13* show the denotations of the measured umbrae. To specify the sunspot groups we used the designation of the *Solnechnye Dannye*.

* * *

In *Figures 4* and *6* the relative coordinates of the most important spots of the groups Nos.203 and 208 of 1969 are expressed in heliographic longitude and latitude differences (ΔL, ΔB) with respect to the main *p* spot; the center of the coordinate system (marked by a double circle) is the position of the spot *1;* the ordinates represent solar meridians and the abscissae are parallel to the solar equator. The spot positions, shown with different symbols, are all arithmetic averages of several single measurements relating to certain time intervals, which relevant data may be found at the right and left lower corner in *Figure 9* and in addition two periods of observations are marked at the bottom in *Figure 6*. The numbers of observations are given in the brackets. Larger numbers and letters show the denotations of the spots, while small numbers mark the day of observation next to the first daily average position.

In *Figure 7* we display in more detail, as an example, the observed motion of the main *f* spot of group 208, i.e. spot *a*. The time change of the Carrington coordinates, i.e. ΔL and ΔB versus time, can be seen, where each small circle represents the result obtained from a single photoheliogram and therefore this Figure may be adopted for forming an opinion on the accuracy of our measurements of spot positions.

Figure 12 for the group No.250 of 1967 is quite similar to *Figures 4* and *6*. Here, for the black symbols, the time of observations concerned are given in the lower left corner of the Figure, while the empty circles and quadrants also show average positions for July 27 and 28 respectively, but related periods of observations as well as numbers of observations are to be found in *TABLE 1*.

The daily average positions of the more important spots of the groups Nos.265 and 268 of 1968 with respect to (spot *1)* the main *p* spot of groups 265, are given in *Figure 14*. Here a spot has the same symbol over all its period of observation, indicated next to the symbols filled in in black, that mark the first day of this period. At the bottom of *Figure 14* the relevant moments of observations and (in brackets) the number of observations are shown.

* * *

In *Figure 9* the relative motion, over several days, of the main *p* spot of five sunspot groups are shown with respect to a steady spot which is the main *p* spot of a sixth group. Concerning the meaning of the spot position to be seen we refer to the explanation that was given in connection with the *Figures 4* and *6*, i.e. the groups 203 and 208 of 1969. We have selected for detailed studies these six sunspot groups of 1969 because in June 1969, at a period of high solar activity, these interesting groups were situated on the same third part of the solar hemisphere between the heliographic longitude 70° and 130°. On this region of the

Sun, simultaneously there was no other group in which the maximal (umbra + penumbra) area of the largest spot exceeded 100 millionths of the solar hemisphere.

The *Figure 10* reveals the motion of the main *p* spots of the six groups in question. The mean Carrington coordinates are given for each day of observations and the relevant rate of the solar differential rotation (according to (4)) are also indicated. The periods of observations are marked on the time axis. It can be seen that the motion of the main *p* spot of group 202 can be considered in approximation as linear and uniform. This fact was the principal reason why we chose this spot as a center of coordinates in *Figure 9*. Under the headline of *Figure 10* the small map makes visible at a glance the relative heliographic places of the six sunspot groups.

The *Figure 15*, which is similar to *Figure 10*, reveals the motion of the main *p* spot (spot *1*) of group 265 of 1968, i.e. the motion of the center of coordinates in *Figure 14*.

The Carrington coordinates of the main spot of group 250 of 1967 i.e. that of the center of coordinates in *Figure 12*, are L =105,8°, B= +26,0° at July 26,4 UT. These coordinates had a change of ΔL = -1,0°, ΔB = -0.3° in 2 days, between July 26,4 UT and 28,4 UT. If the motion in longitude had originated only from the differential rotation then ΔL = -0.6° should be the result (according to (4)).

* * *

By making a thorough examination of the different graphs presented, it is possible to find out several precedents of some interesting facts on sunspot motions. We wish to call attention especially to the peculiarities outlined in the following.

By examining the movement of sunspot groups with respect to the Carrington system of coordinates (see *Figures 10* and *15*) we should come to the conclusion that, in general, only a smaller fraction of motions can be due to the differential rotation.

Sunspot groups 202 and 204 as well as 209 of 1969 during our period of observation consisted almost entirely of a single larger spot and their motions were, in good approximation, linear, as shown in *Figure 10*, but all these groups revealed rotational motions.

The right part of *Figure 1* is self-explanatory. In *Figure 2* the variation of the position angle (ϑ) is seen, where each circle marks an angle measurement on a single heliogram (ϑ is counted from N towards E). In the upper part of *Figure 2* the time-variation of the angle ϑ proves the rotation of the line which connects the p_1 and p_2 umbrae, being in common penumbra (shown in *Figure 1*). It is particularly interesting that spot p_2 of group 202 consisted also of two umbrae (denoted by a and b) within the same penumbra and they also revealed rotation. To put it briefly: the angular velocity of the a - b line of 202 p_2 was several times greater than that of the p_1 - p_2 of 204, and the direction of both rotations was the same on June 6. But we may conclude from the data of measurements, exhibited in the lower halves of *Figure 2*, that the next day, as likely as not, the direction of rotation of 202 p_2 turned. Such a conclusion is also supported by the fact that in group 209 about three days later a similar turning did in fact occur (see Fig.5., p.84 in (1)). In group 209 the pairs of umbrae which were rotating around each other were several times larger than the ones in group 202. (Compare *Figure 8* with Table I, p.80 in (1)). While in group 202 the spot p_2 with its double umbrae was rotating, the whole object was moving in an arc of a circle, which had its center in p_1, as seen in *Figure 1*. (The legend of this Figure is the same as for *Figure 9*, as was explained in the preceding pages.)

In *Figure 8* there are shown some changes of umbra areas within the sunspot groups of 202 and 204.

Sunspot groups 203 and 208 as well as 207 of 1969 all can be considered as "classical" types of normal bipolar groups. First we should like to note, by way of illustration, some rapid variations that often take place in such a type of groups.

The spot *2x* of group 203 (see in *Figure 3)* which was prominent on June 7, we could not recognize next day. Close to its place another spot *2* appeared and moved toward spot *1* on June 10 (as shown in *Figure 4*). They were already embedded in common penumbra on June 11. Analogous case happened in group 208 (compare *Figures 5* and *6*). The spot denoted by *1x* of this group was first observed on June 7, but we were unable to identify it on the following day. Spot *1a* of group 208 also moved toward the large penumbra of spot *1* from the 10th of June and on June 13 already was inside it.

Group 203 still consisted essentially of a tiny *p* spot on June 5, but developed rapidly the following days and after June 9 already began to decay. Group 208, when rotated onto the solar disc on June 5, already showed a fast development that lasted also until June 9. In both cases their main *p* and *f* spot (i.e. spots *1* and *a*) had a large divergent motion. This motion lasted twice as long, more than two days, for group 208 than for group 203. We should call attention to the fact that the area maximum of group 208 became about 50 % higher than that of 203, and group 208 also displayed the longer lasting high speed motion. Comparing the movements in longitude (*L*) of the main *p* spots of groups 203 and 208 with the internal motions of the spots in these groups, i.e. comparing *Figure 10* with *Figures 4* and *6* we find that the high speed with respect to the Carrington coordinates occur simultaneously with great mobilities within the group.

The same holds true regarding the group 207, too, (see Fig.3, p.80 in (2)). The total area of this group was only about 20 % larger than that of the resembling group 208 on the east solar limb on June 5. Eight days later group 207 attained its maximal size, when the total maximal area of group 208 decreased nearly by half. Then the areal ratio of the groups was cca.5. This proportion as well as both total areas remained roughly constant till the groups disappeared at the limb. We note in addition that group 207 (=239) at reappearence after a fortnight, while the area of its main *p* spot grow less by cca. 50 %, became similar to group 209, indicating even certain rotation.

Concerning the moving of the main *p* spots of the groups 207 and 208, a very interesting thing can be seen in *Figure 9*: these two groups of similar type revealed a strikingly high symmetry to the solar equator. Both the positions and the curves of motion show this symmetric feature. On the northern solar hemisphere the principal change of direction of motion was clockwise, but anticlockwise on the southern hemisphere. After a period of fast moving the abrupt turn followed opposite courses on the two hemispheres, the directions of deflection took place if as they were due to Coriolis force. The sweep of the path of group 203 is also in accordance with this observation.

In contrast with the particularly rotational internal motions of the decaying sunspot groups 202, 204 and 209 of 1969, described above, the others of the same year, groups 203 and 208 as well as 207 and the ones of 1967 and 1968, under discussion, reveal quite different types of internal motion. It can hardly be doubted that this dissimilarity is due to differences in the stage of evolution; namely, the groups showing no prominent rotations were still in a strong development phase, at least over several days, during our observational period.

Sunspot groups 250 of 1967 and 265 & 268 of 1968 are objects of more complex types than the ones discussed in the preceding pages.

Group 250 of 1967, when first seen on the sun's disc, near its east limb on July 22, was already a well developed "classical" bipolar group, but next day very close to it fresh spot activity arose. The new formation we may take for a new, separate sunspot group which merged into the old group. This is made clear by the pictures in *Figure 11* and the pattern of motion illustrated in *Figure 12*. The principal old Part I of group 250 consisted of spots *1*, *1a*, *5* and *a*, while the spots *2*, *3*, *4*, *b*, *c*, *d* and *g* formed mainly the young Part II. The *p* and *f* spots of Part II showed intense divergent motions, a well known characteristic of the sunspot groups in their initial phase of development. Here this behaviour lasted for a long time,since we could observe high velocities even on July 27. (See *TABLE 2.)* The Parts I and II in question, i.e. the "two" fused sunspot groups, evidently disturbed each other and, we think, in consequence this particularity advanced the great flare activity observed within the groups.

Regarding the sunspot groups 265 and 268 of 1968, (using the denotation of the *Soln. Dannye)*, first we mention in advance that these objects in our opinion should be taken for three separate groups. The three groups, as seen in *Figures 13* and *14*, are as follows: the first (I) consists of spots *1*,(p_1 of group 265), *1a, 1b, 1c, 1d, 2, 3, 4, a, b, c, d* and probably also the *g;* the second (II) is composed of spots *5, e, h* and *i;* while spots *6, 7, 8, j* and *k* belong to a third (III) group. It seems that for the high flare activity in the group II the other groups I and III can be held responsible. Namely the *f* part of group I was very near to the western part of group II and this fact could have brought about the large spot of group II in which umbrae of opposite magnetic polarity (*e, h, i* and *5*) were embedded in a common penumbra, when group II was first observed on the east solar limb on July 7. Spots *i* and *h* separated after two and three days, respectively. Later we observed spot *i* and spot *6* of group III within a common penumbra for more than 24 hours, from July 10 to 11.

The areal change of some important umbrae of these groups are given in *Figure 16*. Group III did not develop "regularly", probably because of the vicinity of group II. Group I rotated onto the sun's disc on July 6, it did not show significant further development during its disc passage, it began rather disintegrate also proved by the striking rotation of spot *2* around spot *1*, to be seen at a glance in *Figure 13*.

* * *

From the foregoing it is clear that certain characteristic features of sunspot motions are already recognizable. It appears even from the brief discussions that there is close connection between motion and areal development of sunspots. On the other hand we could find no trace of any direct evidence of relationship between the rapidly moving sunspots and the major flares, listed in *TABLE 3*, notwithstanding that there was quite high flare activity in the periods investigated.

R e f e r e n c e s

(1) Dezső,L., Gyertyános,Gy., Kálmán,B., Kovács,Á.: 1971, *Soln. Dannye No.*7, *77.*

(2) *Magnitnye Polya Solnech Pyaten* (Suppl. to *Soln. Dannye).*

(3) *Monthly Bulletin (Solar Phenomena) Oss. Astron. Roma.*

(4) *Greenwich Photoheliographic Results*, 1924, p.*D20* (1926).

TABLE 1

The period (and the number) of observations of the sunspot group 250 of 1967

	UT	
July	26,34 - 26,54	(28)
	27,33 - 27,39	(9)
	41 - 47	(9)
	48 - 54	(8)
	28,33 - 28,40	(11)
	41 - 47	(9)
	49 - 54	(9)

TABLE 2

Some average velocities (v) in the sunspot group 250 of 1967

Spot	*v* km/s	*Spot*	*v* km/s
a	0,02	c	0,2
b	0,05	d	0,3
e	0,1	g	0,5
		3	0,3
from July 26 to July 27		4	0,4
		on July 27	

TABLE 3

Major H-alpha flares in the sunspot groups studied according to *IAU Bulletin on Solar Activity* moments of the maxima of flares of importance ≥ 2. ≥

1967	UT	GROUP 250	
VII.22	12:25	2N	
24	20:20	2B	
25	04:00	2F	
	10:24	2F	
30	6:20	2B	
VIII. 1	17:38	2B	

1968	UT	GROUP II
VII.6	7:20	2B
8	17:15	3B
9	18:17	2B
12	00:09	2N

1969	UT	GROUPS 202	203	207	208
VI.5	10:01				2B
	14:55	3B			
6	6:36			2N	
	7:42				2N
	9:56			2N	
	16:07		2B		
11	16:27				2B
14	21:08			2B	

117

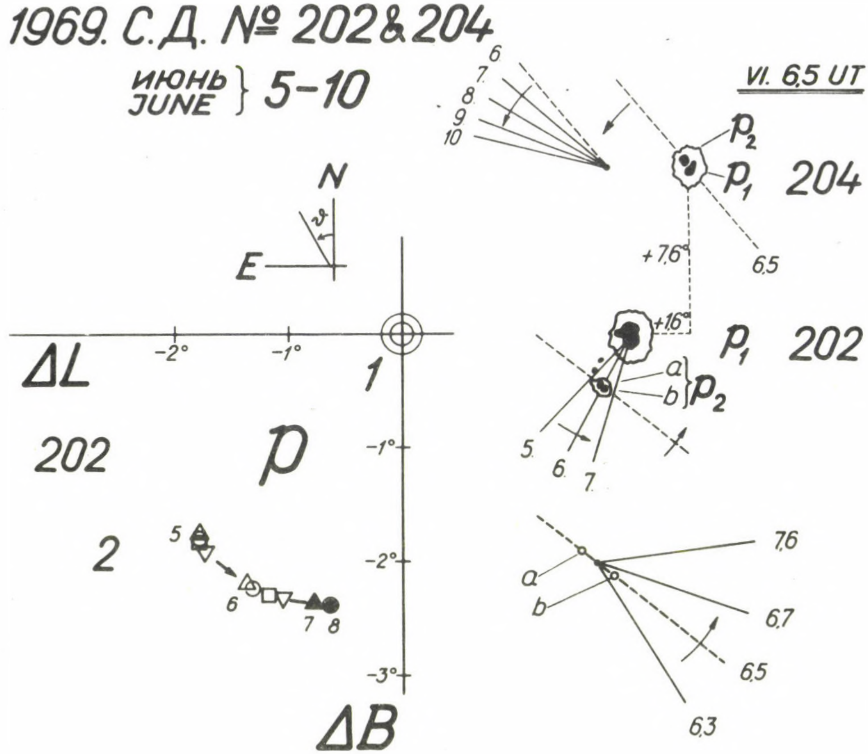

Figure 1. Rotation-like movements in (two near-by) old, shrinking sunspot groups.

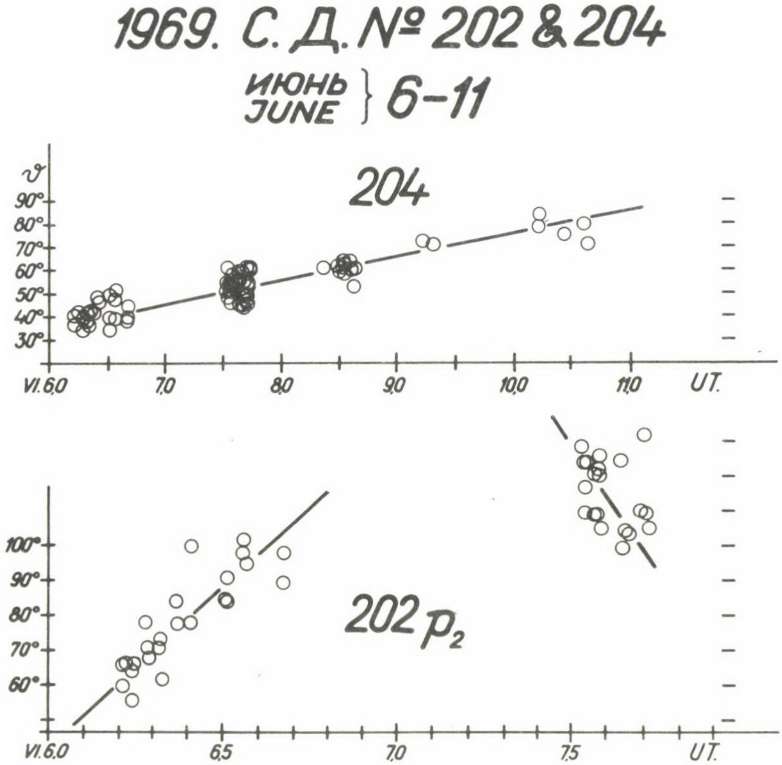

Figure 2. *Data of position angle measurements of the $p_1 - p_2$ line of sunspot group 204 and the $a - b$ line of spot p_2 of group 202, respectively. (Compare Figure 1)*

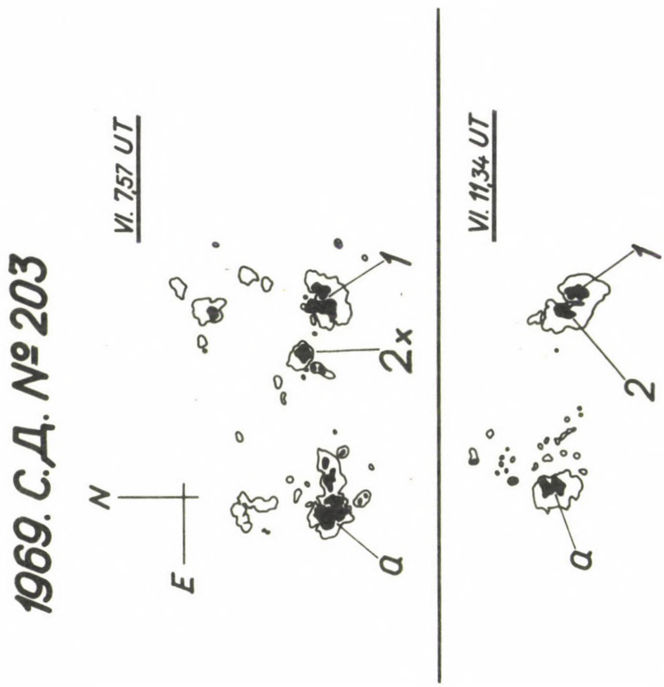

Figure 3.

Figure 4. The course of motion of spot a and 2 with respect to spot 1. (Compare Figure 3.)

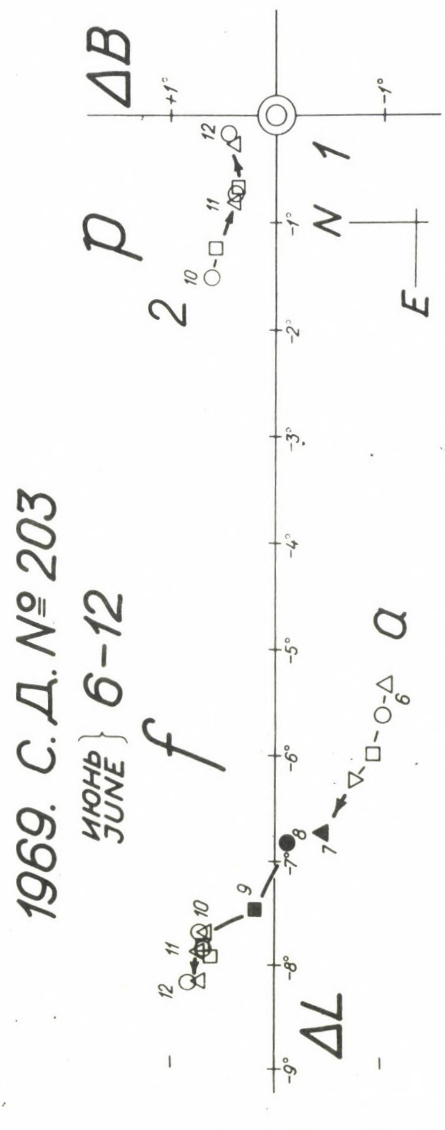

Figure 4.

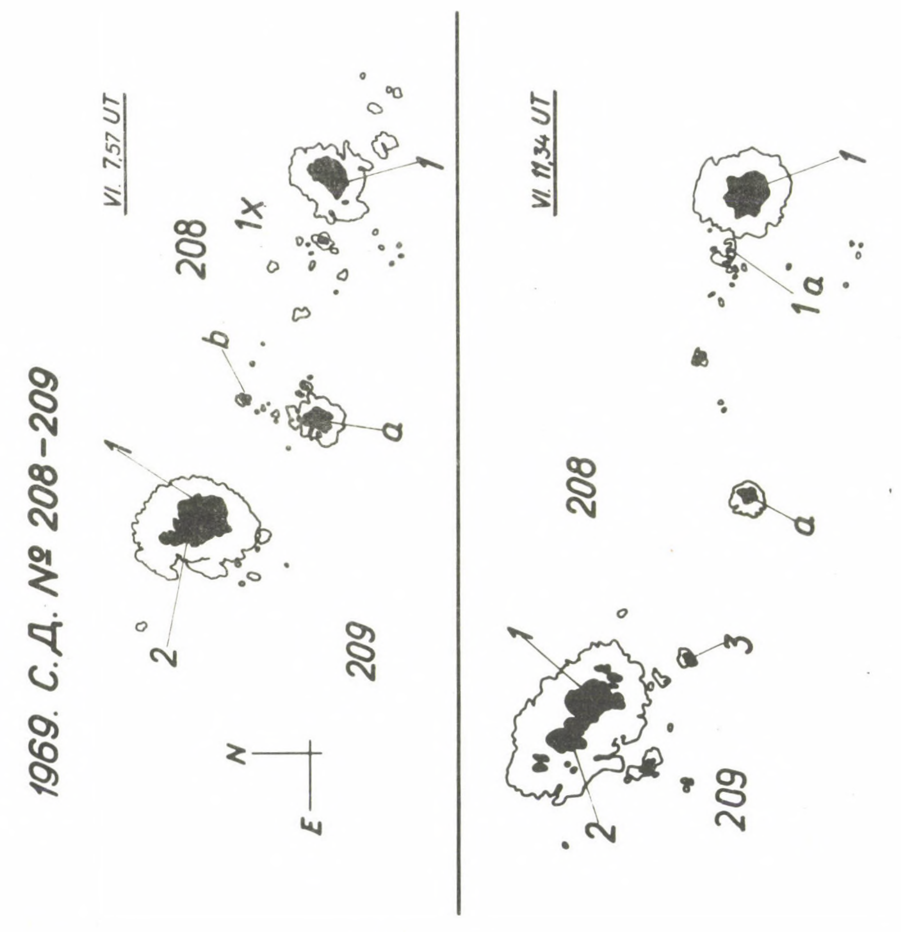

Figure 5..

Figure 6. The course of motion of spots *a*, *b* and *1a* with respect to spot *1*.
(Compare *Figure 5.*)

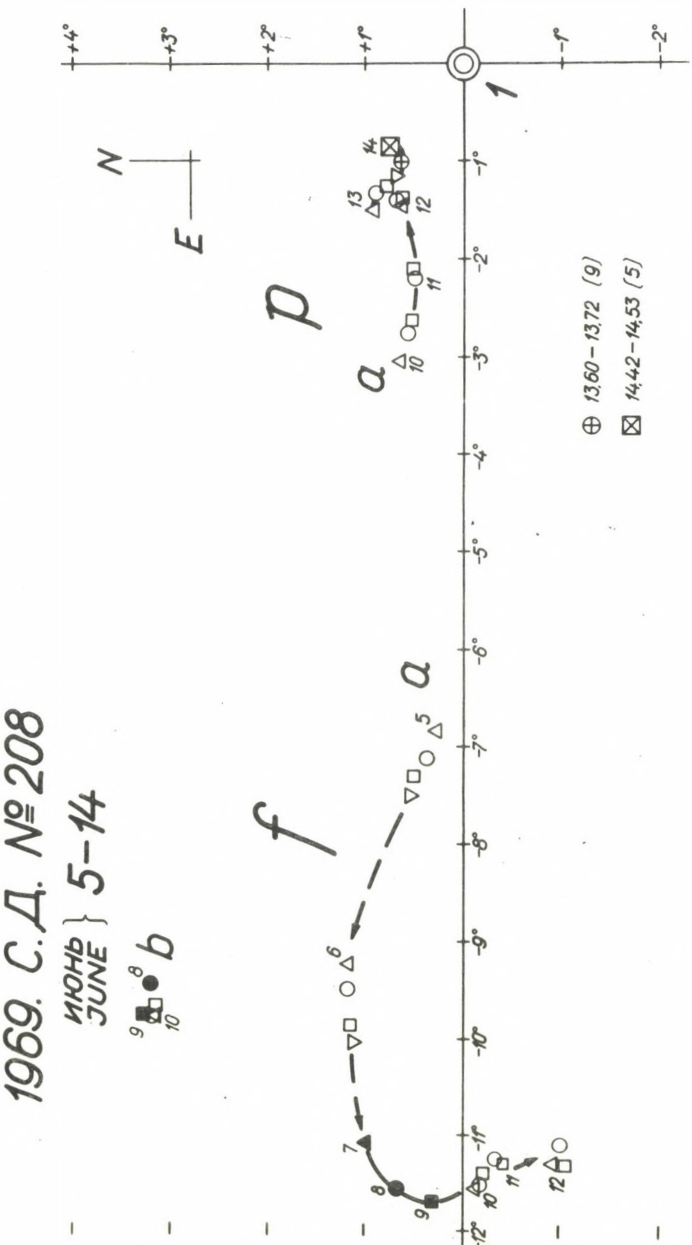

1969. С.Д. № 208
ИЮНЬ JUNE } 5–14
N
E
p
f
a
a
b
⊕ 13,60 – 13,72 (9)
⊠ 14,42 – 14,53 (5)
+4°
+3°
+2°
+1°
-1°
-2°
-3°
-4°
-5°
-6°
-7°
-8°
-9°
-10°
-11°
-12°

Figure 6.

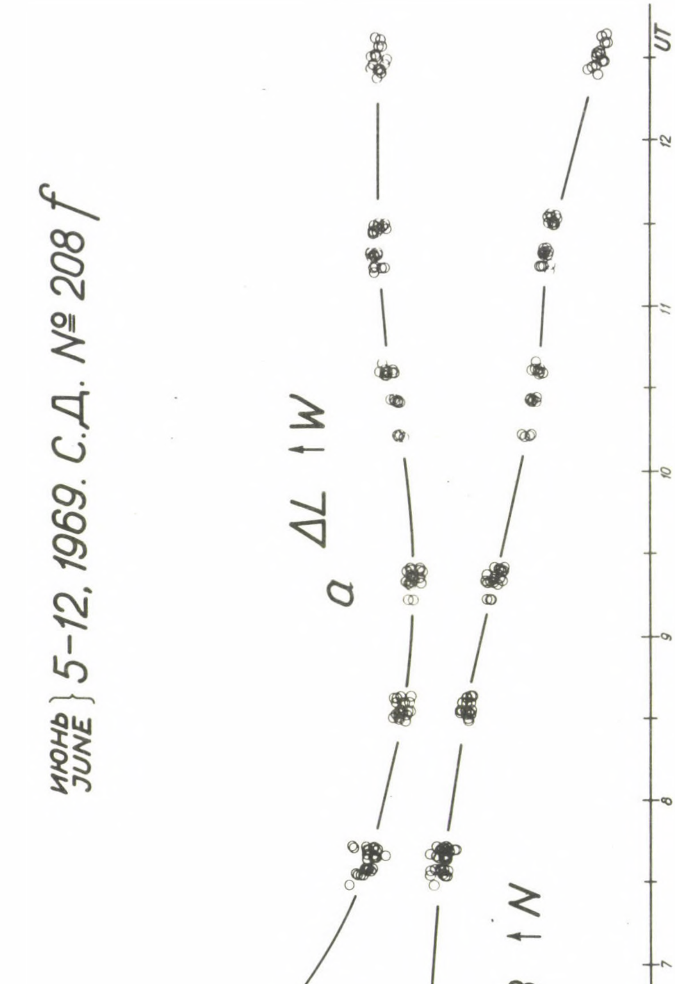

Figure 7.

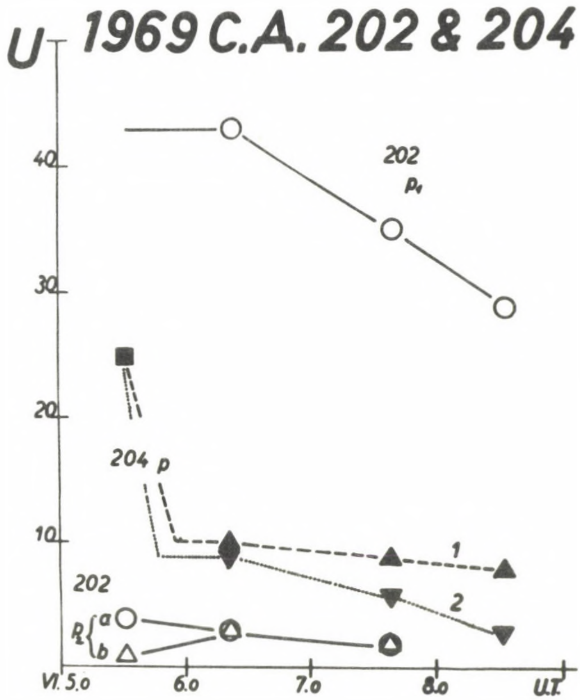

Figure 8. *Changes in some umbral areas (in millionth of the solar hemisphere). (Compare Figure 1.)*

Figure 7. *Data of measurements concerning the change in longitude and latitude of the main f spot a of sunspot group 208. (Compare Figure 5.)*

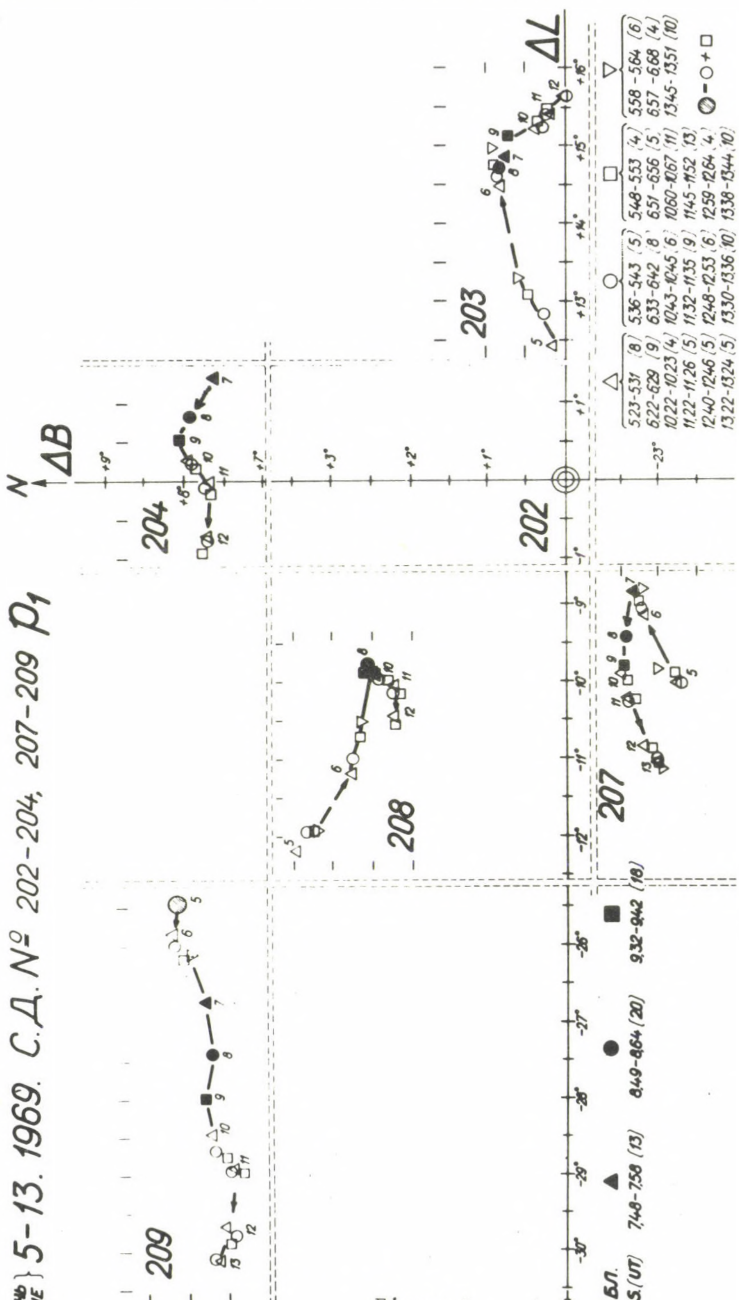
ИЮНЬ
JUNE
5-13. 1969. С.Д. № 202-204, 207-209 p1
N
ΔB
ΔL
E
НАБЛ.
OBS.(UT)
209
208
207
204
203
202

Figure 9.

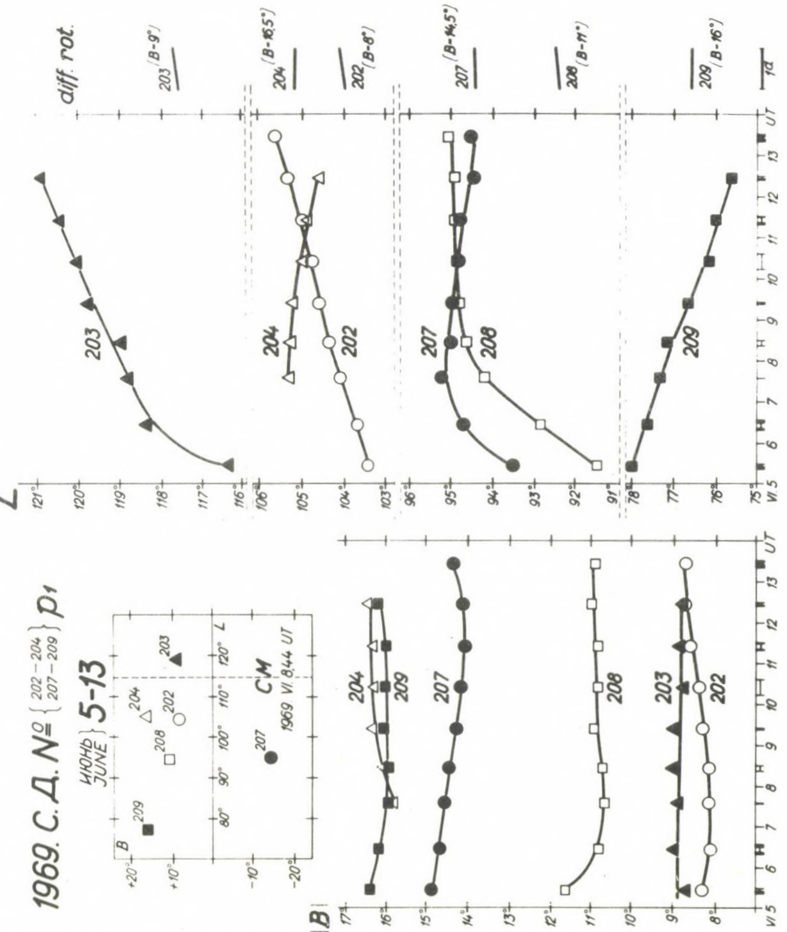

Figure 10. The changes in Carrington coordinates of the main p spots of six sunspot groups.

Figure 9. The course of motion of the main p spot of five sunspot groups with respect to the sixth p spot.

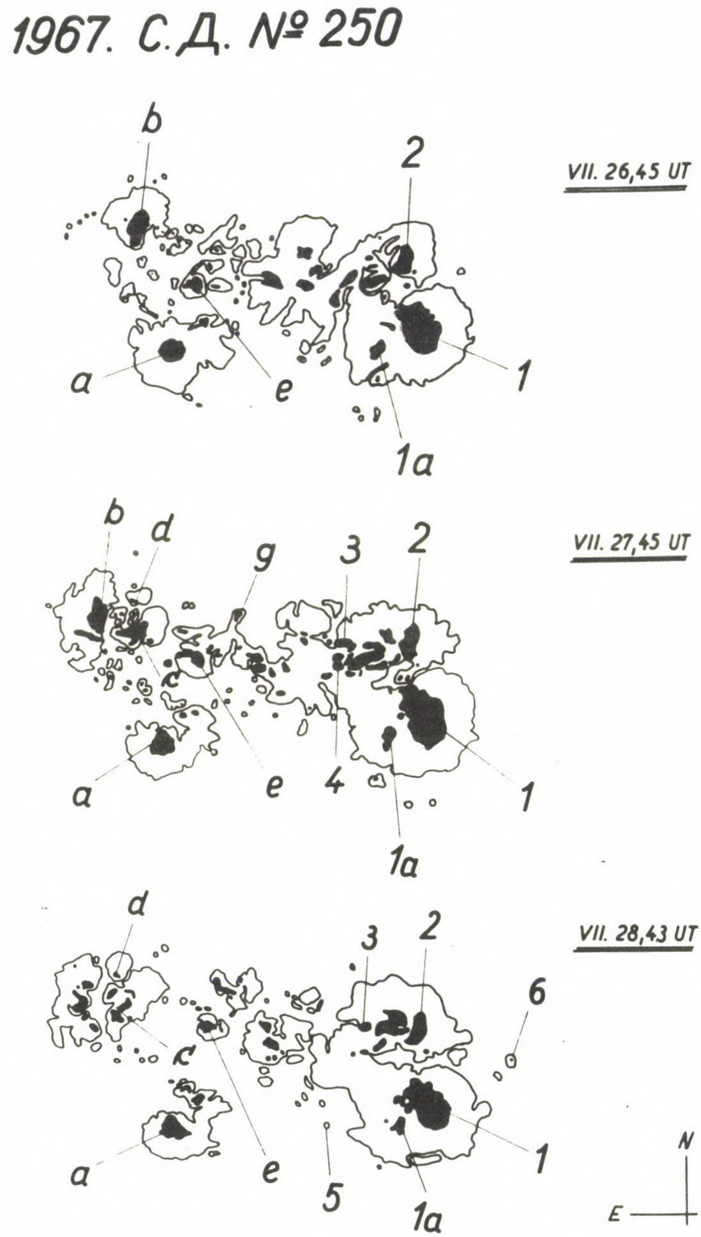
1967. С.Д. № 250
b
2
VII. 26,45 UT
a
e
1
1a
b
d
g
3
2
VII. 27,45 UT
c
a
e
4
1
1a
d
3
2
VII. 28,43 UT
6
c
a
e
5
1
1a
N
E

Figure 11.

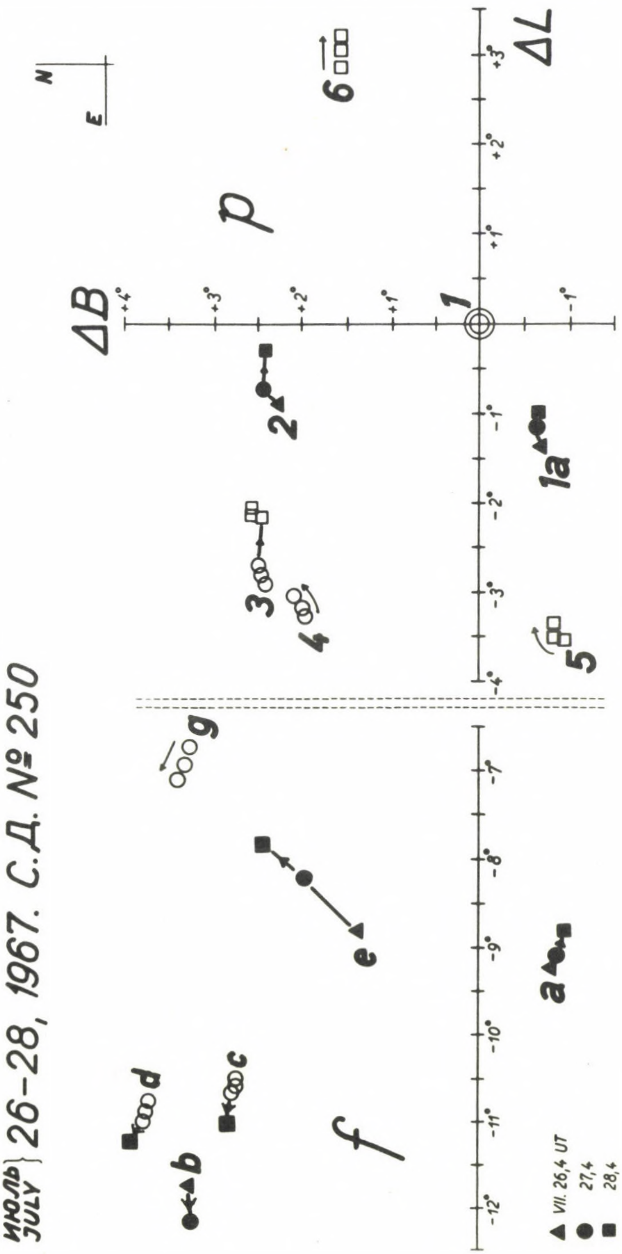

Figure 12. *The course of motion of important spots in a complex sunspot group with respect to spot p .*
(Compare Figure 11.)

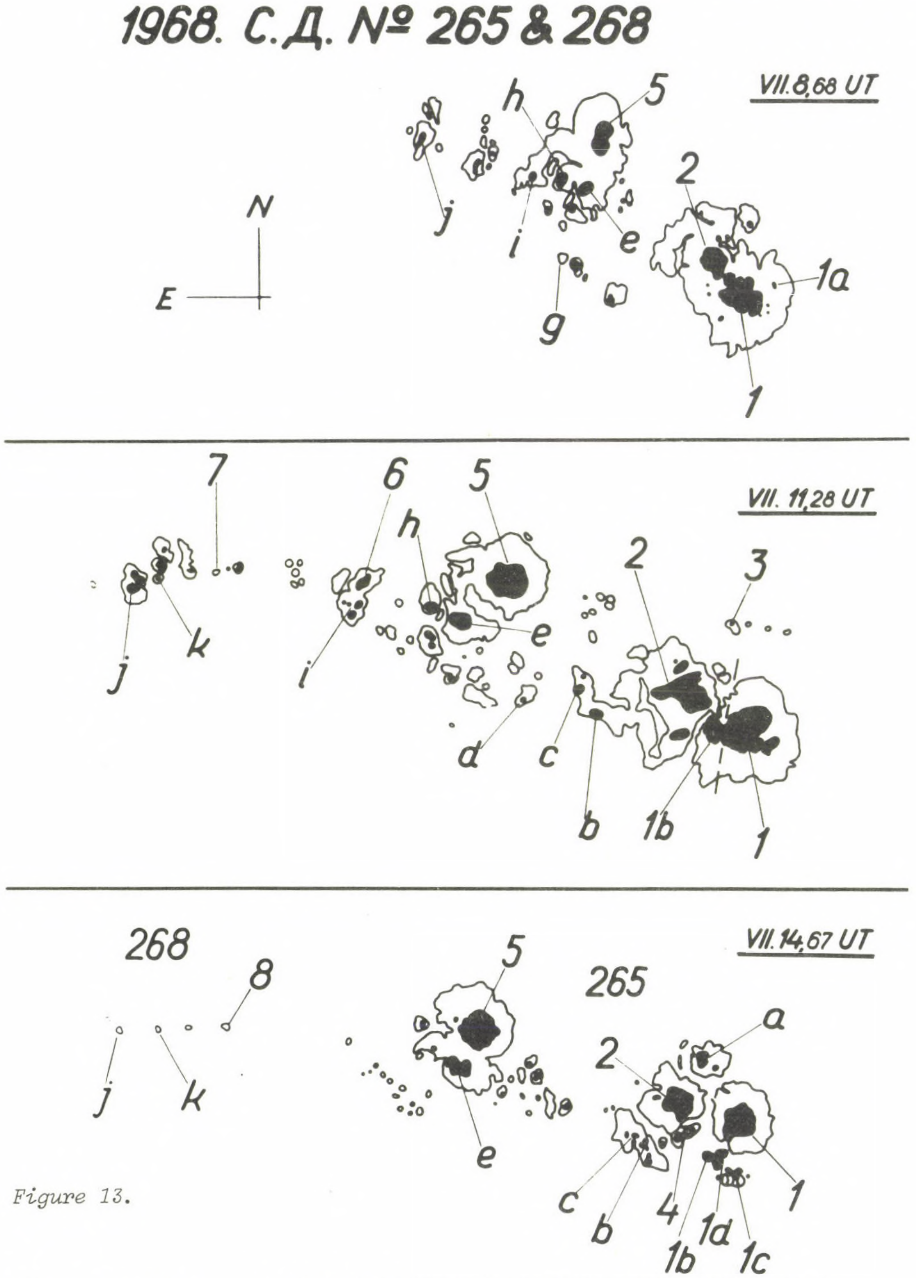

Figure 13.

Figure 14. *The course of spot motions in a large active region with respect to the largest p spot.*
(Compare Figure 13 and 16.)

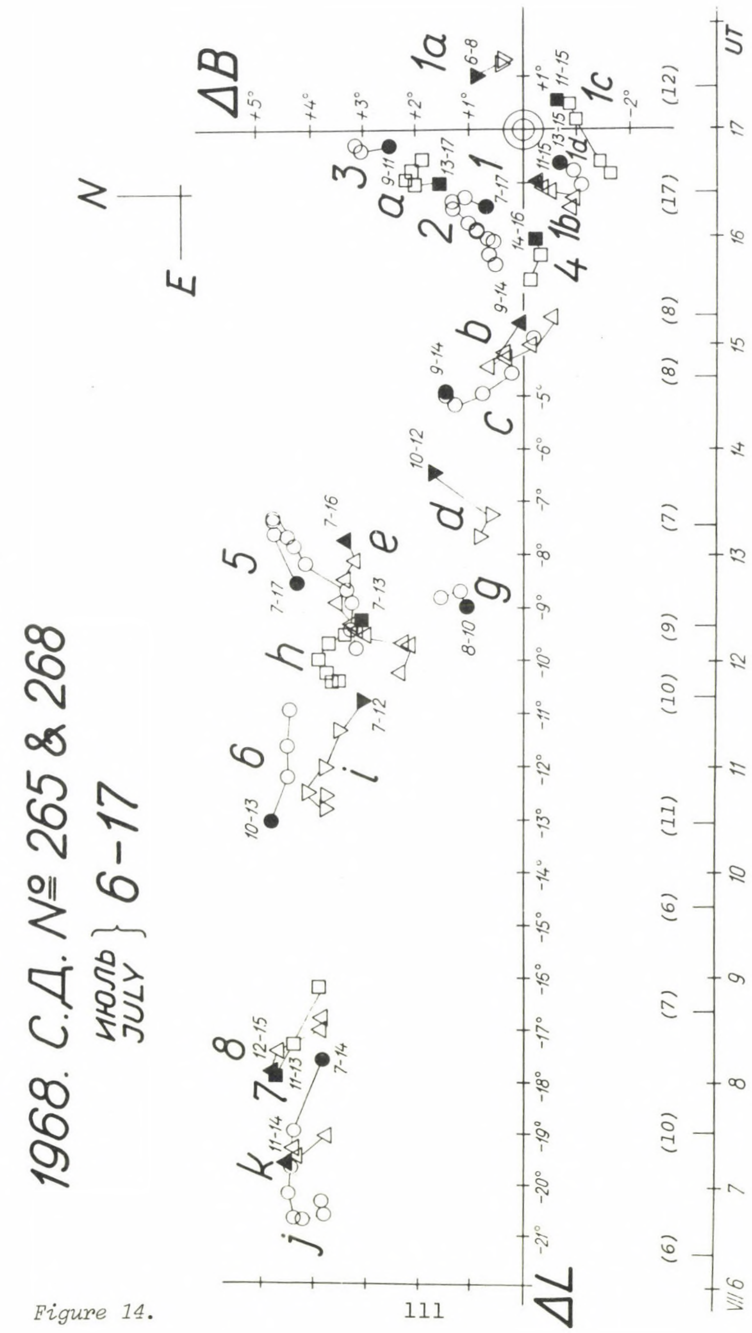

Figure 14.

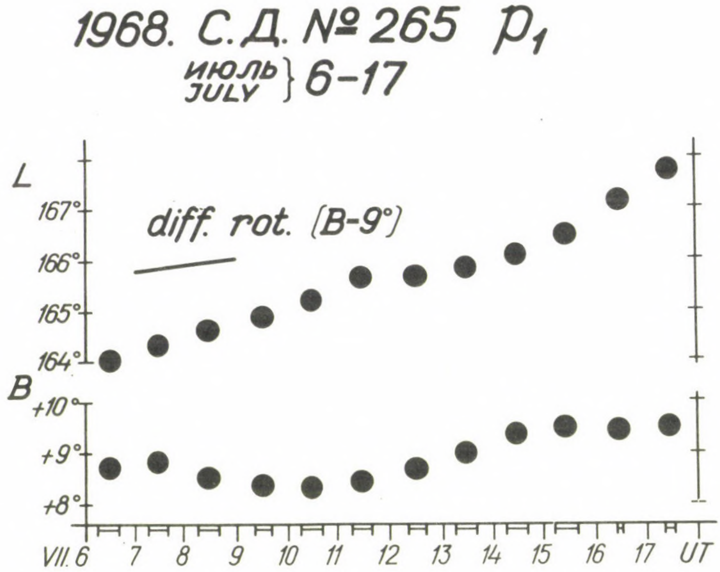

Figure 15. The changes in Carrington coordinates.

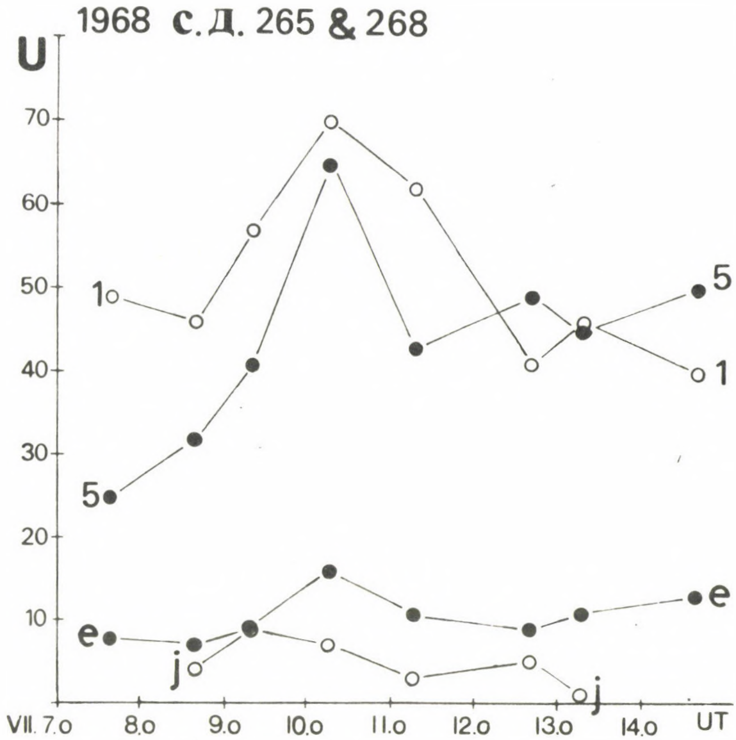

Figure 16. *Changes in some umbral areas (in millionth of the solar hemisphere). (Compare Figure 13.)*

PUBLICATIONS OF DEBRECEN HELIOPHYSICAL OBSERVATORY
Vol. 2 No. 5 1971

THE PARTICLE EMITTING FLARES IN RELATION TO THE PHOTOSPHERIC MAGNETIC FIELDS AND CORONA STRUCTURES

J. SÝKORA

Astronomical Institute of the Slovak Academy
of Sciences, Skalnaté Pleso, Tatranská Lomnica

Abstract:

Atlas of Solar Magnetic Fields 1959-66, the Synoptic Tables of the Green Corona 1947-70 and the List of Type IV Bursts Connected with the Cosmic Ray Increase or PCA Events have been used to study the localization of the large flares in relation to the "supergiant" structures formed by the photospheric magnetic field and by the green corona intensity.

Drop-shaped "supergiant" magnetic field and corona structures are demonstrated. The greatest activity, including the positions of the large flares, is located at the boundary between a head and a tail of the drop--shaped features.

1. Introduction

In our short note we would like to speak about the localization of particle emitting flares, which seem to be in relation to the distribution of some large-scale photospheric magnetic field structures, regarding the emission corona features. This work was stimulated by two facts:

a) During recent years there have been many works demonstrating certain regularities in development and distribution of the photospheric magnetic fields (e.g. Bumba and Howard, 1965a, b; Bumba, 1970a, b; Ambrož et al., 1970) and the large-scale sector structure of interplanetary magnetic field (e.g. Wilcox, 1968; Wilcox and Colburn, 1969). Corona is an intermediate layer between the photosphere and the interplanetary space and therefore it should reflect their, above all, large structural properties (Newkirk, 1967).

b) The study of the localization of the large flares with regard to the regular structure on the solar surface seems to be one of the most hopeful ways for their prediction. Importance of such predictions is still increasing, namely in connection with manned cosmic flights.

We used the following observational data: Atlas of Solar Magnetic Fields 1959-66 (Howard et. al., 1967), Synoptic Tables of the Green Corona 1947-70 (Sýkora, 1970) and List of Type IV Bursts Connected with the Cosmic Ray Increase or PCA Events (Švestka and Olmr, 1966). The interval studied here (1959-1963) was limited by the quality of the magnetic charts, but mainly by the necessary level of solar activity in the 11 - year cycle.

2. Correlation between particle emitting flare positions and "supergiant" features of the green corona

In *Fig. 1* we want to demonstrate what we call the large--scale features. The separated polarities from the magnetic synoptic chart for rotation No. 1428 are shown here. Both polarities (negative - above, positive - below) form drop--shaped features with a head and a tail. The lengths of these drops often exceed 100° in longitude and these features are a result of a long-lasting evolution which usually takes several rotations. These features were found by Dr. Bumba, who spoke about them in detail in his lecture. According to him in a previous cycle (No.19) this structure was better presented by negative polarity which was following one on the northern, more active solar hemisphere. To make the forms of the drop-shaped features more outstanding it is often useful to use a technique of the overlapping of 2 - 3 synoptic charts. In the case of corona we also applied such a method.

Altogether 21 active regions with particle emitting flares were studied. For each active center the synoptic coronal chart ±120° from the flare position was constructed. The coronal data of different corona stations were transformed to a common photometric scale by the method described in Sýkora (1971a, b).

The results are as follows:

1) 14 cases show the drop-shaped structure which is in form and dimension similar to that of the magnetic field. An example is demonstrated in *Fig. 2.* Arrangement of the coronal activity agrees in some cases better with a main body of negative polarity, in other cases with the body of positive polarity. At the same time, as we can imagine from *Fig. 1,* the magnetic drop-shaped features for opposite polarities overlap one another and make a complex magnetic situation which seems to be decisive in the production of particle emitting flares (Bumba et al., 1972).

2) In three cases out of the total number of 21, the coronal body is not realized in spite of the magnetic field showing it very well (see *Fig. 3*). From the face of the magnetic chart (the lowest part of *Fig. 3*) we suppose that this fact is connected with magnetically old and young regions. The lowest isophote visualized in our coronal maps (the central part of *Fig. 3*) is 100 abs. coronal units. Such intensity is characteristic for intermediately active regions. In the case of the old regions (which in this case form the drop-shaped body) the brightness of emission corona does not reach this level and that is why our maps do not reflect these regions.

3) Four cases neither form drop-shaped structure nor they can be explained by the presence of the old fields. It means they are negative in our analysis.

u

4) From the analysis we have made unambiguously it follows that maxima of the emission corona brightness are located above the boundaries of the opposite polarities of the magnetic field, i.e. above the regions with the largest field gradients.

5) *Figs 2* and *3* also demonstrate the main result of this short note. Namely, they present the physical meaning of the drop-shaped features by showing that the particle emitting flares (marked by black points) usually occur in the neighbourhood of the boundary between the main body and the tail of the drop-shaped formation, often in places with relatively low coronal activity. From this fact follows a certain possibility of predicting with some probability occurrence of the large flares.

R e f e r e n c e s

Ambrož,P., Bumba,V., Howard,R., Sýkora,J.: 1970, in R.Howard (ed.) *IAU Symposium No.* 43, *696*.

Bumba,V.: 1970a, *Solar Phys.* 11, *111*.

Bumba,V.: 1970b, *Astrophys. Space Sci. Library* Vol.29, *Part I. 21*.

Bumba,V., Howard,R.: 1965a, *Astrophys. J.* 141, *1492*.

Bumba,V., Howard,R.: 1965b, *Astrophys. J.* 141, *1502*.

Bumba,V., Křivský,L., Sýkora,J.: 1972, *Bull. Astr. Inst. Czech.* 23, *85*.

Howard,R., Bumba,V., Smith,S.F.: 1967, *Carnegie Inst. of Washington Publ. No.* 626.

Newkirk,G.: 1967, *Ann. Rev. Astr. Astrophys.* 5, *213*.

Sýkora,J.: 1970, *unpublished.*

Sýkora,J.: 1971a, *Bull. Astr. Inst. Czech.* 22, *12*.

Sýkora,J.: 1971b, *Solar Phys.* 18, *72*.

Švestka,Ž., Olmr,J.: 1966, *Bull. Astr. Inst. Czech.* 17, *4*.

Wilcox,J.M.: 1968, *Space Sci. Rev.* 8, *258*.

Wilcox,J.M., Colburn, D.S.: 1969, *J. Geophys. Res.* 70, *5793*.

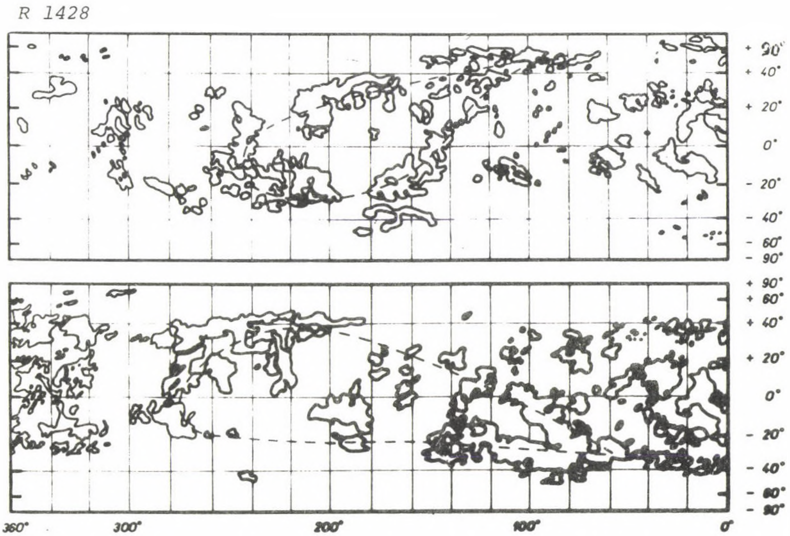

Figure 1. The drop-shaped structure of the photospheric magnetic field on synoptic chart rot.No. 1428. Negative polarity - above, positive polarity - below.

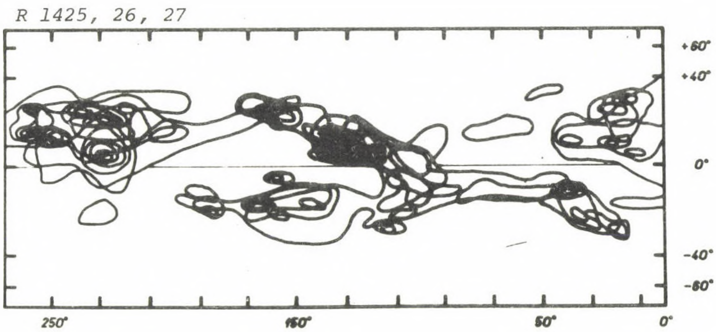

Figure 2. The coronal synoptic chart composed from the synoptic charts for rotations No. 1425, 1426, 1427. The lowest visualized izophote is 100 abs.coronal units. The positions of the particle emitting flares are marked by the black points.

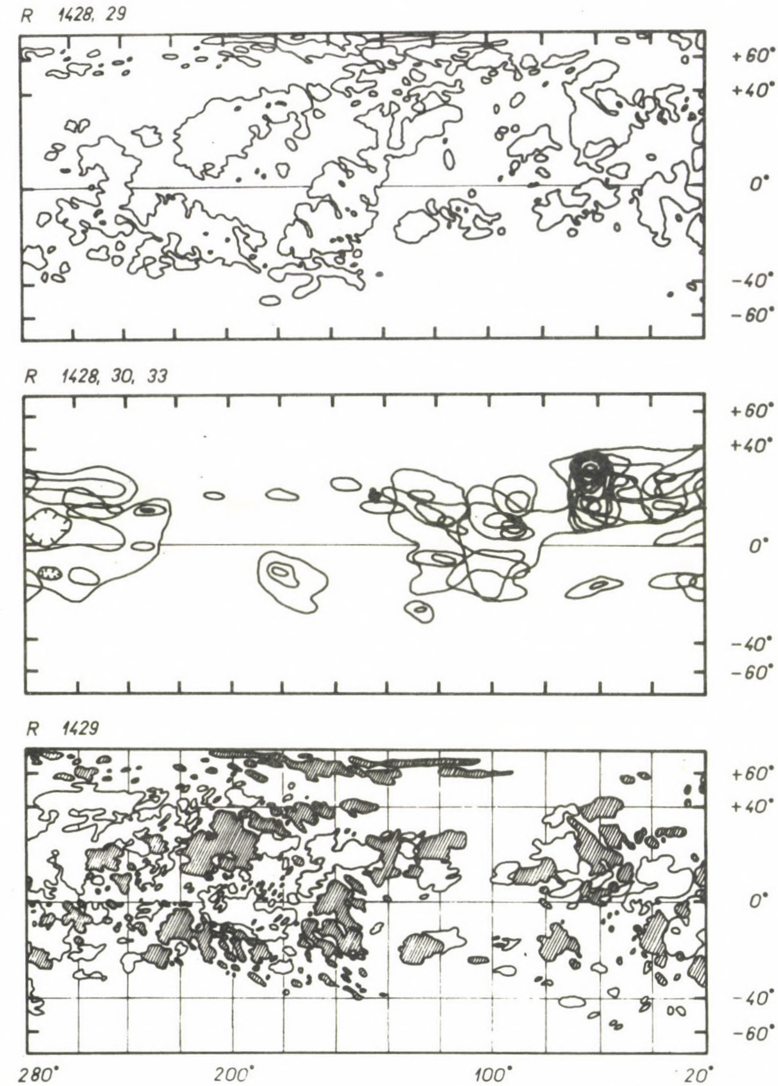

Figure 3. *The negative magnetic polarity synoptic chart (above) shows clearly the drop-shaped structure. In the center the coronal synoptic chart, composed from the charts No. 1428, 1430 and 1433 is demonstrated. There is no drop-shaped structure. The lowest part of this figure shows the magnetic synoptic chart for rotation No. 1429 indicating the old fields in longitudes where the drop is located.*

PUBLICATIONS OF DEBRECEN HELIOPHYSICAL OBSERVATORY
Vol.2 No.6 1971

ON THE RELATION BETWEEN THE SPECTRUM OF THE S-COMPONENT OF RADIO EMISSION AND THE FREQUENCY OF PROTON FLARES

A. K R Ü G E R
Central Institute for Solar-Terrestrial Physics, GDR Acad.Sci., Berlin

As first mentioned by Tanaka and Kakinuma (1964) there is a certain correlation between the spectrum of the S-component of solar radio emission near 3 cm wavelength and the probability of an active region producing energetic events (type IV radio bursts, proton flares). This relationship has been reconsidered with regard to new ground-based and satellite solar observations and a possible theoretical interpretation.

1. Physical properties of the S-component

Parameters used hitherto for a connection with burst activity are flux ratios of the S-component at different observing frequencies ($S_{9400} : S_{3750}$; $S_{9400} : S_{1500}$) which are expected to be roughly proportional to $N_e \cdot f(T)$ so far as thermal models are concerned. For non-thermal models a certain amount of superthermal radiation would influence the flux at short cm-wavelengths. As the indicator for the magnetic field strength inside the source region the frequency of the spectral maximum of the S-component ν_{max} is expected.

For comparison the flux of the slowly varying soft X-ray emission is proportional to $N_e^2 f(T,\nu,..)$.

2. Statistical results

Correlation coefficients calculated half-yearly for the period 1966-69 between different solar parameters with the frequency of type IV bursts and proton flares give the following main results:

a) The correlation is best ($r \approx 0.25 \pm 0.05$) for both the radio emission at 3 cm and X-ray emission in the 0-8 A band;

b) The correlation is not always significant for sunspot numbers and ν_{max}.

3. Discussion

The dominating influence of the short wave radio spectrum over the frequency of the spectral maximum leads to the conclusion that the average magnitudes of magnetic fields inside active regions are not the main point for a connection with a production of energetic events. This is also supported by the same degree of correlation with the X-ray emission which is not directly controlled by the magnetic field. It cannot be excluded that a certain variable amount of nonthermal energy is reflecting both the change of the shortwave S-component spectrum and the probability of producing instabilities leading to flare-burst events.

R e f e r e n c e

Tanaka,H., Kakinuma,T.: 1964, *Report Ionosph. Space Res. Japan* 18, *32-44*.

PUBLICATIONS OF DEBRECEN HELIOPHYSICAL OBSERVATORY
Vol.2 No.7 1971

ON SOME PROBLEMS RELATED TO THE G.L.E. OF FEBRUARY 25, 1969

T. FORTINI, M. TORELLI

Osservatorio Astronomico di Roma

Abstract:

1) The G.L.E. of February 25, 1969 was localized close to the main spot of a narrow island of strong north magnetic polarity embedded in a region of southern polarities. The configuration was determined by the interaction of a preexisting south polarity spot with new fields born on its western side after February 22.

2) The cross-section of the flare parallel to the solar surface appears rather modest. The extended brightening of the flare is rather due to large loops seen in projection toward the solar disk.

3) The radio emission exceptionally intense in the dm range has not given to the radio spectrum the characteristic deep U-shape of other proton events.

1. Introduction

1968 has been rather rich in corpuscular events widely spread in longitude and latitude on the solar surface. The flare of February 25, 1969 started a long period of particle events almost all localized on the same place of the solar surface. For many rotations until the end of the year the activity was concentrated in two almost 180° separated longitudes. This particular period should be examined in detail in the light of recent studies on the solar activity (Bumba, 1971; Ambrož, 1971). In this discussion,however, we confine our attention to the short term elaboration of the event of February 25, 1969 and to its description.

On February 16 a large supercomplex embracing almost 120° in longitude in the northern hemisphere appeared on the east limb. For many days the Fraunhofer maps showed a rather enhanced coronal emission. However, before February 22 the polarities of the spots in the whole supercomplex were quite regularly distributed (*Fig.1.*).

The production of the flares was not efficient before February 22; on this day new fields of both polarities began to emerge around the western spot (indicated by an arrow on *Fig.1*) of the main active center of the complex,particularly on its western side. This phase marked an increase in the number of flares, many of them localized at the coordinates of the flare of February 25. The interval February 22 - February 25 should be considered the time of elaboration of the G.L.E. of February 25.

On February 24 the magnetic fields of the main spot were already complicatedly intermixed. However the north magnetic polarities in the spot were limited between two filaments (A and B in *Fig. 2*) in a still quite open configuration. Our H-alpha and white light pictures of the morning, compared with the observations at later times obtained in the western earth hemisphere (çourtesy of P. Mc Intosh, Boulder) do not show substantial changes for many hours. The situation changed in the early hours of February 25, probably after a 2B flare on February 24 at $23^{h}06^{m}$ U.T. The angle in between the two filaments is narrowed and the north polarities are now contained in a narrow isle in the spot.

2. The G.L.E. of February 25

From our optical and the Heinrich Hertz radio records (courtesy of A.Krüger, Berlin) the event may be divided in two main phases (*Fig. 2*). In this preliminary research we have concentrated our attention on the first phase.

The first brightening paralleled by a soft enhancement in the radio flux patterns a preexisting thread-plage between and around spots all of south polarity. At 9^h05^m U.T. a bright point lights beside the north polarity spot, but beyond the inversion line in the south polarity part of the configuration (point X_1 in *Fig.2*). The lightening of a second zone (point X_2) close to the spot on the northern magnetic site marks the decisive phase of the flare with a rapid increase of the mm and cm flux. The increase is so steep that we attribute to this moment the blasting of the electromagnetic and possibly corpuscular radiation. The optical configuration is rather unusual (Křivský, Švestka, 1970). We do not have the two classical rows of spots of opposite polarities; the flare after the brightening of the points X_1 and X_2 is developing in the high chromosphere and low corona and what we observe is only its projection against the disc.

It is well known that the event has been very impulsive from the point of view of particle acceleration (Manno, Page 1970; Datlowe, 1971) on the other hand the P.C.A. was not outstanding, only 2 decibels. This event should confirm the interpration of Švestka (1970) that "the size of the volume where the acceleration takes place determines the number of the accelerated particles and the entity of the P.C.A.". We believe that in this case the volume of the shotting particles was modest, close to the points X_1 and X_2 (*Fig.2*). On the other hand the north polarity was narrowly embedded and it has probably strenghtened the acceleration process producing particles of high energy.

The radio emission was very peculiar, but we have not examined in detail the radio records. The fundamental points are: 1/ the spectrum at the maximum emission did not present the characteristic U-shape of particle events (Castelli, Aarons, 1967) because of a rather unusual emission in the decimetric range; 2/ the lack of type II burst.

References

Ambrož,P.: 1971, *this Volume.*

Bumba,V.: 1971, *this Volume.*

Castelli,J.P., Aaarons,M.: *J. Geophys. Res.* 72, *5491.*

Datlowe,D.: 1971, *Solar Phys.* 17,*436.*

Krivský,L., Švestka,Z.: 1971, *Space Research* X,*817.*

Manno,V., Page,D.E., (eds.) 1970, *Astrophys. and Space Sci.Library* Vol. 19, *Part VII.*

Švestka,Ž.: 1971, *Astrophys. and Space Sci. Library* Vol.29,*Part I,72.*

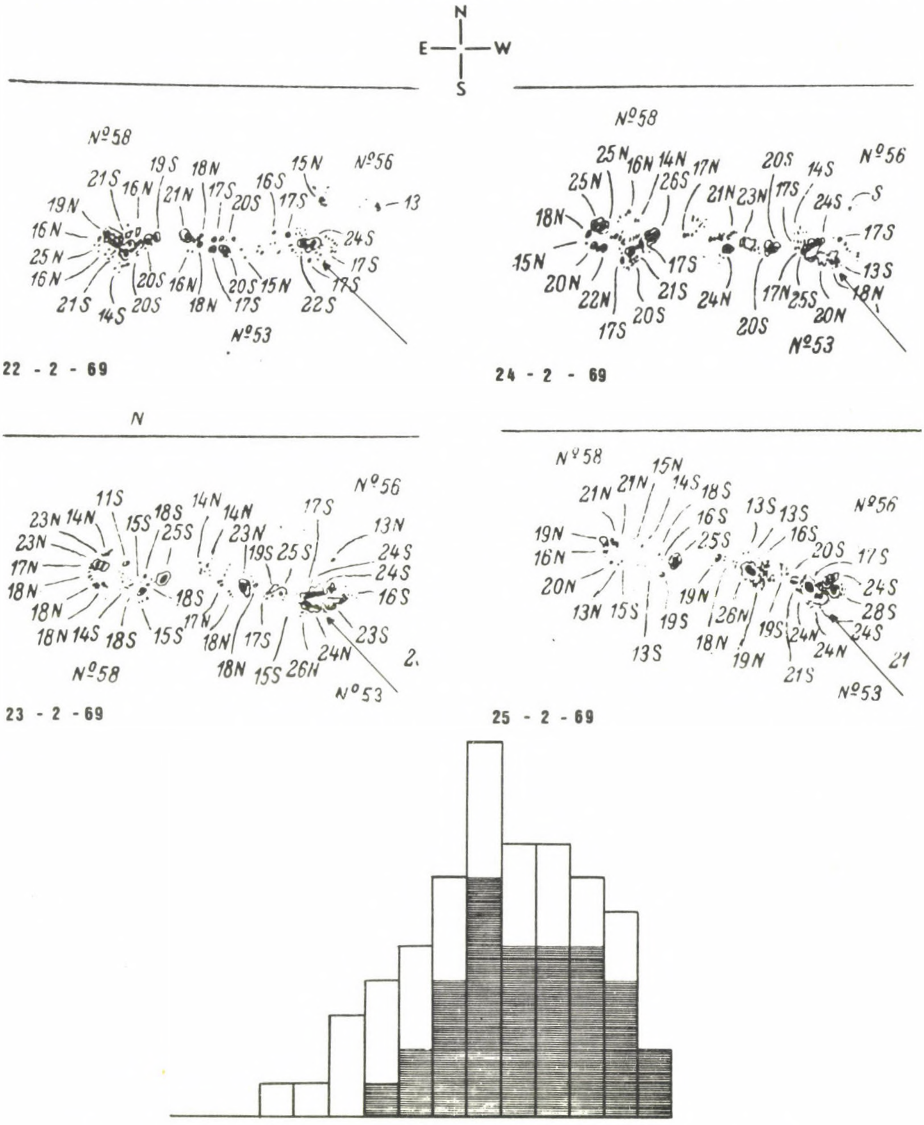

Figure 1. Above: Sunspot drawings and magnetic fields, from Solnechnye Dannye. (the arrow indicates the location where new magnetic flux is emerging)
Below: Hystogram of the flares in the active region (shaded area: flares at the exact location N13 L72 of the February 25 G.L.E.)

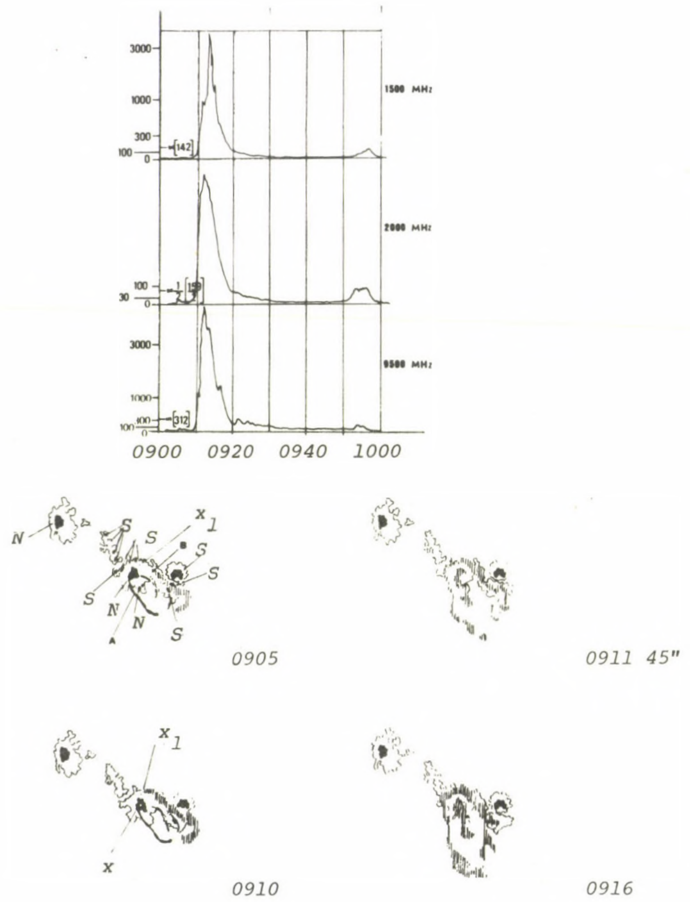

Figure 2. *Above: H.Hertz Institute 9500-2000-1500 MHz fluxes*
Below: Schematic phases of the flare
Sunspot umbra: black
H-alpha flare emission: shaded
x_1 *and* x_2*: bright points*
A and B: filaments

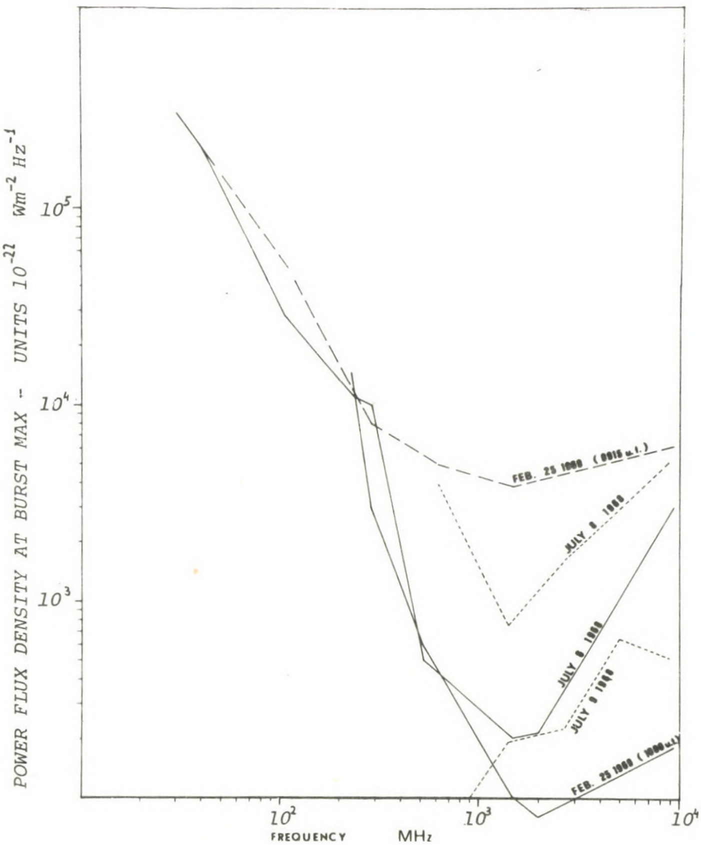

Figure 3. Radio spectrum at maximum emission from the H.Hertz Institute data.

PUBLICATIONS OF DEBRECEN HELIOPHYSICAL OBSERVATORY
Vol. 2 No. 8 1971

ON THE CROSS-CORRELATION FUNCTION OF VELOCITY AND MAGNETIC FIELD IN THE PHOTOSPHERE

I. K. C S A D A

Konkoly Observatory of the Hungarian Acad. of Sci., Budapest

Abstract:

The fluctuations of the velocity and the magnetic field observed in the photosphere are usually analysed by the correlation method. Some results obtained in this way were published by G.Y. Vasilyeva and A.K. Tchandaev (1967). I had many discussions with the authors about their results, but there is still an open question, namely, the physical meaning of the correlation functions, especially that of the cross-correlation function of the velocity and the magnetic field.

In the present paper, first, a short comment will be given to this question, proposing a modification of the published cross-correlation function, second, the physical meaning of the correlation function will be discussed.

The representation of the autocorrelation function by a symmetrized, i.e. an even function form, is a generally accepted convention. However, such a symmetrization cannot be applied to the cross-correlation function because of its skew symmetry, or odd-function character (i.e. it has zero at the origin and the absolute value remains unaltered while the sign changes as we are going through the origin). The observed values have to be separated to even and odd terms by use of the formulae

$$R^{+}(l) = \frac{R(l) + R(-l)}{2} \qquad R^{-}(l) = \frac{R(l) - R(-l)}{2}$$

It is supposed that the odd terms (i.e. the second equation) have a physical meaning since they represent the values of the cross-correlation function which are comparable with the even character autocorrelation function of the velocity and with that of the magnetic field represented by the first equation.

A magnetohydrodynamic theory of the correlation function was published by Chandrasekhar (1955). The basic problem in this paper is the determination of the autocorrelation function of the magnetic field. Similarly to the assumptions used in earlier theories of the velocity correlation in ordinar-y hydrodynamics, Chandrasekhar assumed a negligibly small contribution from the magnetic fluctuations to the averages. This step in generally accepted in the case of isotropic turbulences and its correctness has been confirmed by laboratory experiments.

The explanation of the above result is very simple, as we can consider the fluctuation relative to the mean velocity. The statistical results are unaffected by such a transformation and if the inertia terms are negligible, this transformation can be replaced formally by the omission of the mean velocity in the analysis.

The magnetic field strength will not reduce by such a transformation. This is an essential difference between the statistics of the velocity and the magnetic field and therefore we can conclude that the average of the magnetic fluctuations should not be ignored in a more general analysis.

In the present treatment the mean velocity will be omitted but the effect of the mean magnetic field on the correlation functions will be taken into account.

Let us introduce into the equation of motion and into the equation of the magnetic field the transformation

$$v_i = v_i' \quad , \quad H_i = \overline{H}_i + H_i' \quad , \quad p = \overline{p} + p' \tag{1}$$

and ρ is supposed to be constant.

Defining the correlation functions in tensorial form, we get for

1. The autocorrelation function of the velocity

$$v_{ij}(\vec{l},\tau) = \frac{\overline{v_i'(\vec{x},t)\ v_j''(\vec{x}+\vec{l}\ ,\ t+\tau)}}{\overline{v_i'v_j'}} \tag{2}$$

2. The autocorrelation function of the magnetic field

$$H_{ij}(\vec{l},\tau) = \frac{\overline{h_i'(\vec{x},t)\ h_j''(\vec{x}+\vec{l}\ ,\ t+\tau)}}{\overline{h_i'h_j'}}\ . \tag{3}$$

3. The cross-correlation function of the velocity and magnetic field

$$R_{ij}(\vec{l},\tau) = \frac{\overline{v_i'(\vec{x},t)\ h_j''(\vec{x}+\vec{l}\ ,\ t+\tau)}}{\overline{v_i'h_j'}} \tag{4}$$

where

$$h_i = \frac{H_i}{\sqrt{4\pi\rho}}$$

and $\vec{l}$ is the distance between the points P_2 and P_1 to which the correlations are related.

Let us note that

$$l^2 = l_1^2 + l_2^2 + l_3^2$$

Using the substitution (1), we obtain the equations

$$\frac{\partial v_i'}{\partial t'} + \frac{\partial}{\partial x_k'}(v_i'v_k' - \bar{h}_i h_k' - h_i'h_k') = \frac{\partial\bar{\omega}}{\partial x_i'} + f_i + \nu\Delta' v_i' \tag{5}$$

$$\frac{\partial h_j''}{\partial t''} + \frac{\partial}{\partial x_k''}(h_j''v_k'' - v_j''h_k'' - \bar{h}_k v_j'') = n\Delta'' h_j'' \tag{6}$$

where

$$\bar{\omega} = \frac{H^2}{4\pi\rho} + p, \quad \text{and } t'' - t' = \tau, \quad \vec{x}'' - \vec{x}' = \vec{l}$$

and $\vec{f}$ denotes the external forces.

Multiplying now (5) by h_j'' and (6) by v_i' and averaging out time and space we introduce as new coordinates l and α (instead

)

of x_1, x_2, x_3, the third coordinate x_3 remains unaltered) we obtain

$$-(\nu+\kappa)\Delta\overline{v_i h_j} R_{ij}(l) = \bar{h} \cos\alpha \frac{\partial}{\partial l} \left[(v')^2 V_{ij} - (h')^2 H_{ij}) \right] \quad (7)$$

where α is the angle between the actual direction of $\vec{l}$ and that of the average field.

Let us approximate V_{ij} and H_{ij} by the forms

$$V_{ij} = \frac{V_L - V_T}{l} l_i l_j + V_T \delta_{ij} \quad (8)$$

$$H_{ij} = \frac{H_L - H_T}{l} l_i l_j + H_T \delta_{ij} \quad (9)$$

where V_T and H_T are the transversal, V_L and H_L the longitudinal invariants of the correlation tensors. The transversal constituents are observable if $\vec{l}$ is perpendicular to the line of sight, while the longitudinal components are observed if $\vec{l}$ is parallel to the line of sight. In the case of solar observations the fluctuation in terms of the transversal constituents can be analysed in the solar center, while those in the longitudinal components at the limb.

Typical forms of the two components of the velocity correlation as measured in laboratory generated isotropic turbulence are shown in *Fig. 1*, (1), (4).

As a more general rule, it can be shown that the autocorrelation function has a limb effect which can be

S decribed by the well defined formula

$$V_p = V_T + (V_L - V_T) \sin p$$

where p is the distance measured from the center of the disc. The family of the correlations to be expected in terms of the

parameter p is shown in *Fig. 1*. A comparsion of this formula with the observation should give a criterion of the application of the isotropic turbulence to the solar atmosphere.

In the following we shall restrict out problem to the center and thus the correlation tensors V_{ij} and H_{ij} will be replaced in (7) by V_T, H_T and R. Then we find

$$(\kappa+\nu)\Delta R = -h \cos\alpha \frac{d}{dl}\left(\frac{v'}{h'} V_T - \frac{h'}{v'} H_T\right).$$

Since in this representation the transversal cross--correlation is a function of the coordinates l and α we can try to find a solution in the form

$$R = A\int_0^l V_T dl - B\int_0^l H_T dl$$

where

$$A = -\frac{\bar{h}\cos\alpha}{\nu+\kappa}\frac{v'}{h'} \quad \text{and} \quad B = -\frac{\bar{h}\cos\alpha}{\nu+\kappa}\frac{h'}{v'} .$$

This equation suggests some elementary consequences for the magnetohydrodynamic turbulence and its application to solar physics.

As R(l) must be zero if $l \to \infty$ (i.e. the fluctuations which are too far from one another cannot be in any correlation), we have

$$(v')^2 L_V = (h')^2 L_H$$

where $L_V = \int_0^\infty l V_T dl$ and $L_H = \int_0^\infty l H_H dl$ are the scales of velocity and the magneto turbulence, respectively. In an alternative form we can write

$$E_M L_M = E_V L_V \qquad (8)$$

where $E_V = \frac{1}{2}\rho(v')^2$ and $E_M = H^2/8\pi$ are the kinetic and magnetic energies, respectively. It follows from (8) that the ratio of the two energy fluctuation is equal to the ratio of the scales of the two turbulences. In the case of equipartition of the energies

$$E_M = E_V \quad \text{and} \quad L_M = L_V$$

and the cross correlation must be identically zero.

The cross correlation function must also be identically zero if the magnetic fluctuations do not contribute at all to the average. This is the case considered in Chandrasekhar's paper.

If there is no equipartition and the contribution from the magnetic fluctuation to the average is not zero, the cross correlation shows a characteristic variation with the direction of $\vec{l}$ (see *Fig.2*). This fact offers the possibility of finding the orientation of the average magnetic field in the photosphere.

Finally *Fig. 3* shows some results for the comparison of the cross correlation deduced from the observed values of the autocorrelation functions with the values obtained for the cross correlation directly from the observations.

References

Vassilyeva, G.Y., Tchandaev,A.K.: 1968, *IAU Symposium No.* 35,*236*.

Chandrasekhar,S.: 1955, *Proc. Roy. Soc. A.*233, *322*.

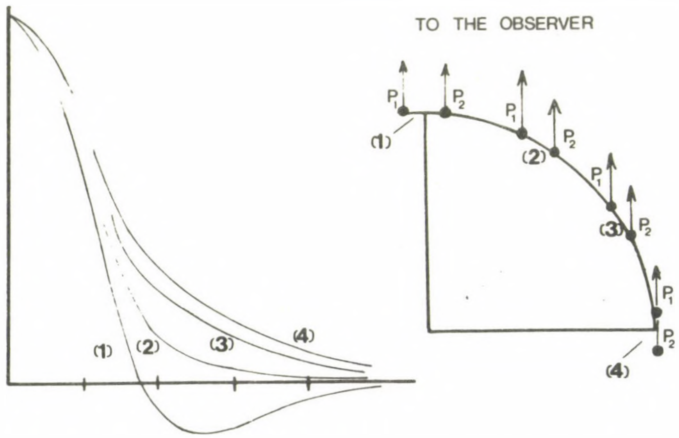

Figure 1. Typical forms of the correlations. (1) and (4) show the transversal correlation and the longitudinal correlation, respectively. The limb effect of the correlation function, as would be observed on the solar surface, is also presented. In this sense (1) is observed at the center ($p = 0°$), (2) at $p = 30°$, (3) at $p = 60°$, and (4) at the limb ($p = 90°$).

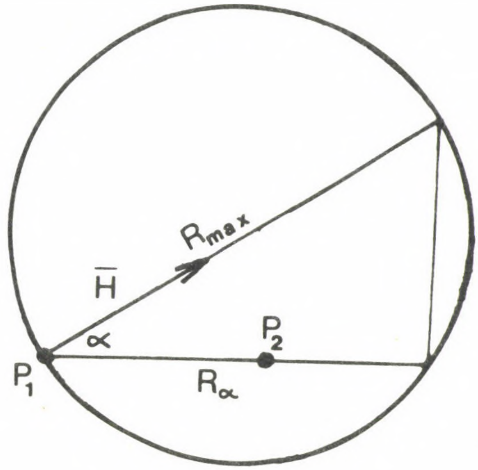

Figure 2.

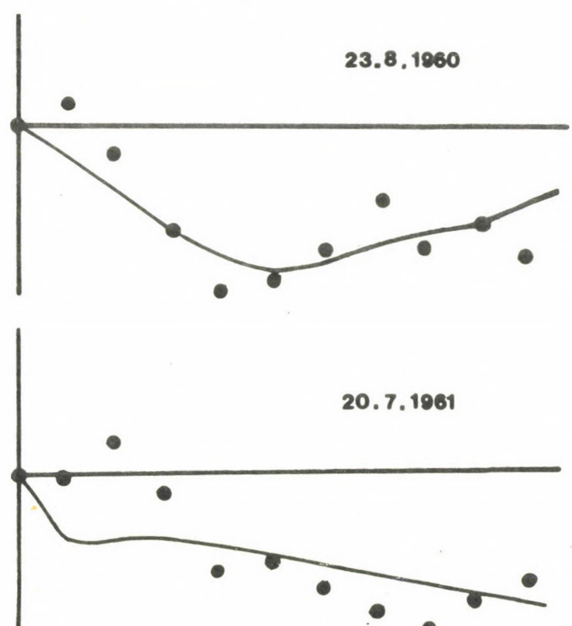

Figure 3. The cross-correlation function of the velocity and magnetic field as is observed at the surface (dots) (G.Y.Vassilyeva and A.K.Tchandaev) and derived from the autocorrelation functions (solid lines).

PUBLICATIONS OF DEBRECEN HELIOPHYSICAL OBSERVATORY
Vol. 2 No.9 1971

A THEORETICAL MODEL OF THE SOLAR CHROMOSPHERE

M. M A R I K

Astronomy Dep., Eötvös University, Budapest

Abstract:
A theoretical model of the solar chromosphere is given. The calculations have been made based on supposing a thermodynamic equilibrium state in the chromosphere. The results show that the temperature in the chromosphere increases with height.

In the course of calculations approaches are used in many cases and therefore the calculated model can be considered as a first approximation only.

To calculate the model the following four conditions have been assumed:

I. The Emission Coefficient

The energy, emitted by the solar matter in the chromosphere and in the low corona was given by theoretical calculations in (1) as follows:

For the hydrogen, lines and continuum: $1{,}30\cdot10^{-21}n_e^2T^{-\frac{1}{2}}$ erg $s^{-1}cm^{-3}$

For the helium, lines and continuum: $3{,}96\cdot10^{-21}n_e^2T^{-\frac{1}{2}}$ "

For the other elements, lines and continuum:

$$1,01\cdot 10^{-21} n_e^2\, T^{-\frac{1}{2}} \mathrm{erg\,s^{-1}cm^{-3}}$$

For all the elements, lines and continuum:

$$\varepsilon_e^1 = 6,00\cdot 10^{-21} n_e^2\, T^{-\frac{1}{2}}\ \mathrm{erg\ s^{-1}cm^{-3}}$$

For the free-free transitions:

2

$$\varepsilon_e^2 = 1,93\ 10^{-27} n_e^2 T^{-\frac{1}{2}}\ \mathrm{erg\ s^{-1}cm^{-3}}$$

where n_e is the electron density and T is the temperature.

If the temperature is below 10^6 °K, ε_e^2 is negligibly small as compared to $\varepsilon^1{}_e$ Considering $T < 10^6$ °K the emission coefficient can be approximated as follows:

$$\varepsilon_e \approx 6.10^{-21}\ n_e{}^2\ T^{-\frac{1}{2}}\ \mathrm{erg\ s^{-1}cm^{-3}}$$

To calculate the model in a simple way let us suppose that the hydrogen is fully ionised and the other elements are not ionised. This supposition is exact in the higher chromosphere only. In this case the emission coefficient can be approximated as follows:

$$\varepsilon_e = 6,51\cdot 10^{26}\ \rho^2\ T^{-\frac{1}{2}}\mathrm{erg\ \ s^{-1}\ cm^{-3}} \qquad (1)$$

where ρ is the densitiy of the matter.

II. The Absorption Coefficient

The generation of magnetoacoustic waves was discussed by Kulsrud in (2).Pikel'ner and Lifshitz (3) have suggested that the magnetoacoustic waves, generated in the solar convective zone, are transforming into weak shock waves in the layer of $V_A \approx V_S$. (V_A is the Alfvén velocity and V_S is the velocity of the sound.) The chromosphere is heated by these weak shock waves according to Osterbrock (4), Pikel'ner and Lifshitz (3), Marik (5) and others. The heating of the corona occurs by other mechanisms. The absorption coefficient for weak shock waves was given in the chromosphere by Osterbrock(4):

$$\varepsilon_\alpha = \frac{2^{\frac{1}{2}}}{4\ \rho^{\frac{1}{2}}\ V_S^{\frac{5}{2}}}\ F^{\frac{3}{2}} \qquad (2)$$

where F is the energy flux of weak shock waves.

The energy flux, F has been calculated in (5):

$$F = F_o \left[1 + 0{,}177\, F_o^{\frac{1}{2}}\, t_o^{-1} \int_0^h \rho^{-\frac{1}{2}}\, V_S^{-\frac{5}{2}}\, dh\right]^{-2} , \qquad (3)$$

where F_o is the energy flux of shock waves by $h = 0$ and t_o is the passing time of the shock waves. Generally

$$t_o = (0{,}1 - 0{,}5)\ P,$$

where P is the characteristic period of the shock waves.

III. The Hydrostatical Equilibrium

We suppose that the chromosphere is in a hydrostatical equilibrium state. In this case:

$$P' = \frac{dP}{dh} = - \rho g \ , \qquad (4)$$

where g is the gravitational acceleration.

IV. The Equation of State

The equation of state of ideal gases is used:

$$P = \frac{\rho}{\mu} RT \ , \qquad (5)$$

where R is the gas constant and μ is the mean molecular weight. μ

The calculation of the model is based on supposing a thermodynamic equilibrium state in the chromosphere. In this case the emitted and the absorbed energy per second and cubic centimeter must equal each other,

$$\varepsilon_e = \varepsilon_a$$

or using equations (1) and (3):

$$\frac{2^{\frac{1}{2}}}{4\, \rho^{1/2} V_S^{5/2}} \cdot \frac{F_o^{\frac{3}{2}}}{\left[1 + 0{,}177\, F_o^{1/2} t_o^{-1} \int_0^h \rho^{-1/2}\, V_S^{5/2} dh\right]^3} = 6{,}51 \cdot 10^{26}\, \rho^2\, T^{-1/2} \qquad (6)$$

The velocity of the sound is:

$$V_S = \left(\gamma \frac{P}{\rho}\right)^{1/2} , \qquad (7)$$

where γ is the ratio of specific heats.

Substituting equation (7) into equation (6), eliminating T by equation (5) and ρ by equation (4) we get:

$$1 + A \int_0^h P^{-5/4} dh = B\ (P')^{-7/12} P^{1/4} \ , \tag{8}$$

where $A = -\ 0{,}177\ g^{-3/4}\ F_o^{1/2} t_o^{-1} \gamma^{5/4}$ and

$$B = -\ 8{,}159 \cdot 10^{-10} g^{7/12} \left(\frac{\mu}{R}\right)^{1/6} \gamma^{-5/12} F_o^{1/2} .$$

After differentiating the equation (8) we get:

$$P\ P'' + (P')^2 \left[\frac{3}{7} + C\ (P')^{1/3}\right] = 0 \ , \tag{9}$$

where $C = \frac{12\ A}{7B} = 3{,}718 \cdot 10^{8}\ g^{-4/3} \left(\frac{R}{\mu}\right)^{1/6} \gamma^{-5/6} t_o^{-1}$.

P'

The solution of equation (9) for P' is:

$$P' = D\left[\ \beta\ P^{1/7} - 1\ \right]^{-3} ,$$

where $D = 3{,}066 \cdot 10^{-13}\ t_o^3$ (for the mean molecular weight $\mu = 0{,}872$ was taken and for the gravitational acceleration $g = 2{,}736 \cdot 10^4 \mathrm{cm\ s^{-2}}$), β is a constant of integration.

If $P = P_o$ and $P' = -\ \rho_o g$ by $h = 0$,

$$P' = -\ \rho\ g = D \left[\left(\frac{P}{P_o}\right)^{1/7} \alpha - 1\right]^3 \tag{10}$$

where

$$\alpha = 1 - 2{,}293 \cdot 10^{-6}\ t_o\ \rho^{-1/3} .$$

The solution of differential equation (10) for P is:

$$P \left[\frac{7}{10}\ \alpha^3 \left(\frac{P}{P_o}\right)^{3/7} - \frac{7}{3}\ \alpha^2 \left(\frac{P}{P_o}\right)^{2/7} + \frac{21}{8}\ \alpha \left(\frac{P}{P_o}\right)^{1/7}\right] = D\ (h - h_1) \ , \tag{11}$$

where h_1 is a constant of integration. Considering $P = P_o$ by $h = 0$, we get,

$$\frac{P}{P_o} \left[\frac{7}{10}\ \alpha^3 \left(\frac{P}{P_o}\right)^{3/7} - \frac{7}{3}\ \alpha^2 \left(\frac{P}{P_o}\right)^{2/7} + \frac{21}{8}\ \alpha \left(\frac{P}{P_o}\right)^{1/7} - 1\right] - \tag{12}$$

$$-\left[\frac{7}{10}\ \alpha^3 - \frac{7}{3}\ \alpha^2 + \frac{21}{8}\ \alpha - 1\right] = \frac{D}{P_o}\ h .$$

150

Giving various values for P_0, ρ_0 and t_0 function $P(h)$ can be calculated by equation (12). Function $\rho(h)$ can be obtained by equation (10) and $T(h)$ by equation (5).

Functions $P(h)$, $\rho(h)$ and $T(h)$ do not depend on the energy flux of weak shock waves F_0 directly, but t_0 depends on the magnetic field strength.

Fig. 1. shows the temperature as functioned by the height in the chromosphere. By the level $h=0$ has been taken $P_0 = 1{,}31$ din cm^{-2} and $\rho_0 = 4{,}90 \cdot 10^{-9}$ g cm^{-3}. For t_0: 10, 15, 20 and 30 seconds have been taken succesively. *Fig. 1.* shows that the temperature reaches 10^6 degrees when $t_0=15$ s and 4.10^4 degrees when $t_0= 20$ s at 10^4 km height above the photosphere. As, according to observations, the characteristic period of the shock waves in the chromosphere is about 100 seconds, and $t_0 = (0{,}1-0{,}5)$ P, these results are not in contradiction with the observations.

These results do not show the rapid change of temperature, observed in the chromosphere, because an approximation has been used for the emission coefficient by the calculations.

In a following paper a model of the chromosphere will be made by numerical calculations using the numerical values of the emission coefficient given in (6).

The author is grateful to S.B. Pikel'ner and V. Letfus for the valuable discussions of this paper.

R e f e r e n c e s

(1) Unsöld,A.: 1955, *Physik der Sternatmosphären*, (Springer) *670*.

(2) Kulsrud,R.: 1955, *Astrophys. J.* 121, *461*.

(3) Pikel'ner,S., Lifshitz,M.: 1964, *Astron. Zhurn. Akad. Nauk SSSR* 41,*1007*.

(4) Osterbrock,D.: 1961, *Astrophys. J.* 134,*347*.

(5) Marik,M.: 1966, *Astron. Zhurn. Akad. Nauk SSSR* 43,*400*.

(6) Cox,D., Daltabuit,E.: 1971, *Astrophys. J.*167, *113*.

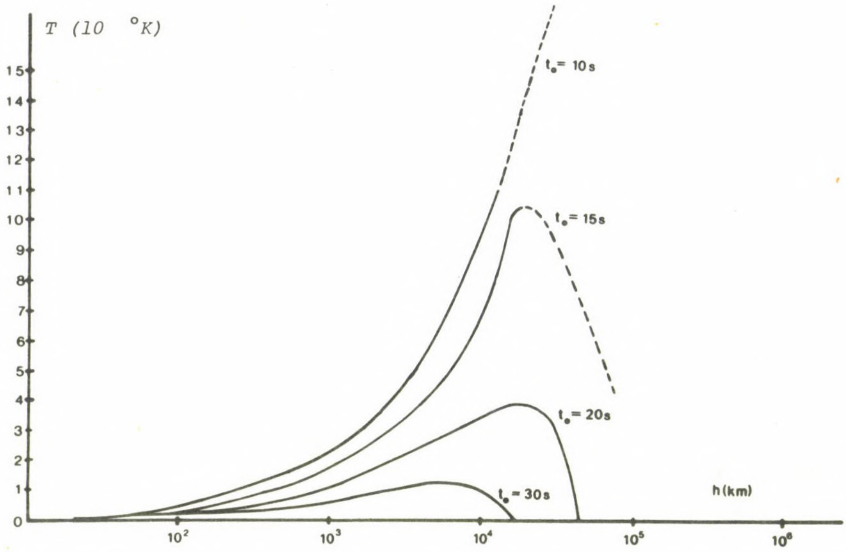
T (10 °K)
15
14
13
12
11
10
9
8
7
6
5
4
3
2
1
0
t_e= 10s
t_e= 15s
t_e= 20s
t_e= 30s
h(km)
10^2
10^3
10^4
10^5
10^6

Figure 1.

PUBLICATIONS OF DEBRECEN HELIOPHYSICAL OBSERVATORY
Vol. 2 No.10 1971

SPECTRAL EVIDENCE FOR SPIRAL MOTIONS IN PROMINENCES

B. ROMPOLT

Astronomical Observatory, Wrocław University, Wrocław

Abstract:

On the basis of the observed zigzag-shaped H-alpha lines in prominence spectra, the conclusion is made that in some thin threads of prominences material flows along the helix-like trajectory. From two active prominences a pitch of about 13 000 km, a width of the helix structure of 1500 km at most, and a velocity of 150 km/s along the helix trajectories are evaluated. A lower limit of magnetic field sufficient for keeping the spiraling matter is estimated to be 20 gauss.

1. Introduction

The aim of the present paper is to report and discuss the results of the spectral researches which seem to give evidence for the existence of helical mass motion along the helix-shaped magnetic tubes, in some fine filaments of prominences.

The helical and rotational mass motions as well as the helix-shaped magnetic fields have attracted more attention from solar observers and theoreticians, especially in the last few years. It is so, because the twisted magnetic fields have been recognized as the best source of energy for solar flares.

The present observational facts and theoretical arguments indicating the existence of the helical fluxtubes and the helical or rotational mass motions in the solar atmosphere are reviewed in an other paper of this issue (Rompolt, 1971 a).

2. Observations

During my stay at the Ondřejov Observatory in Czechoslovakia, in 1963, I recorded spectra of loop type prominences using a multi-camera horizontal spectrograph (Valniček et al., 1959). Spectral lines from the top part of several loops had a wavy appearance resembling the letter 's'. After detailed analysis of the Doppler displacenets in the observed lines it became clear that some rotational mass motion must take place in loops or at least in certain filaments of the loops, because no kind of motion could be responsible for the observed 's' - shaped lines coming from the top part of the horseshoe loops.

It must be stressed here that if we take spectra of prominences with solar telescopes giving the Sun's image between 10 and 30 cm in diameter, then, the usually used width of the spectrograph slit is comparable to the width of the fine filament of a prominence (about 1 arc second) - see Ciurla and Rompolt (1965). In other words, the image of a filament may pass as a whole through the spectrograph slit. It is evident that spectral observations of such fine structures ought to be carried under conditions of exceptionally good visibility with telescopes of high spatial and spectral resolution and of good guiding.

Encouraged by the observations made at Ondrejov, I realized a more refined observational program of investigation of motions in fine filaments of active prominences, during my stay at the Sayanian Mountain Observatory of the Siberian Institute IZMIRAN, in 1969.

The observations were made using the solar horizontal telescope ACU-5 with the 165 mm Sun's image, and the 7-m horizontal spectrograph ASP-20. At such a scale of the Sun's image and at the spectrograph slit set to 0.1 mm, the width of the slit corresponded to nearly 1000 km at the center of the disk - it is more than 1 arc second. The H-alpha lines of prominences were photographed in the 4-th order of the spectrum at the dispersion of about 3 mm/A.

On some occasions a three-mirror solar image rotator giving the possibility of obtaining any desirable spectral cut across the prominence and a biaxial pointing control of the telescope was used.

Simultaneously with spectra, the H-alpha images of the prominence were taken by means of a H-alpha attachment for solar spectrographs, constructed at the Wroclaw Astronomical Observatory. A part of the image, reflected off the polished slit jaws, passes through an objective, then through a Solz type birefringent filter having a rather wide 8 A passband centered on H-alpha, and finally is photographed by a camera. The resulting slit-jaw pictures record the position of the slit on the prominence image. The passband of the birefringent filter may be shifted in the range of $\pm$ 5 A by a simple inclination of the filter - thus, those parts of a prominence which have a considerable line-of-sight velocity component can be observed and recorded under the best visibility and best contrast. In order to diminish the amount of scattered light in the spectrograph, the image of the solar disk was covered with a metal disk placed at the entrance slit - where the solar image is formed - during taking the spectra and the H-alpha pictures.

In this place, I would like to call the attention of observers of prominences to the fact that the usually used narrow-passband filters (0.5 A) in the H-alpha attachments for solar spectrographs did not yield a perfect correspondence between the knots of active prominences recorded on filtergrams and spectrograms. In other words, if a narrow-passband filter is adjusted to the center of the H-alpha line then some prominence knots having adequately large line-of-sight components may not be recorded on the filtergrams, while on the spectrograms they will. So, in my opinion, the slit-jaw filtergrams of prominences taken with the H-alpha attachment equipped with a wide passband filter (5 - 10 A), yield more information and make easier the reducing procedure.

On 8 September 1969, and also on 11 September 1969, I was successful in finding in certain places of two active prominences the zigzag-shaped H-alpha lines that I was looking for.

The first prominence was situated at the west solar limb and consisted of a system of flattened, horizontally oriented arches (filaments) being at nearly flare brightness (see *Figure 1a*). Behind the arches there were two very faint loop structures, the radiation of which could not contribute of the recorded H-alpha light emitted by the arches.

The second prominence at the NW solar limb was in the form of a broad loop structure, which consisted of a number of thin loops (see *Figure 1b*).

In *Figures 1a* and *1b*, together with the outlines of the prominences, the positions and the widths of the spectrograph slit are indicated. The recorded zigzag-shaped H-alpha lines in the two prominences are shown in *Figures 2a* and *2b*, respectively.

The zigzag-shaped H-alpha lines were observed in both prominences only at strictly defined places. For example, the shape of the line - taken at 2 arc seconds to the right from the position indicated in *Figure 1b* - is shown in *Figure 3*. It is quite different from the shape of the line shown in *Figure 2b*.

3. Results and Discussion

An interesting feature of both zigzag-shaped lines is that both inclined, contiguous streaks of the H-alpha line converge to a point in the far wings; so, the zigzag-line goes continuously, without interruption, from the bottom to the top.

In order to find an explanation for the shape of the observed lines, several mechanisms like wave propagation, pinch-effect,expansion, rotation and spiral motion were discussed (hereafter the words "spiral" and "helix" will be treated as synonymous). Not one from the above specified mechanisms, except spiral motion, appeared to be able to produce the observed zigzag-shaped lines.

A zigzag-shaped line cannot be expected from a wavy disturbance propagating along a filament, the orientation of which - in the case of limb observations and known overall geometry of the prominences - ought to be rather perpendicular than parallel to the line-of-sight. Moreover, the second line (*Figure 2b)*, with pointed ends of the zigzags at the short-wave part of the spectrum and rounded at the long-wave, is hardly to be interpreted by wave stimulated motions.

The pinch-effect is also to be excluded. In order to give the lines under discussion a pinch must take place simultaneously in several regions distributed at nearly equal distances along a filament strongly inclined to the line-of--sight. Outflows of plasma with line-of-sight velocity components directed towards and from the observer ought to accompany the pinches. The distances between the pinch regions, the amount and specific axis distribution of gained velocities ought to be adequately matched. Of course, such a circumstance where all the mentioned conditions would be fulfilled at the same time is of small probability. In these terms, however, the shape of the second line cannot be explained.

The expansion (or contraction) of a filament is unable to produce any inclined to the direction of dispersion emission streaks - indepedently of the orientation of the expanding filament with regard to the slit.

The rotation - contrary to expansion - may produce inclined streaks, but only in that case when the slit is more or less perpendicularly oriented to the axis of the rotating filament. Here, in order to have a continuous zigzag-shaped line, some additonal conditions must be fulfilled; for example, filaments in projection onto the slit plane ought to be packed one close to the other, the direction of rotation must be opposite in alternately laying filaments, diameters of filaments and rate of rotation ought to be adequately matched. This is schematically explained in *Figure 4* (cf. Rompolt, 1971 a). Each figure of that type ought to be deciphered as follows: on the left hand side of a picture an outline of the spectrograph slit is given; against the slit an outline of a projected feature under investigation is shown - here the open circle denotes motion from the ovserver, and arrows indicate motion in the direction perpendicular to the line--of-sight, as seen at the side of a solar feature, being nearer to the observer; on the right hand side of a picture a part of the spectrum with the expected appearance of a line is displayed; the vertical line indicates the theoretical line center.

There is another possibility to get the zigzag-shaped line too, with other collocations of several rotating filaments, but much more complicated; this case will not be discussed here. So, it becomes evident that it is barely possible to obtain a zigzag-shaped line from several fortuitously adjusted inclined streaks, generated by a number of rotating filaments.

Arguments concerning the cases of expansion and rotation are documented in the next paper of this series (Rompolt, 1971 b).

The zigzag-shaped line may be formed in yet another way, which seems to be also of small chance - namely, a conglomerate of incidentally Doppler-shifted lines arranged in the form of a zigzag.

Finally, after considering and discarding the possibilities discussed above, and others I was left with the conviction that the gas motion along a helical trajectory gives the best and the most reasonable explanation for the observed zigzag-shaped lines.

In order to get the observed Doppler-displacements, the entire image of a projected helical structure must pass through the slit. In our case the diameter of the spiral structures ought not to be larger than 1000 km, if the effect of trembling the image across the slit is neglected.

When we make a projection of a spiral with its axis perpendicularly oriented to the line-of-sight, then the resulting image will have a zigzag form (*Figure 5a*). An unexpected coicidence takes place here: the shape of the Doppler-displacements of a line resulting from the spiral motion of material is, in general character, the same as the image of the projected spiral. This is schematically explained in *Figure 6a*. There is a rather good general resemblance between the observed zigzag-line (*Figure 2a*) and the expected appearance of a line resulting from the spiral motion (*Figure 6a*).

Some fainter emission in those places of the line where the Doppler-displacement is the largest (the converging streaks numbered 3 and 4 in *Figure 7a*), may be caused by locally higher velocity of the material flowing along the helix-like tube. Plasma radiation coming out from the region of the higher velocity is smeared out over a larger area in the spectrum - hence the fainter emission. The higher velocity may be gained in local choke of the helix-shaped magnetic tube.

The H-alpha line of the second prominence (*Figure 2b*), with pointed ends of the zigzags at the short-wave part of the spectrum and rounded at the long-wave may also be explained by a helix-like model. In this case inclination smaller than 90° of the axis of the helical filament to the line-of-sight is necessary. Under such an inclination, the image of the projected spiral will be of the form presented in *Figure 5b*. As the inclination still decreases, the image of the projected spiral will be like in *Figures 5c* and *5d*.. A scheme explaining the formation of the line presented in *Figure 2b* is given in *Figure 6b*.

At orientations other than those presented in *Figures 6a* and *6b*, of a helix-shaped filament with regard to the slit one can get essentially various images of the spectrum. Some examples are shown in *Figures 8a* and *8b*. It should be noted that similar inclined spectral features are observed on some occasions in the prominence spectra (e.g. *Figures 9a* and *9b*).

The photographically reproduced equidensitometric maps of both observed H-alpha lines reflect the zigzag form of the lines (*Figures 10a* and *10b*).

In *Figures 7a* and *7b* the numeration of the projected half-coils along which microphotometric traces were made, and the distances between the coils of the helical filaments are given.

The intensity profiles constructed along the inclined half-coils, for the first and the second prominence, are presented in *Figures 11a* and *11b*, respectively. In the case of spectral features, in the formation of which the effects of motion are expected to prevail over the other effects of line broadening, the photometric procedure carried out along the inclined features gives the best and the quickest information concerning the motion, as one can infer from a photometric procedure usually carried along the direction of dispersion. This remark will be argued in more detail in a forthcoming paper. It is easily seen from the upper scale of the presented profiles that the line-of-sight velocity components in some half-coils are of several tenths of kilometers per second. The profiles of the discussed lines are much broader than that of stable prominences.

In order to obtain a more reliable evaluation of the line-of-sight velocity components of the helical motion, a Doppler profile of a prominence having a temperature of 10 000 °K, and a 8 km/s turbulent velocity was used (these values are somewhat higher than the typical ones in stable prominences). Wings of the computed profile were fitted to the wings of the observed profiles, just as *Figure 12* shows for profile No.2 of the second prominence (cf. Machado, 1971). This procedure allows us to gain a rough estimation of the maximum line-of-sight velocity component, which appeared to be of around 40 km/s in both prominences.

Thus, if the proposed helix-like model interpretation is correct, we get for the spiral filaments the following average dimensions: the pitch - 13 000 km (see *Figure 7*), the width of the spiral structures - maximum 1500 km (when we take into account the effect of slight trembling of the prominence image across the slit).

Using the value of 40 km/s of the obtained line-of-sight velocity component, and 1500 km for the evaluated maximum width of the spiral, we obtain for the velocity along the spiral trajectory the value of around 150 km/s. In other words, the matter performs one complete turn along the spiral trajectory in every 90 seconds. If the width of the spiral structures were smaller than 1500 km, then the space velocity of spiralling should be adequately larger. The evaluated space velocity is comparable to the velocity of surges.

Nowadays, there is growing evidence that the matter visualized in various solar filamentary features is flowing along and guided by magnetic tubes (Tsap, 1964; Smith, 1968; Deubner and Göring, 1970; Foukal, 1971 a and b; Prata, 1971; Zirin, 1972). Moreover, more than 90 % of the magnetic flux in active regions (excluding the sunspots) is channelled in narrow filaments (Frazier and Stenflo, 1972). Therefore it is reasonable to assume that the described H-alpha helical filaments represent a type of helix-shaped magnetic channel.

It is evident that the plasma spiralling at a velocity of about 150 km/s, without being kept and guided by a magnetic field, would change significantly the shape of its initial spiral trajectory in consequence of the centrifugal force, in a time of the order of several seconds; this in turn would lead to a picture of the spectral lines quite different to the one observed. If it is not so in our case - the zigzag-shaped lines indicating spiral mass motion were observed in both prominences in a time of around 10 minutes - the magnetic field must be needed for keeping and guiding the spiralling matter.

167

Let us try to evaluate the magnetic field strength of helix--shaped magnetic tube responsible for keeping the matter in motion along the helical trajectory. With a tube-shaped model we can give a rough estimation of the lower limit for the magnetic field assumed to produce a sufficient pressure gradient. In order to do this, the centrifugal force of the spiral motion exerted against a unit area must be compared with the magnetic pressure (cf. Warwick, 1957). In the case of our spiral filaments, with scalar rotational velocities of the order of 150 km/s, the lower limit of the magnetic field is somewhere round 20 gauss. In computations, a value of 500 km was accepted for the diameter of the filament spiral tube and for the mean gyroradius of the spiral motion. So, even if our estimation was incorrect in one respect and instead of a 20 gauss field a field ten times larger was necessary for keeping the spiralling matter, it is known that magnetic fields of up to some hundreds of gauss exist in prominences (e.g., Zirin and Severny, 1961; Harvey, 1968; Smolkov, 1971; Smolkov et al., 1971).

Another example of a zigzag-like H-alpha line produced by the upper part of a limb flare observed on 30 July 1969 is shown in *Figure 13*. *Figure 14* gives some other lines having the shape resembling the lines discussed here, but without any information concerning the position of the slit relative to the prominence. Some of the lines I had the privilege to select from the spectral archives of the Crimean and Kislovodsk Observatories.

4. Conclusion

Spectral observations reported in the present paper indicate the presence of spiral motions in some small scale filaments of some prominences. This in turn allows us to judge that the helix-shaped magnetic filaments visualized by the spiralling matter do exist in the Sun's atmosphere. Magnetic fields of that type were recognized as the best accumulators or energy for solar flares (Gold and Hoyle, 1960; Alfvén, 1968; Anzer, 1968; Kiepenheuer, 1968; Nakagawa et al., 1971).

Acknowledgements

It is a pleasure to record here my sincere thanks to Professor V.E. Stepanov the Director of the Irkutsk Institute SibIZMIRAN, and to the staff of the Sayanian Mountain Observatory for their hospitality during my visit in 1969. It is also my pleasant duty to thank Dr. R.B. Teplitskaya, Mrs. N.M. Firstova and Mr. V.S. Bashkirzev for their kind assitance during the observations.

R e f e r e n c e s

Alfvén,H.: 1968, *Nobel Symp.* 9, *189.*

Anzer,U.: 1968, *Solar Phys.* 3, *298.*

Ciurla,T., Rompolt,B.: 1965, *Publ. Astr. Inst. Czech.* 51, *100.*

Deubner,F.L., Gőhring,R.: 1970, *IAU Symp.* 43, *190.*

Foukal,P.: 1971a, *Solar Phys.*19, *59.*

Foukal,P.: 1971b, *Solar Phys.*20, *298.*

Frazier,E.N., Stenflo,J.O.: 1972, *Solar Phys.* 27, *330.*

Gold,T., Hoyle,F.: 1960, *Monthly Notices R.A.S.*120,*89.*

Harvey,J.W.: 1968, *Astron.J.* 73,*Part II, S 62.*

Kiepenheuer,K.O.: 1968, *Nobel Symp.* 9, *123.*

Machado,M.E.: 1971, *Bull. Astr. Inst. Czech.* 22, *117.*

Nakagawa,Y., Raadu.M.A., Billings,D.E., McNamara,D.: 1971, *Solar Phys.* 19, *72.*

Prata,S.W.: 1971, *Solar Phys.* 20, *310.*

Rompolt,B.: 1971a, *the review paper in this Volume.*

Rompolt,B.: 1971b, *to be published in Acta Univ. Wratislaviensis (1975).*

Smith,S.F.: 1968, *IAU Symp.* 35, *267.*

Smolkov,G.Y.: 1971, *Issledovanja po Geomagnetizmu, Aeronomii i Fizike Solnca* 2,*140.*

Smolkov,G.Y., Rompolt,B., Bashkirtzev,V.S., Zubkova,G.N.: 1971, *Issledovanja po Geomagnetizmu, Aeronomii i Fizike Solnca* 20, *242.*

Tsap,T.T.: 1964, *Izv. Krym. Astr. Obs.* 31, *200.*

Valniček,B., Letfus,V., Blaha,M., Švestka,Ž., Seidl,Z.: 1959, *Bull. Astr. Inst. Czech.* 10, *149.*

Warwick,J.W.: 1957, *Astrophys. J.* 125, *811.*

Zirin,H.: 1972, *Solar Phys.* 22, *34.*

Zirin,H., Severny,A.B.: 1961, *Observatory* 81, *155.*

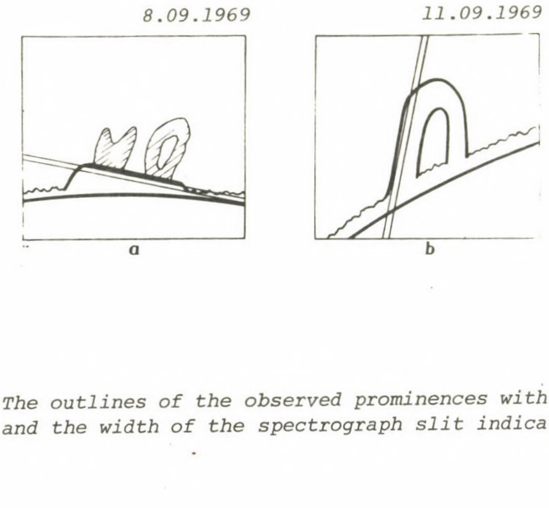

Figure 1. The outlines of the observed prominences with the position and the width of the spectrograph slit indicated.

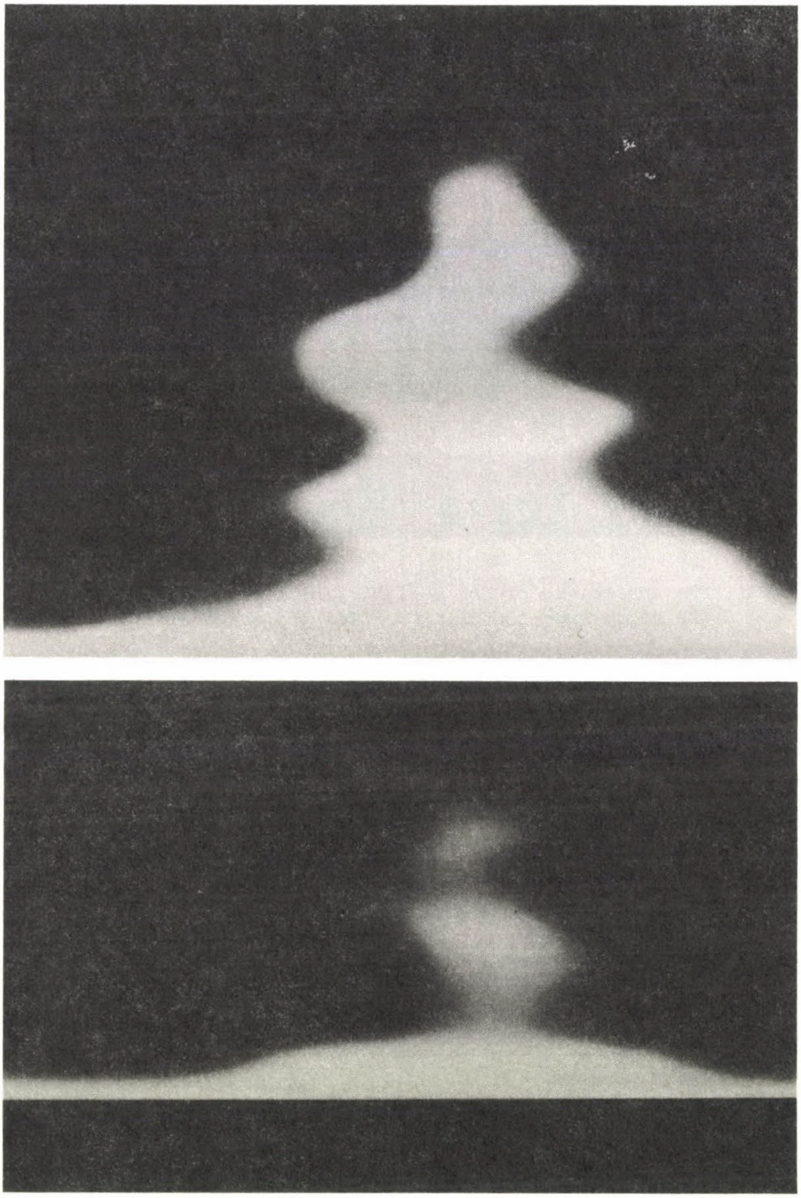

a

b

Figure 2. *The zigzag-shaped H-alpha lines observed in the two active prominences.*

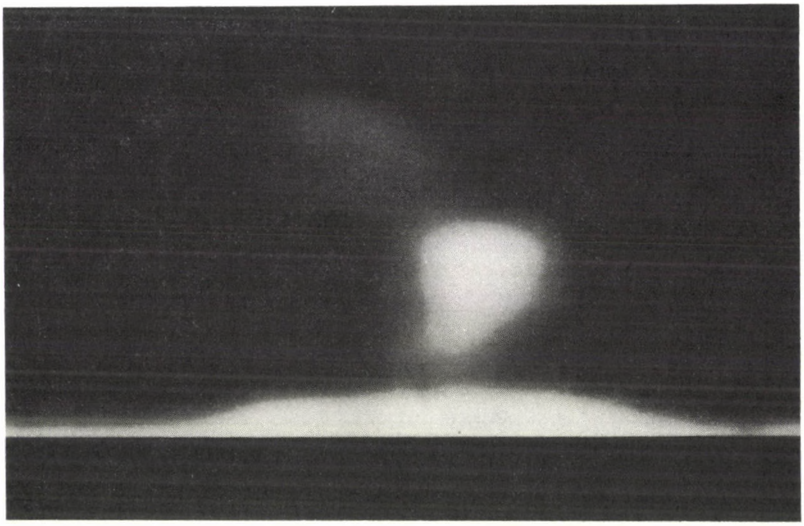

Figure 3. *The appearance of the H-alpha line taken at 2 arc seconds to the right from the slit position indicated in Figure 1b.*

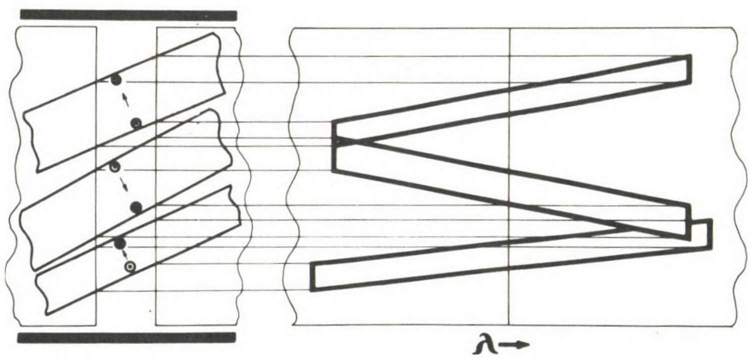

Figure 4. *The schematic drawing explaining the way in which a zigzag--shaped line may be produced by a set of rotating, tightly packed filaments.*

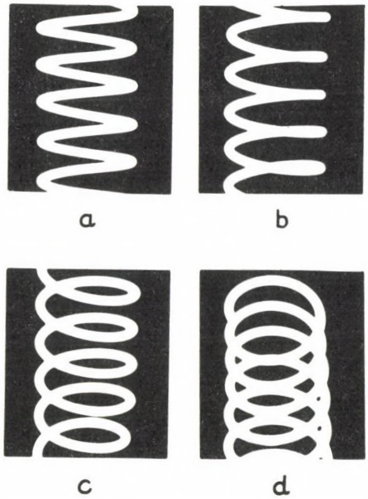

Figure 5. The shadow-projections of a spiral.

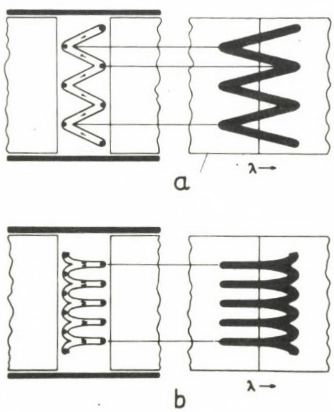

Figure 6. The sketches illustrating the mechanism of formation of the lines presented in Figure 2a and 2b.

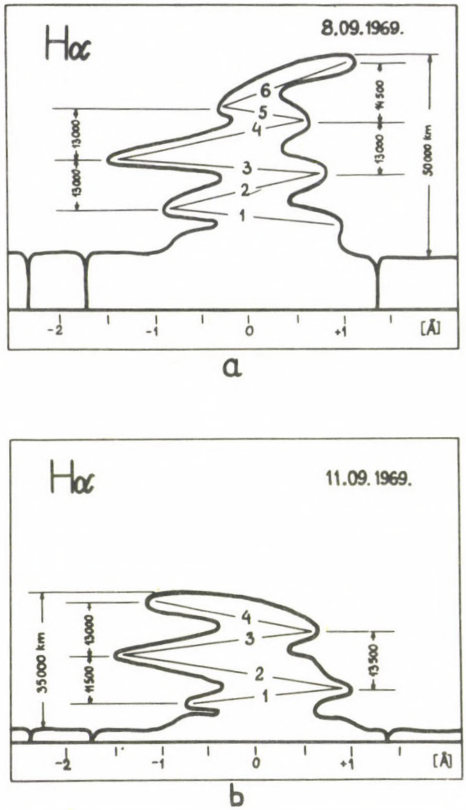

Figure 7. The outlines of the H-alpha lines with the numeration of the emission streaks (half-coils) along which microphotometric measurements were made. The distances between the coils of the helical filaments are also given.

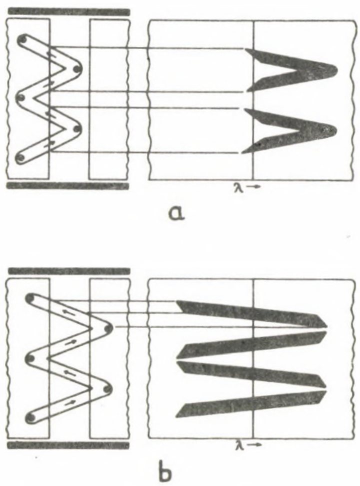

Figure 8. The lines to be expected from positions other than in Figure 6 of the spiral filament with regard to the slit.

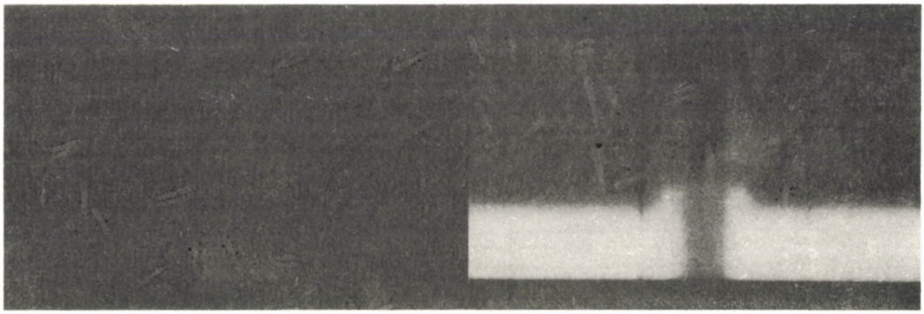

a *b*

Figure 9. The H-alpha lines of prominences, having shapes similar to those predicted by the mechanisms presented in Figure 8 (courtesy A.B.Severny).

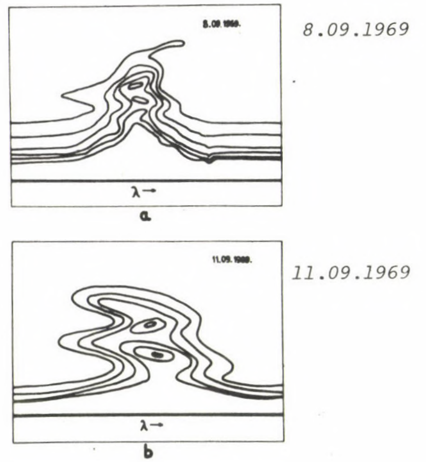

Figure 10. *The photographically reproduced equidensitometric maps of the observed zigzag-shaped H-alpha lines.*

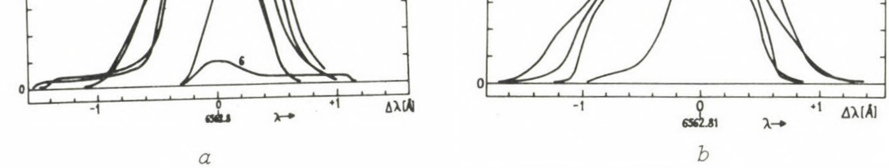

Figure 11. *The intensity profiles constructed along the inclined streaks (half-coils) of the observed zigzag-shaped H-alpha lines.*

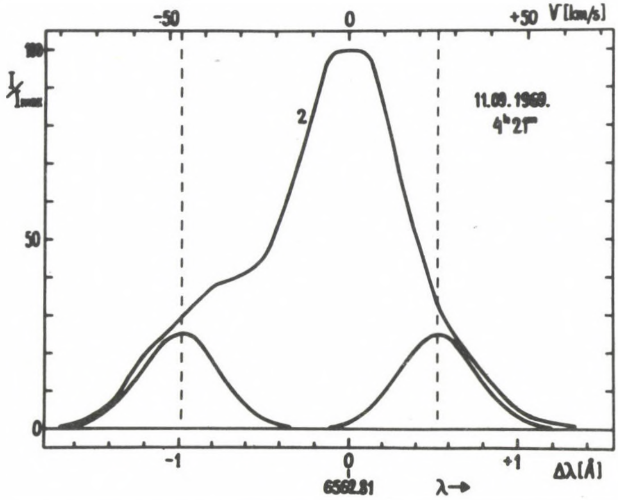

Figure 12. *The method of estimation of the maximum line-of-sight velocity component.*

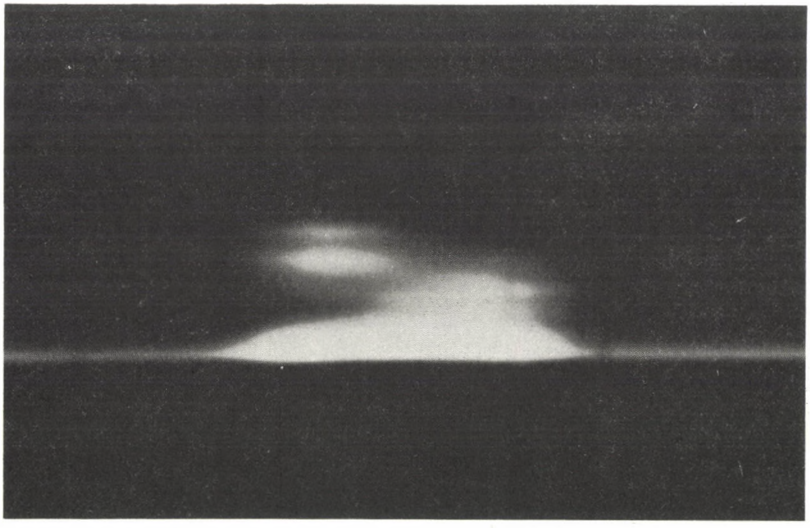

Figure 13. *The zigzag-like H-alpha line produced by the upper part of a limb flare observed on 30 July 1969.*

Figure 14a.

Figure 14b.

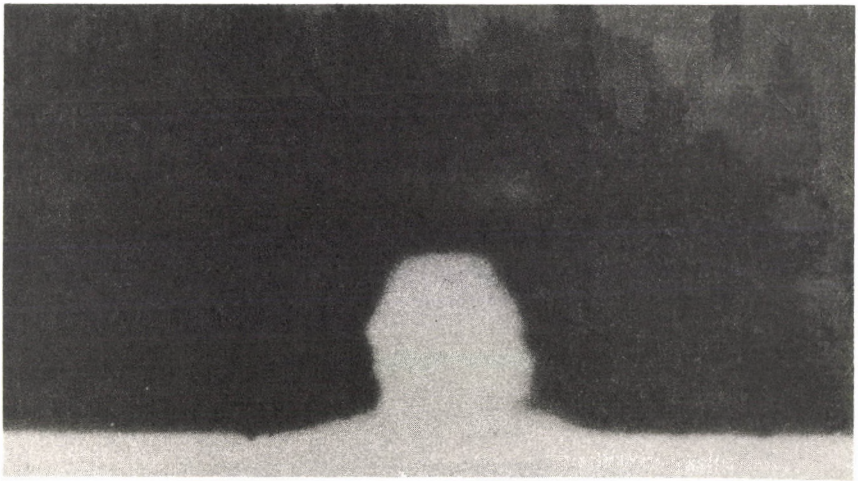

Figure 14c.

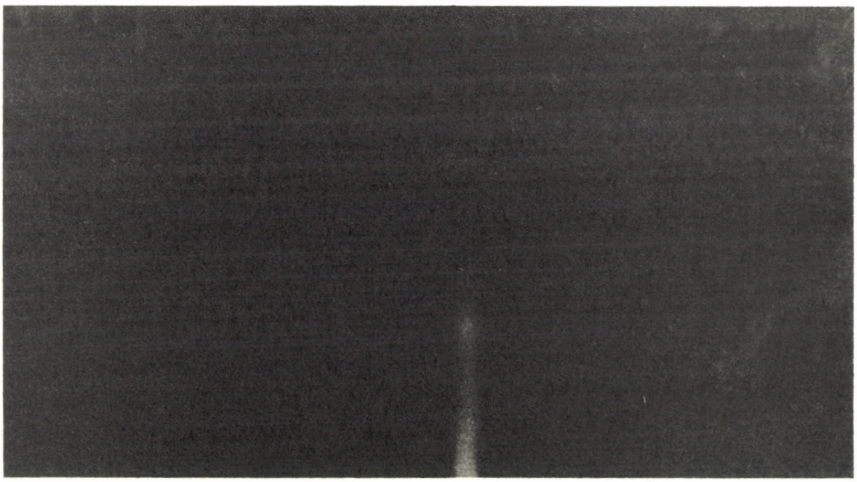

Figure 14d.

Figure 14. Other examples of prominence lines suspected to be produced by spiralling matter (*Figure 14a*, *c* and *d* courtesy *A.B.Severny*; *Figure 14b* courtesy *V.I.Makarov* and *G.M.Nikolsky*).

PUBLICATIONS OF DEBRECEN HELIOPHYSICAL OBSERVATORY

H-ALPHA HYDROGEN LINES OF TWO SCREENING THEMSELVES PROMINENCES OF JULY 29, 1969

B. ROMPOLT, A. SPODENKIEWICZ

Astronomical Observatory of the Wrocław University, Wrocław

Abstract:

One arch of a quiescent prominence of July 29, 1969 observed at the NW solar limb, obscured partly the other one. A rare and favorable situation arose for examination of the modification of the shape of profiles of optically thick emission lines of prominences caused by an additional emitting layer, which appeared into the line-of-sight.

Profiles of the H-alpha line coming from a single arch of the prominence show flattened top parts, while the profiles from two arches (into the line-of-sight) are double-peaked. This fact, along with a rough estimation of some physical parameters in the prominence, seems to support the view that the non-coherent scattering of the solar radiation must play an important role in the line formation of prominences.

1. Introduction

On July 29, 1969, at the NW solar limb, a quiescent prominence composed of a system of arches was seen nearly edge on, partly in emission against the sky, and partly in absorption against the disk. One arch of the prominence, protruding above the limb and situated nearer the observer, partly obscured the other one situated farther on. A rare and favorable situation arose for examination of the modification of the shape of profiles of optically thick emission lines of prominences caused by an additional emitting layer, which appeared into the line-of-sight.

2. Observations and Measurements

The observations were carried out at the Sayan Mountain Observatory of the Siberian Institute of Terrestrial Magnetism, Ionosphere and Radio Propagation with the help of the solar horizontal telescope ACU-5 and the 7-m spectrograph ASP-20. The sun's diameter at the slit was 165 mm. The H-alpha line was photographed on H-alpha ZP2 ORWO plates, in the 4-th order of spectrum at the dispersion of 2.7 mm/A. The exposure was 3 seconds. The plates were calibrated at the telescope after observations by means of a nine-step wedge at the center of the disk.

The H-alpha slit-jaw pictures recording the position of the slit on the prominence image were taken simultaneously with spectra.

Special attention was paid to the photometric procedure in order to diminish photometric errors - the accuracy of the intensity measurements was of about 1 %. Spectra were measured with a Zeiss photoelectric recording microphotometer "Lirepho--2".

The grating ghosts were very faint and spread out well beyond the wings of the prominence emission lines. Each part of the profile suffered from the ghosts by the same proportional loss of light; hence, though the central intensity of the prominence H-alpha line was diminished, the shape of the profile was unaltered.

The lines of the prominence photographed above the limb, against the sky background, were superimposed on the spectrum of the sun's light scattered into the earth's atmosphere and into the instrument. All H-alpha lines were corrected for the superimposed scattered light.

According to our evaluation, the instrumental smearing was unimportant for the broad H-alpha lines.

3. Results of Measurements and Discussion

Several spectral cuts across the prominence were taken during the observations. For the present analysis only, the most interesting, H-alpha cut was choosen. The orientation of the slit crossing the prominence, established on the basis of the H-alpha filtergram, is schematically shown in *Figure 1a*. Arrows indicate the places from which photometric traces on the H-alpha-spectrogram (*Figure 1b*) were taken. The dotted line in *Figure 1a* is the outline of the prominence arch situated nearer the observer.

Besides the H-alpha-line profiles, the equidensitometric map of the H-alpha - line was obtained using the photographic photometric procedure based on the Sabattier effect (see *Figure 2*). One can see a marked darkening in the lower part of the centre of the H-alpha-line, while just above it there is a violent increase of brightening.

Figures 3 and *4* show six profiles of the observed H-alpha-line. In the abcissa distances from the centre of the H-alpha-line are plotted in Å; in the ordinate the relative intensities I/I_0 are plotted, where I_0 is the intensity of the continuum close to the H-alpha-line at the centre of the Sun's disk. The number of a profile corresponds to the number of the photometric trace indicated in *Figure 1*.

S

I/I_0

The profiles numbered 1, 2 and 3 in *Figure 3* are from the lower part of the H-alpha-line, formed by the radiation in two self-screening arches of the prominence (cf. *Figure 1a*). These profiles have the double-peaked tops characteristic of lines produced by non-coherent scattering of the solar radiation in an optically thick medium. The profiles numbered 4, 5 and 6 in *Figure 4* are from the higher part of the H-alpha-line, which is formed by the radiation coming out from only one arch of the prominence, situated farther on from the observer (cf. *Figure 1a*). These profiles show flattened tops (4 and 5) or nearly gaussian shape (6); this indicates that they are produced - contrary to the profiles 1, 2 and 3 - in an optically thinner layer.

In order to gain an insight into the process of modification of the Ha-alpha line by an additional layer, a rough estimation of some physical parameters in the prominence was derived from the profiles of the observed line.

Yakovkin and Zeldina (1966) calculated a series of H-alpha profiles for the case of completely non-coherent scattering and plane-parallel geometry. These profiles, for some values of the optical thickness τ_0 and for the Doppler width $\Delta\lambda_D = 0.33$ Å, are shown in *Figure 5* by solid lines. It is interesting to note that the double-peaked top appears for $\tau_0 > 5$.

Yakovkin and Zeldina (1966) noticed that some physical parameters like τ_0 and $\Delta\lambda_D$ may be derived with a good approximation from the observed double-peaked profiles using the well known relation

(1)

$$I_v = \bar{B}\,(1 - e^{-\tau_v}), \tag{1}$$

instead of solving the more complicated integral equation for the case of completely non-coherent scattering

(2)

$$I_V = \int_0^{\tau_0} B\,(t)\, e^{-(\tau_0 - t)e^{-v^2}} e^{-v^2}\, dt. \tag{2}$$

In equation (1) and (2) I_v is the intensity at a distance $v = \frac{\Delta\lambda}{\Delta\lambda_D}$ from the line center, and $\bar{B}$ - the source function constant at all optical depths in a prominence, B - the source function dependent on the optical depths.

Profile (1) has a flattened top part, while profile (2) a double-peaked - for larger values of the optical thickness. In order to obtain a satisfactory approximation in deriving parameters τ_0 and $\Delta\lambda_D$ on the basis of profile (1), one must fit this profile to a wing and a peak of an observed double--peaked profile, which is assumed to result from completely non-coherent scattering mechanism of line formation and to be described by profile (2). Such a procedure is justified to some extent by the fact that profile (1) originates from the exact profile (2) by putting the source function $B(t)$ in the formula (2) to be constant at all depths in the prominence.

A rough estimation of τ_0 and $\Delta\lambda_D$ in the observed prominence was made by comparing the observed profiles with the theoretical ones (1), under an assumption that both self-screening prominences are of a plane-parallel form. The process of comparison of the observed and theoretical profiles (1) was carried out by the method of "six cuts" proposed by Yakovkin and Zeldina (1960). The obtained values of τ_0 and $\Delta\lambda_D$ are listed in *TABLE 1* along with the maximum intensity - I_m , the intensity of the line center - I_c the half-width - $2\Delta\lambda_{\frac{1}{2}}$ the equivalent width - A and the height above the solar limb - h . The same parameters, but derived from the solution of the exact equation (2) - after Yakovkin and Zeldina (1966) - are given for comparison in the bottom part of *TABLE 1*.

We can see from the *TABLE 1* that profiles 1, 2 and 3 (two prominences into the line-of-sight) are characterized by an optical thickness about twice as large as profiles 4, 5 and 6 (a single prominence into the line-of-sight). On the other hand the Doppler widths for almost all profiles observed (excluding Nr 1 - here the H-alpha line may be affected by the chromosphere) are nearly the same.

One of our profiles (Nr 3) is shown in *Figure 5* by a dashed line - for comparison with the theoretical profiles computed according to equation (2). The agreement is quite good. We may conclude, on the base of this rough analysis, that the non-coherent scattering of solar radiation seem really to play an important role in prominences.

Acknowledgements

One of the authors (B. Rompolt) wishes to express his deepest thanks to Professor V.E. Stepanov. Owing to his kind invitation, the author had the valuable opportunity to stay and to observe prominences at the SibIZMIRAN solar observatory. It is also a pleasure to acknowledge the assistance of Dr. R. B. Teplitskaya, Mrs. N.M. Firstova and V.S. Bashkirtzev in the observations.

R e f e r e n c e s

Yakovkin,N.A., Zeldina,M.Y.: 1960, *Soln. Dannye* No. 12, *67*.
Yakovkin,N.A., Zeldina,M.Y.: 1966, *Voprosy Astrofiziki* (Kiev) *5*.

TABLE 1.

Physical parameters derived from the observed and theoretical H-alpha line profiles.

profiles:	τ_0	I_{max}	I_c	$\Delta\lambda_D$, A	$2\Delta\lambda_{1/2}$, A	A, mA	h"
observational nr1	*13*	*.119*	*.110*	*.41*	*1.35*	*168*	*12*
" 2	*14*	*.104*	*.095*	*.35*	*1.30*	*139*	*20*
" 3	*14*	*.090*	*.081*	*.33*	*1.27*	*127*	*30*
" 4	*6.3*	*.108*	*.108*	*.34*	*1.00*	*123*	*38*
" 5	*6.3*	*.099*	*.099*	*.32*	*0.94*	*97*	*45*
" 6	*5.6*	*.086*	*.086*	*.31*	*0.88*	*78*	*55*
theoretical	*5*	*.076*	*.076*	*.33*	*0.92*	*72*	*30*
"	*10*	*.086*	*.079*	*.33*	*1.06*	*90*	*30*
"	*100*	*.138*	*.096*	*.33*	*1.50*	*172*	*30*

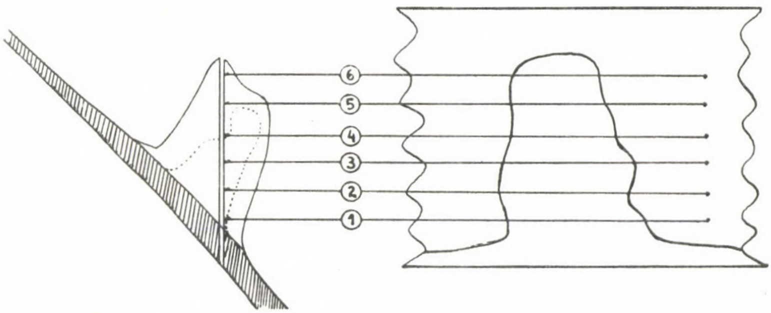

a *b*

Figure 1. *a - The orientation of the spectrograph slit crossing the prominence. Arrows indicate the places from which photometric traces on the H-alpha-spectrogram were taken. The dotted line shows the outline of the prominence situated nearer to the observer.*

b - The outline of the H-alpha line with photometric traces indicated.

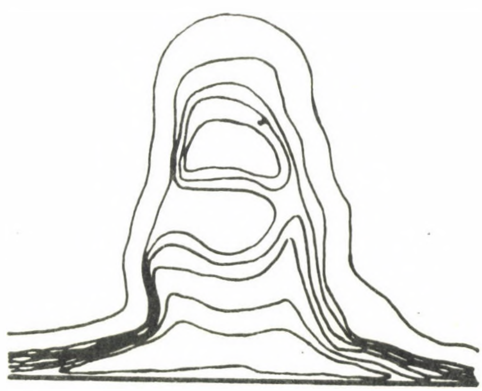

Figure 2. The equidensitometric map of the H-alpha line.

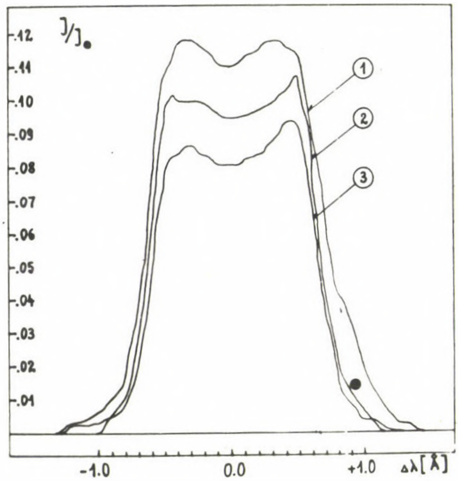

Figure 3. *The H-alpha line profiles from the lower part of the H-alpha line, where two prominences were into the line-of-sight.*

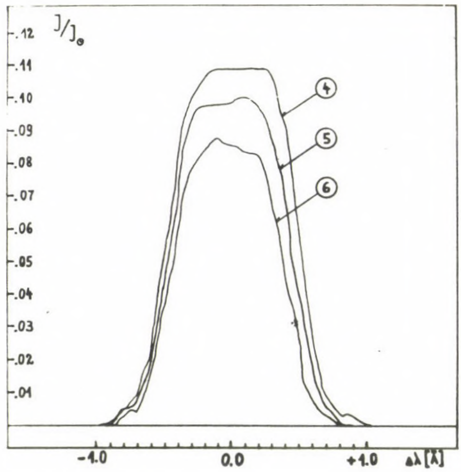

Figure 4. *The H-alpha line profiles from the upper part of the H-alpha line, where only a single prominence was in the line-of-sight.*

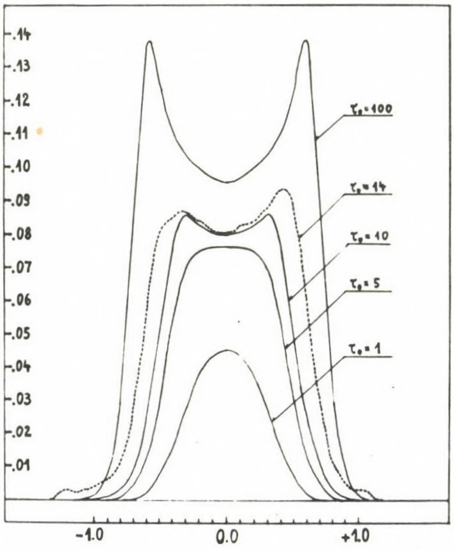

Figure 5. *The theoretical H-alpha line profiles for completely non-coherent scattering (solid lines) together with an observed one - Nr3 (dotted line).*

PUBLICATIONS OF DEBRECEN HELIOPHYSICAL OBSERVATORY

RADIO-BURSTS CONNECTED WITH SPRAYS OF JULY 6, 1968

I. G A R C Z Y N S K A, B. R O M P O L T

Astronomical Observatory of the Wrocław University, Wrocław

Abstract:
Two sprays were observed in H-alpha light on July 6, 1968 at the time of brightening of chromospheric flares. The sprays were accompanied by very intensive radio-bursts on various frequencies. The heights of the origin of these radio-bursts were estimated assuming the Newkirk model of the electron density distribution. These heights were compared with the observed heights of the visible front of the sprays. The comparison indicates the existence of a relation between the shock-wave producing radiobursts and the H-alpha spray. The distance between the "radio" and "optical" heights increases with time.

A complex of loop prominences was observed in H-alpha line at the eastern limb on July 6, 1968 by Fortini and Torelli (1970) and Rompolt, Kozar and Szumiejko (1969 - further quoted as Paper I) who also described in detail the results of their observations. At the base of the loop prominences several limb flares were seen.

Rompolt et al. (1969) observed two sprays that took place during chromospheric flares: the first flare at 7^h17^m U.T., the second at 9^h44^m U.T. In IAU Quarterly Bulletin (1968) both flares were classified as flares of importance 2n. However, these sprays were not seen by Fortini and Torelli - probably due to the narrow-band filter used. The Wroclaw coronograph, that was used for the sprays observations by Rompolt et al. (1969), was equipped with a wider filter of 8 Å shiftable band-pass.

In the present paper an attempt to investigate the possible connection between the observed sprays and strong radio-bursts simultaneously recorded in a wide range of frequencies is undertaken.

At $7^h17^m30^s$ U.T. a limb flare of importance 2n started to expand from a chromospheric brightening. At the same time the flare spray was ejected from the south base of the loops, and, more precisely, from the place where the arms of the two loops L_1 and L_2 converged (see *Figure 1*). The initial compact bulk of the spray fell into separate blobs, which moved nearly radially upwards from the point of the first appearance. The projected velocities of the brightest blobs of the sprays were estimated in Paper I for various heights - they ranged from 300 to 1150 km/s for the first spray, and from 90 to 720 km/s for the second. In the present paper the observational data have been reviewed to determine the front velocities of blob complexes.

Some time after each flare brightening the matter of the prominence QPl (in the S-region) was swept out in the opposite direction to the flare. This effect might have been caused by disturbances travelling horizontally over the solar surface and originating in the flare region. The distance between the flare and the prominence, and the time interval between the starting time of the flare and the beginning of the sweeping of matter permit the estimation of the mean velocity for these disturbances around 200 km/s.

It looks as if the observed process of the matter sweep from the stable prominence QPl is nothing else but the effect of the slowly propagating disturbances, usually observed against the disk, and seen just above the limb.

For the second spray a strong deviation (up to 90°) from the initial direction of its motion was observed. This deviation must have been produced by respectively strong factors, since initial blob velocities were high.

It may be found that the time-interval between the starting time of the flare in the S-region and the beginning of the spray was comparable with that needed for the disturbance to cover the distance between the flare and the point where the spray started. A possible explanation for the deviation of the second spray trajectory is that is resulted in the interaction between the spray and the disturbance. It is interesting to note that, beginning from some altitude above the photosphere, the blobs of spray were moving straightforward.

During both sprays the intensive radio-bursts classified as of type II, III and IV, were observed in various observatories in a wide range of frequencies (H.H.I., 1968; H.H.I., 1969; Q.B.S.A., 1968; Solnechnye Dannye, 1968; Osservazioni Solari, 1968). For this investigation the unpublished radio data from Cracow, Gorki, Ondrejov and Torun observatories have been kindly put at our disposal. S

According to Croom (1969) the unusually intense radio--bursts were observed in the milimeter and centimeter ranges: at 4.2 mm - $47 \cdot 10^3$ flux units, at 1.6 cm - $25\text{-}30 \cdot 10^3$ f.u. and at 10.7 cm - 1000 f.u. "Normally observed maximum values of flux density do not exceed 10^4, 10^3 and 400 f.u. at these frequencies, respectively (Croom, 1969). Such an "abnormal" intensity may be understood as the result of the self-radiation of the spray, which may be generated in the interaction of the spray whith the disturbance spreading out from the flare. e

The "intensity versus frequency" dependence for these radio-bursts shows the "U" shape in the range of $10 - 10^5$ MHz (Croom, 1969), which is characteristic for the proton bursts.

The latter was confirmed by the "Pioneer" - 6 and 7 particle flux measurements (Solar Geophysical Data, October 1968) - energies up to more than 190 MeV. These phenomena are usually correlated with the X-ray radiation.

The first SC geomagnetic storm that was probably connected with flares observed on July 8, took place on July 9. Its connection with the flares of July 6 could be real if the particle trajectories between the Sun and the Earth would have been strongly curved.

All those radio-bursts (spectral types II - meter and IV - cm and dcm) that happened during the second spray have been selected to determine their starting times.

A comparison of optical observations of the sprays travelling upwards in the corona with the frequency drift-rates of radio-bursts enables one to conclude that there are some connections between these phenomena. The detailed investigation of these connections is the subject of the present paper.

Let us consider the motion of an agent producing the radioemission in the solar corona. Such an agent may be identified with a shock-wave in which radio-waves of frequencies equal to the frequencies of plasma self-oscillations determined by the electron concentration of the shock-front are generated. The Newkirk's model of electron concentration for a coronal streamer (1961) multiplied by a factor of two has been used in this work following after Weiss (1963) and after Young et al. (1961).

The frequency of self-oscillations ω has been calculated using the formula:

$$\omega = 5.64 \cdot 10^4 \sqrt{N_e}\ s^{-1}$$

where N_e is the electron concentration. As a result the altitude of radiating region may be determined.

Figures 2 and *3* give the time dependence fo the subsequent positions for the radio-frequency radiating regions and the positions of the spray front obtained from the direct optical observations. It may be seen from these figures that the distance between the radio-frequency region (indicating position of the shockwave front) and the front of the spray increased with time. This fact may be understood if one assumes that only the densest part of the spray material was seen in the H-alpha line. In other words, the front of the shock-wave produced by the spray must have been well ahead of the spray. c

Figure 4 shows the dependence of the distance h between radio and optical regions versus altitude Δh above the photosphere. It is seen that Δh was constant up to the height of 95 000 km for the first spray, and, subsequently, it quickly increased. For the second spray Δh constantly increased with h. This different behaviour may be caused by different conditions of motion for the both sprays. The first one appeared at a root of the system of loops and was restrained by a strong magnetic field, which stabilized the system. The second spray appeared between the quiescent prominence and the system of loops, where the magnetic field in this region of the corona was probably weak and open. c

The mean velocities of both shock-waves, as well as the velocities of visible edges of the sprays will now be considered. It may be seen that a mean velocity of the first spray remained constant and was equal to 500 km/s, which, at first sight, contradicts the results obtained in the Paper I, where the maximum velocities of separate blobs were found to be of the order of 1150 km/s. This discrepancy disappears if one recalls that the velocity of the edge was determined from slow (500 km/s) and weakly radiating blobs moving in the corona ahead of the fast and bright blobs. The shock-wave velocity constantly increased in this case.

For the second spray the shock-wave velocity and the edge-of-the-spray velocity increased with the height above c the photosphere up to the values of 3300 km/s and 750 km/s, respectively.

The results obtained here support the hypothesis on the connection of sprays and shock-waves producing radio-bursts. Unfortunately, the small number of spray observations has prevented us from making more the general conclusion that the described relation always exists.

The hypothesis on the existence of a non-visible matter in the region between the shock-wave and the spray could be confirmed by overexposed broad-band H-alpha filter (with shiftable band-pass) observations and simultaneous radio observations with the use of a radio-heliograph. This kind of observation may provide direct measurement of the height of the radio emission region. It would make it possible to avoid the use of the model for the electron concentration distribution in the corona. Such models are approximate and represent only a global averaged distribution, and not the actual situation above active regions.

R e f e r e n c e s

Croom,D.L., Powell,R.I.: 1969, *Nature* 122, *945*.

ESSA: 1968, *Solar Geophysical Data,* (Boulder).

Fortini,T., Torelli,M.: 1970, *Solar Phys.* 11, *425*.

HHI Solar Data: 1968, 19.

HHI Suppl. Ser. Solar Data: 1969, 1, No. 5.

IAU Quarterly Bulletin on Solar Activity: 1968.

Young,C.W., Spencer,C.L., Moreton,G.E., Roberts,J.A.: 1961, *Astrophys. J.* 133, *243*.

Newkirk,G.: 1961, *Astrophys. J.* 133, *983*.

Osservazioni Solari: 1968, III. *No.11* (Trieste).

Riddle,A.C., Sheridan,K.V.: 1971, *Proc. ASA* 2, *62*.

Rompolt,B., Kozar,T., Szumiejko,E.: 1969, *Geod. Geoph. Veroff.* (Berlin) R, II, H.13, *55*.

Sheridan,K.V.: 1970, *Proc. ASA* 1, *376*.

Soln. Dannye 1968, N.7.

Weiss,A.A.: 1963, *Australian J. Phys.* 16, *240*.

TABLE I

Compilation of bursts data of the events of 6 July 1968

	Freq.	*Start Time*	*Time of Max*	*Spectral Type*	*Max.Flux Inst.(s.u.)*	*Hight of radio radiating region (10^3 km)*	*Observational Data*
Spray I	*810*	7^h16^m0	–	*f*	–	*17*	*Krakow*
	650	*7 16.2*	$7^h20^m.6$	*f*	*7,5*	*22*	*Gorki*
	430	*7 17.0*	–	*f*	–	*30*	*Krakow*
	260	*7 20.0*	–	*III*	*75*	*100*	*Soln.Dan.*
	234	*7 20.3*	*7 21.1*	*III*	*3500*	*120*	*HHI*
	234	*7 20.5*	*7 21.2*	*III*	*3500*	*120*	*Soln.Dan.*
	200	*7 20.7*	*7 21.8*	–	*9750*	*140*	*Quart.Bull.*
	111	*7 20.6*	*7 22.1*	*III*	*500*	*290*	*HHI*
	111	*7 20.9*	*7 21.1*	*III*	*500*	*290*	*Soln. Dan.*
Spray II	*71000*	*9 44*	*9 46.5*	–	*47000*	*0*	*Slough*
	19000	*9 42.2*	*9 45.0*	–	*18000*	*0*	*Slough*
	2800	*9 42.6*	*9 44.8*	–	*700*	*0*	*Slough*
	510	*9 43.0*	*9 49.2*	*IV*	*250*	*25*	*HHI*
	808	*9 43.5*	–	–	–	*17*	*Soln.Dan.*
	536	*9 44.0*	–	*III+II*	*280*	*25*	*Soln.Dan.*
	367	*9 45.0*	*9 47.5*	*IV*	*170*	*40*	*HHI*
	287	*9 45.0*	*9 46.5*	*II,III,IV*	*10000*	*80*	*HHI*
	239	*9 44.7*	*9 46.5*	*f*	*7500*	*115*	*Triest*
	234	*9 45.0*	*9 46.5*	*III*	*10000*	*118*	*Soln.Dan.*
	111	*9 47.0*	*9 48.5*	*II*	*22000*	*290*	*HHI*
	64	*9 48.0*	*9 48.6*	*II*	*9000*	*470*	*HHI*
	40	*9 49.0*	*9 49.9*	*II*	*75000*	*700*	*HHI*

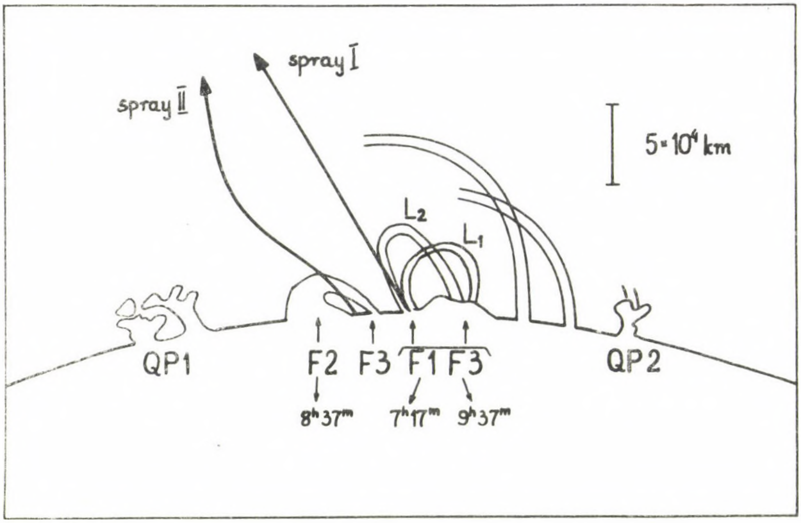

Figure 1. Schematic presentation of events in the limb active region of July 6, 1968.

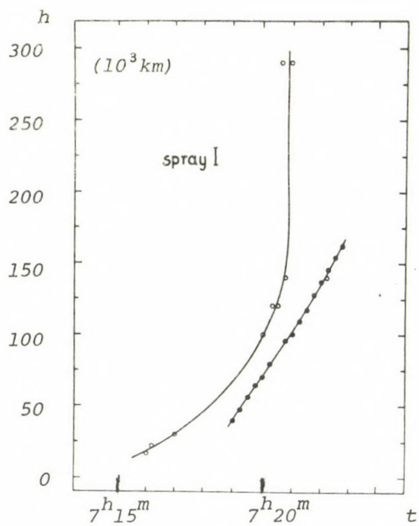

Figure 2. The time dependence of the altitudes for the radio-frequency radiating regions (open circles), and for the optical front (dots) of the spray I.

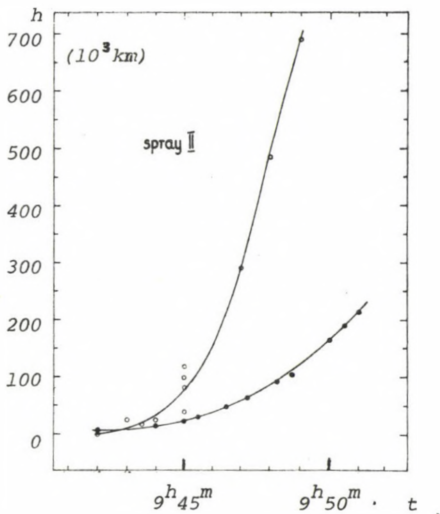

Figure 3. The time dependence of the altitudes for the radio-frequency radiating regions (open circles), and for the optical front (dots) of the spray II.

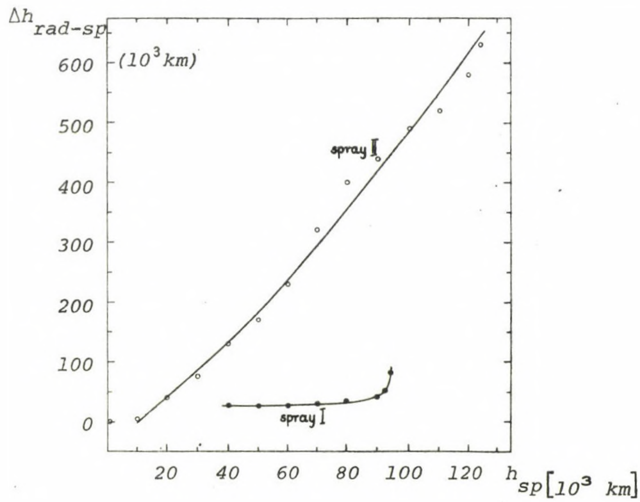

Figure 4. The dependence of the distance Δh between radio and optical regions versus altitude h for the spray I and II.

PUBLICATIONS OF DEBRECEN HELIOPHYSICAL OBSERVATORY

ROTATIONAL MASS MOTIONS AND TWISTED MAGNETIC FIELDS IN SOLAR PHENOMA

B. ROMPOLT
Astronomical Observatory, Wrocław University, Wrocław

Abstract:
A review paper reporting the results of observational and theoretical research giving evidence of the existence of rotational and helical mass motions as well as of twisted magnetic fields in some solar phenomena.

1. Introduction

The problem of the existence of helix-shaped magnetic fields in the chromosphere and in the corona seems to be significant for the better understanding of the mechanism of solar flares and of other active phenomena (Alfvén, 1968; Anzer, 1968a and b; Gold 1968; Kiepenheuer,1968; Nakagawa et al., 1971). Beginning from Gold and Hoyle's (1960) theory of solar flares, recent theories more and more often imply the twisted magnetic fields in flares, e.g. Alfvén and Carlqvist (1967), Anzer (1968a) Carlqvist (1969), De Jager (1969), Raadu (1972). Twisted magnetic fields seem to be the best accumulator of energy for solar flares. These are reasons why rotational mass motions and twisted magnetic fields have attracted more and more attention in the last few years. Arguments in favour of the presence of helical structures, and helical or rotational mass motions in the Sun's atmosphere yield the observations of prominences, flares, spicules, plages, sunspots, and also the theoretical studies. A great part of this evidence is dispersed and hidden in the literature, often even forgotten. A concise review of this evidence is given below.

The review will contain the evidence - without differentiation - based on the observed lines, inclined to the direction of dispersion in spite of the fact that the inclined lines may result not only from helical structures (while taking the spectral cuts with an adequate orientation of the spectrograph slit), but also from the rotational mass motion in filamentary or spherical structures (Rompolt, 1971 a and b). Moreover, the inclination produced by the closely wound helical structure is nearly the same as produced by a structure rotating around its axis - if of course the orientation with respect to the spectrograph slit and the amount of rotation of both types of structures is similar. The writer (Rompolt, 1971 a and b) has shown that other mechanisms as rotation can hardly be responsible for producing the inclination. So, the effect of inclination of spectral lines (streaks) to the direction of dispersion is hereafter believed to be produced by rotational or helical mass motions.

The observed H-alpha filtergrams, wavy (or sinusoidally) fine filaments in prominences, are considered throughout the paper as manifestation of a helical (or spiral) structure in real space. A spiral trajectory in three-dimensional space, with the axis of a spiral more or less perpendicular to the line of sight, is seen in the plane projection as a wavy line.

2. Prominences

It is generally known that a considerable part of flares brighten up in already existing prominences. The prominences give the most evidence indicating the helical mass motions and the helix-shaped magnetic fields. Spiral trajectories were found in nearly all types of prominences. Taking this into account, the helical structures in prominences are reviewed first.

2.1 TORNADO PROMINENCES

Spiral structures in prominences have been known for over a hundred years. The earliest observations were secured with a spectroscope. Pictures, which probably represent the first twisted prominences were drawn by Zöllner (1870) and by Young (1881). These kinds of prominences were extensively studied in a series of papers by Pettit (1925; 1932; 1941; 1943; 1946 a; 1950), and classified by him as the tornado type. The main features of the tornado prominences are: the diameter of the helix structure - on average 12000 km - ranges from 6000 km to 22000 km; the height - on average 53000 km - ranges from 25000 km to 100000 km. Tornadoes occasionally have only one or two turns, but sometimes they show a very tight twist. In every case a faint, diffuse stream issues from the top of the helix, often bent over, and in some cases spreading out to the chromosphere. The peripherial velocity recorded on some occasions in tornadoes was of the order of 50 km/s, but in one case amounted only to about 3 km/s (Pettit, 1946 a). Tornado prominences have been observed to disappear with increasing velocity of rotation, and also by eruptions.

Two types of tornado prominences have been considered by Pettit (1950). A columnar tornado of type IVa with a tight helical structure often difficult to recognize, and a skeleton tornado of type IVb with the clearly seen helical structure in the form of two interlacing streamers spiraled in opposite directions.

Probably the largest tornado prominence ever recorded was photographed by Richardson (1940) on 7 July 1940. Its height was 240000 km and the diameter 17000 km at the base, tapering to 8000 km at the height 120000 km. This tapering part of the prominence was tightly twisted. Higher up the prominence broke up into separate knots some being as bright as the flare. The velocities of several knots ranged from 20 to 60 km/s.

A large prominence with a pronounced helical structure recorded by Kristenson (see Öhman, 1968 a) seems to be skeleton type tornado.

An interesting observation of a tornado was reported by Harvey (1969). The spectrum of the prominence shows that the rotation in the outer shell and in the core was of opposite direction.

2.2 ERUPTIVE PROMINENCES

It is widely known that a spiralling motion of matter is often observed during the eruptive phase of stable prominences. Spiralling material is especially clearly seen in the legs of eruptive arches, while flowing into the chromosphere.

The first indications of the existence of spiral filaments in eruptive prominences could probably be deduced from the wavy filaments seen in the photographs presented by Pettit (1925; 1932).

Evidence for the presence of helical motions in this type of prominence is given by Severny and Khokhlova (1953), Kleczek (1963; 1968), Zirin (1968) and Rybanský (1971). The largest eruptive arch with a pronounced helical structure ever observed, is the well known eruption of 4 June 1946 (Roberts, 1946). The top of the expanding arch before it faded reached a height of about 1 700 000 km (Pettit, 1946 b). The average velocity of the expansion was 140 km/s. Rybanský (1971), on the basis of the observed rotational motions of the individual knots of an eruptive prominence, found that the angular velocity of motion was around 6° per 1 minute.

A spiralling motion of material during the phase of eruption is especially clearly seen in the prominence movies of the Pic-du-Midi, Climax, and Sacramento Peak observatories.

Spectral observations also indicate that rotatory mass motion must be present in the eruptive prominences. Spectra taken by Ellison (1947) with the slit crossing both legs of an eruptive arch show a rapid rotation of the order of 200 km/s (in opposite direction in every leg) by the inclination of the lines.

2.3 FUNNELS

Streamers forming a funnel-type prominence often display a wavy shape in H-alpha filtergrams (Kleczek, 1968; Rompolt, 1971 c). This is especially conspicuous if the funnel is not tightly filled by the matter. Such wavy shaped streamers one may find, for example, in the funnel shown by Pettit and McMath (1937).

2.4 LOOPS

On rare occasions the lapsed-time H-alpha pictures show spiral motion in the arms of the loop-type prominences (Rompolt, 1971 c; Palus, 1972). Spiral motion of material is sometimes visible also in the top part of the loops.

Severny (1968 a) gives an example of the inclined H-alpha line produced by a loop prominence observed in absorption against the disk. The H-alpha spectra taken from a system of loop prominences developed on 4 May

1960, just after a flare, show a cluster of inclined emission streaks. Machado (1971) using these spectra determined the rotational velocity in prominence streamers (15 km/s) from the angle of inclination of the streaks.

Some dark filaments associated with the appearance and the development of an active center (emerging magnetic flux tubes) also seem to rotate. Observations of these features reported by Martres and Soru-Escaut (1971) show that the traces of the filaments seen in both wings of the H-alpha line are close but not superimposed.

The zigzag-shaped H-alpha emission lines taken by the writer (Rompolt, 1971 a) from the individual filaments of two loop-like prominences give direct arguments in favour of the presence of spiral motions in certain loops. The velocity of material following the spiral path was around 150 km/s. The lower limit of the magnetic field strength - sufficient for keeping the spiralling matter - was evaluated at 20 Gauss.

"Dashes" - the spectral lines produced by a kind of loop (Billings, 1957; Prokofjeva, 1957) also show on inclination to the direction of dispersion (see Shpitalnaja, 1964; Krat, 1968).

2.5 CORONAL RAIN

Palus (1972) reported the results of trajectory measurements of two knots of a coronal rain prominence. The determined trajectories show spiral pattern with the pitch and the amplitude decreasing while approaching the chromosphere. The best approximation to the observed paths of knots appeared to be a hyperbolic spiral on a cone surface.

2.6 SURGES

Surges observed at the limb under good visibility and good resolution appear sometimes to grow upward with a twisting motion from the chromosphere (Kleczek, 1968; Dizer, 1968). Twisted motions of some surges were probably known to Pettit (1943). He denoted spiral streamers in surges by wavy lines in his schematic drawing illustrating various types of prominences. The most conspicuous twisted motion of surge material is seen in the Climax prominence film "Explosions on the Sun", where the ejection of the classical surge of 12 June 1946 is presented (see also Kiepenheuer, 1953, Figures 50 and 51).

Tilted H-alpha absorption lines are often produced by dark surges (Őhman et al., 1968). Koval and Stepanjan (1972) revealed that dark surges shooting from the neighboring chromosphere to a newly forming sunspot exhibit inclined H-alpha absorption lines.

On some occasions H-alpha pictures of limb surges show bright, equally spaced structures inclined to the long axis of the surge body (Rompolt, 1971 c). This provides an additional argument in favour of the helical internal structure of some surges.

2.7 SPRAYS

Blobs of spray as a rule move with high speed along virtually straight trajectories. In many cases, however, blobs rose with a spiralling motion visualized by small deviations of the projected trajectories from the straight lines. The wavy motion of blobs is recognizable in the cinematographic projection.

A spiralling motion in some events was reported by Warwick (1957), Berge (1959), Kleczek (1968), and Rompolt et al. (1969). Warwick (1957) has used the twisting motion of some sprays to evaluate the magnetic field strength in the corona. Rompolt (1971 c), on the basis of measurements of projected trajectories of 18 blobs in 5 sprays, concluded that the radius of spiral motion of blobs is in the range of 1000 - 9000 km, and the pitch is in the range of 36000-160000 km.The most often occuring value for the radius of spiral motion of blobs and the pitch is 2000 km and 60000 km respectively.

Inclined spectral streaks were observed in a spray by Öhman et al. (1967) indicating that essential rotatory mass motion must be present in spray blobs.

2.8 QUIESCENT PROMINENCES

One may expect from the helical structures observed during the phase of eruption of the quiescent prominences that fine helical structures ought to be present in these prominences also during their stable phase. Usually the characteristic scale of helical structures is too small to be visible against the filamentary background of a prominence. However, when looking at photographs of threadlike quiescent prominences, taken under conditions of excellent visibility and high resolution, one may notice that some of the fine prominence filaments exhibit a regular wavy shape - see for example photographs reproduced by Menzel and Wolbach (1960), and by Dunn (1972). The writer (Rompolt, 1971 c) has selected a number of H-alpha pictures of quiescent prominences in which fine wavy filaments are clearly seen. Spiral structures in quiescent prominences were also observed by Ambrož (1970).

Machado and Gallegos (1972) come to the conclusion - on the basis of the monochromatic images (H-alpha $\pm$ 0.5 A) of a relatively stable prominence-that the upper stream of the prominence is strongly twisted in a helix.

Severny and Khokhlova (1953) represent the opinion that the flow of the stable prominences material, deviating from the straight trajectories, is of a random and chaotic character.

On many occasions spectral lines of stable prominences, observed in absorption against the disk, show an inclination to the direction of dispersion (Öhman et al., 1968; Rompolt, 1971 b). Öhman (1951), while searching for dark filaments in prominences, found that sometimes wavy--shaped dark lanes appear in the core of H-alpha line of quiescent prominences seen at the limb. A similar wavy appearance of H-alpha and K CaII lines, but seen in emission at the limb, was revealed by Engvold and Livingston (1971). The authors do not exclude the rotation as one of the possible mechanisms explaining the observed shape of the lines.

2.9 SMOKE RINGS

Ring-shaped objects resembling plasmoids, named by Öhman et al. (1968) "smoke rings", are associated with flares and prominences.

The H-alpha filtergrams of the smoke rings, and the appearance of their H-alpha emission streaks allow one to judge that within a smoke ring rotational motions must be present (Öhman et al., 1968; Öhman, 1969,1970).

The smoke ring observed by Hagen and Neidig (1970) was ejected from a flare of the class 1B. It lasted in the ring-shaped form for less than 2 minutes. Radio emission recordings indicate that formation of the ring must have been performed at a height of 30000-45000 km. The observed smoke ring had the following diemensions: outer diameter - 21 200 km, hole diameter - 6 200 km, and ring cross - section diameter - 7 500 km. The projected velocity of the motion of the smoke ring was of up to 136 km/s.

Kawaguchi et al. (1972) report the observations of a smoke ring formed from a knot ejected by a small prominence. The dimensions of the smoke ring were: outer diameter - 22 000 km, and inner diameter - 6 000 km. The projected mean velocity of ejection was found to be 170 km/s. The smoke ring persisted for less than 3 minutes.

Similar, as in plasma smoke rings, rotations have been obtained in laboratory experiments by Lindberg et al. (1960), and by Bostick (1966).

2.10 THEORY

A twisted magnetic tube, with both ends anchored deep in the photosphere will tend to maintain its size instead of spreading out, as an untwisted tube would do. The observational facts indicating that various kinds of small structures like fine structure in loop prominences, fibrils, and chromospheric filaments are of roughly uniform width over a considerable length argue in favour of such spirally wound magnetic tubes.

Theoretical arguments given by Anzer and Tandberg-Hanssen (1970) support the notion that helical structures ought to be present in quiescent prominences. Their model for quiescent prominences is described by two magnetic fields, one produced by photospheric or subphotospheric currents, the other due to currents along the long axis of prominence. The resulting magnetic field has a helical form. It seems that the same mechanism, in some cases, could be resposible for the spiral structures observed in active region prominences.

Kuperus (1971) - contrary to the Kippenhahn - Schlüter (1957) supporting field configuration - proposed another configuration of the spiral field able to support the prominence material. His field is in the form of a long spiral tube horizontally oriented. Such a field configuration could also account for the observed ∼ 15° inclination between the filament (quiescent prominence seen on the disk in absorption) and its magnetic field (Anzer and Tandberg-Hanssen, 1970).

Merkulenko (1968 a) dealt with - on the basis of the variational principle - the process of lifting the magnetic field in the corona by the instability of a twisted magnetic tube. In the opinion of Merkulenko (1968 b), during the time of lifting a twisted magnetic tube the expansion and decomposition of the main tube takes place into separate filaments with longitudinal currents. The problem of magnetic ropes arising in the convective zone and the resulting mass motion was studied by Solovjev (1971 a and c) - also on the basis of the variational principle. Solovjev (1971 b) pointed out that magnetic ropes arising in the subphotospheric medium due to magnetic buoyancy are in the form of the pointed loops, whose edge is directed to the photosphere. He also investigated the structure of a magnetic rope over the photosphere (Solovjev, 1972).

Raadu and Nakagava (1971) show that the loop prominences formed after flares ought to exhibit a small twist. The largest twist occurs for the magnetic field with the smallest scale height, while the angle of twist decreases with increasing scale height.

On the other hand, Pneuman (1971) theoretically investigated the height dependence rate of the rotation of initially poloidal loop configurations, as influenced by differential rotation of the footpoints. He found the tendency for an outward increase in angular velocity distribution along closed magnetic loops in the lower corona. This effect appeared to be most pronounced at high latitudes and either small, absent, or even reversed at the equator.

3. Flares

3.1 OBSERVATIONS

There are observations indicating the presence of rotational as well as spiral motions in flares.

Inclined emission lines as produced by some flares were reported by Severny (1959 a), Öhman (1968 b and c, 1970, 1972), Öhman et al. (1968). Tilted emission lines are also clearly seen in the spectra of a weak limb flare presented by Kurochka et al. (1971). Öhman (1968 b and c, 1970, 1972) attributes the double-peaked and inclined H-alpha emission streaks of flares to the rapid rotatory mass motions.

The tilted streaks occur on rare occasions in flares observed against the disk. They appear more often in limb flares. It is necessary to say that we observe different parts of the flare when observing it on the disk and on the limb (Švestka, 1964). In the disk flares we observe their lower and denser region where the superposition of many filaments takes place (Švestka, 1951, 1965). On the limb the upper region of flares - much more extensive and rarefied - is seen. This upper region is practically transparent (with exception of hydrogen H-alpha - H-delta lines).

Öhman (1972) reports the observations of the inclined emission of the H CaII line of a flare close to the limb, accompanied by the periodic asymmetry of the absorption line of AlI 3961. The observations are interpreted as a rotational motion of a prominence material ejected from a rotating flare. The period of rotation of the AlI prominence is about 32 minutes, and the velocity 13 km/s.

A spiralling motion at a macroscopic scale was observed in a flare by Prokofjeva (Krat, 1968, Figure 10).

In the flare of 25 July 1959 the motion of two details seemed to be rotational and probably spiral in form; the velocity of this spiral motion was different for each detail (Ogir, 1971).

The detwisting prominence described by Valniček (1968) was also observed by the writer at the Wrocław Astronomical Observatory, and because of its unusual brightness it was classified as a flare. One of the bright streamers followed a spiral trajectory with the projected velocity of 50 km/s.

According to Menzel et al. (1956), the mass of an elevated limb flare showed during the expansion the internal filamentary structure in the form of a twisted loop. The summit of the rising mass acquired in one minute - as a spray - an upward velocity of 1130 km/s.

Martres et al. (1971) observed - while searching for evidence of the role of photospheric motions in the building up of the flare productive magnetic patterns - that the bright H-alpha faculae are associated with $v_{\parallel}$ structures different from a classical Evershed flow and are particularly anomalous in the regions and periods of high flare occurrence. In most cases the flares, usually occurring at "crossings" of the lines $v_{\parallel} = 0$ ($v \neq 0$) and $H_{\parallel} = 0$ showed an abrupt change of the direction of the line $v_{\parallel}=0$. This suggests a kind of vortex motion.

Sunspot groups showing vortex structure indicating the rotation have been found to be associated with an increased occurrence of energetic flares (Sakurai, 1967; McIntosh, 1969, 1970; Sawyer and Smith, 1970).

There are also some observational arguments that the temporary changes of the H-alpha-vortex structure take place during the more important flares (Severny, 1969 b). Moreover, McIntosh (1969, 1970) mentions the rotation of spots as a pre-flare indicator.

Observations of magnetic field in active regions demonstrate that some flares are associated with regions of strong rotation of the transversal magnetic field (Severny, 1968 b). The rotation of directions of the transverse component of the magnetic field by 90° was found at the place where the flare appeared - by comparing these directions before and after the flare (Severny, 1969 a).

According to the suggestion of C. de Jager (1968) one may find evidence of the occurrence of the twisted magnetic fields in flare regions in Severny's photospheric magnetic field measurements. Vectors of the magnetic field in initial flare knots are not exactly directed to the next knot, but are inclined in that direction.

3.2 MOUSTACHES

Inclined moustaches are observed on some occasions both at the limb and on the disk (Severny, 1957, 1968 a; Öhman, 1968 c).

The main features of the inclined moustaches according to Severny (1968 a) are the following: besides the symmetric there are also the asymmetric and one-sided inclined moustaches; some of the moustaches change the sense of their inclination to the direction of dispersion within a few minutes; in some instances the inclined emission streaks of moustaches appear only for some lines, while the other lines do not display the inclination or show a slight inclination in the reversed direction. Severny (1957) found the line-widths of hydrogen and "metallic" moustaches to be nearly the same - this in turn indicates that in moustaches the macroscopic motions must be of importance for the mechanism of line broadening.

In order to account for the observed behaviour of the moustaches Severny (1965 a) proposed a model in the form of a transparent jet, or spherical shell, in which the broadening is due to a gradient of velocities. Later on Severny (1968 a) replaced this transparent model of moustaches by an opaque one of an expanding structure. However, as was already mentioned in the Introduction, not one of the expanding models may satisfactorily account for the observed inclination of lines.As one of the possible mechanisms of formation of moustaches Severny (1968 a) admits also the motion along a spiral trajectory.

Öhman (1968 b and c), on the other hand, has suggested that the inclined lines of moustaches may be produced by the rapid rotatory mass motion.

Recently reported observations by Bruzek (1972) indicate that moustaches are located at the base of the structured H-alpha chromosphere, and coincide with continuous facular granules. Lines of moustaches observed against the disc exhibit an absorbing and slightly Doppler - shifted streak, which in the core of H-alpha line is usually inclined to the direction of dispersion.

3.3 THEORY

Gold and Hoyle (1960), and following them several other authors, have considered the storage of free energy in twisted magnetic fields, i.e., in currents parallel to the magnetic field. The twist and the current might partly be preexistent in the field before it crosses the photosphere, but the major part will be induced afterwards by photospheric convection with rotational components. The flare will occur when twisted magnetic loops of opposite direction of the magnetic field and opposite twist coalesce. Such loops attract each other, and the annihilation of the longitudinal component of the field where they meet leads to a sudden constriction of the current, and through this, to a dissipation of the energy associated with that current.

Anzer (1968 a) has proposed a model of solar flares in which the accumulation, storage and energy release may be the consequence of the twisted magnetic fields. It is known that flares usually occur in the neighbourhood of sunspots. In the opinion of Danielson (1961 a and b), a penumbra filament - with magnetic field predominantly horizontally oriented - is in a state of rolling convection where the axis of rotation is parallel to the filament. Electrical conductivities are sufficiently high for the magnetic field to be frozen into convective rolls over the lifetime of the rolls. A magnetic tube extending out from a penumbra filament is usually anchored in an adjacent spot or somewhere in the neighbouring photosphere. It is obvius that both ends of such a magnetic tube can be in a different state of rotational motion, as a result of which the tube will be twisted up about its long axis. So, the initially current-free magnetic field may be transformed by a twist into the force-free field; in other words, the rotation induces currents which flow along the field. The energy of the twisted field is higher than the energy of the current-free field. The excess of energy is produced by the kinetic energy of rotational motions. As long as the stability of the magnetic field takes place, the process of accumulation of energy goes on. The energy release in solar flares proceeds when an instability occurs.

The problem of stability of the magnetic fields with helical lines of force was treated by Alfvén (1950 b), Lundquist (1951), Dungey and Loughhead (1954), and Agrawal (1969).

Anzer (1968 a and b) in connection with his flare model (Anzer, 1968 a) has studied the stability of certain force-free magnetic fields of uniform cylindrical symmetry. He found that for any degree of twist all force-free magnetic fields are unstable to the kink instability. On the other hand, Anzer has shown that the unstable perturbations are of helical symmetry, and therefore the fields with helical symmetry may exist in the neighbourhood of the cylindrically symmetric fields. These helical fields are stable if their twist is sufficiently small.

The stability analysis made by Anzer (1968 a and b) was performed for a periodic perturbation on an infinite flux rope. Recently Raadu (1972) carried out the stability analysis of the force-free field to a kink perturbation. Contrary to Anzer, he has considered a flux rope of a finite length imposing rigid boundary conditions at the ends. It was shown that for all the cases investigated by Anzer the kink instability is supressed by allowing a moderate degree of twisting and by taking a sufficiently short length of the flux rope. Thus, the fields of cylindrical configuration may accumulate and store the flare energy. The kink instability, and energy release, may occur when for a given finite length the degree of twisting becomes higher than a finite critical value.

Takakura and Kai (1966) have proposed a model of the flare structure where the high energy flare plasma has been identified as trapped particles in the field line system connencting two spots of opposite polarity. This model was in some extent modified by C. de Jager (1969) who introduced helically shaped magnetic fields instead of the field of Takakura and Kai.

According to the theory of solar flares (wich postulates the importance of the current filaments with high impedance regions) proposed by Alfvén and Carlqvist (1967), and Carlqvist (1968, 1969), the rotational mass motion is generated as a consequence of electric current system instabilities or their equivalent magnetic fields rearrangements. Carlqvist (1968, 1969) considers an energy as large as that of a flare to be stored in the twisted magnetic field of a current filament. If the current density of the filament becomes sufficiently large, an instability develops which leads to the creation of a high-impedance region in the filament. In turn, the stored magnetic energy is dissipated, and the filamentary current decreases. As a result, the helical magnetic field lines inside the filament should be twisted back and straightened. If the magnetic field lines can be considered to be frozen into the plasma during the energy release - the magnetic field will then force the filamentary plasma to rotate. Carlqvist admits that moustaches can be explained by the rotational motion of the current filament during the energy release. The observed emission of moustaches may come from rotating small dense parts of the filament. An upper limit to the velocity of rotation, v_0 may be estimated considering a filament of the length L with the azimuthal and axial components of the magnetic field nearly equal on the border of the filament. During the time of energy release, t_0 when the magnetic field lines are to be twisted back and straightened, the plasma starts to rotate near the high-impedance region with a velocity of $v_0 \sim L/2t_0$ With $L=10^8$m and $t_0=10^2$s the velocity of rotation is $v_0 \approx 5 \cdot 10^5$m/s, which corresponds to a Doppler displacement of 11 A of the H-alpha line. This is comparable with extension of the emission wings of the moustaches.

It is obvious that the energy of a magnetic field increases with the twisting of the magnetic lines of force. Nakagawa et al. (1971) have evaluated that a small twist of the magnetic field of a spot is sufficient to produce a flare. If the potential field $(\theta=0)$ of a typical spot - containing the amount of magnetic energy of the order of 10^{33} erg - is twisted to the spiral-angle of $\theta=60°$, then the magnetic energy increases twice. The twist from $\theta=20°$ to $30°$ gives an energy increase of 10^{32} erg.

A model of the storage of flare energy, efficient acceleration of electrons, and triggering of the flares was recently proposed by Takakura (1971 a and b). This model involves the rotation of two spherical clouds in the same direction in the presence of magnetic fields of opposite polarities - without satisfying the condition of freezing. These rotating spheres are responsible for the generation of quasi-static electric fields, in which electrons are effectively accelerated. The electrons excite plasma waves which make the conductivity lower by several orders in the lower corona. As a result, the electromagnetic energy (I^2L) stored before the onset of the flare is rapidly converted in about 10 s into the heat due to the ohmic loss.

4. Spicules

4.1 OBSERVATIONS

The majority of emission lines of individual spicules exhibit inclination to the direction of dispersion. Observations of inclined lines in the limb emission spectra of spicules were reported by Michard (1954), Athay and Bessey (1964), Giovanelli et al. (1965), Beckers (1966, 1968), Beckers et al. (1966), Livschitz (1966), Nikolsky and Sazanov (1966), Nikolsky (1970), Jefferies (1967), Noyes (1967), and Mamedov and Orudzhev

(1969).

Fine absorption features recorded in the disk spectra often show inclinations. These are observed not only in quiet regions (Beckers, 1964; Zirin, 1966; Figure 19b) but also in active regions (Haugen, 1967; Öhman, 1968 b; Öhman et. al., 1968). Some of the features are suspected to be spicules seen on the disk.

The observed tilt of the lines of some spicules is - in the opinion of Beckers (1966, 1968), Beckers et al. (1966), Jefferies (1967), Noyes (1967), Pasachoff (1968), Pasachoff et al. (1968), Rodionov (1968), Mamedov and Orudzhev (1969) - due to spicular rotation.

Noyes (1967) gives an interesting record of the time development of one of the tilted features observed in the H CaII line at a fixed height above the limb. It is clearly seen that the tilt undergoes a steady evolution of its inclination passing through zero and, afterwards, reversing the direction of inclination. The broad and doubly-peaked profile at the phase of maximum inclination becomes narrower and narrower as the line acquires the zero-tilt. Moreover, the line center exhibits a shift toward the red by 16 km/s at the phase of the zero-tilt. A reasonable explanation of this event must be founded on the rotational mass motion. Other observations indicating the different velocities on the opposite sides of spicules were reported by Pasachoff et al. (1968). A series of filtergrams taken simultaneously at $\pm$ 0.3 A from the center of the K - line show that more than half of the investigated spicules exhibit a definite difference in position of about 450 km between the +0.3 A and -0.3 A images.

4.2 THEORY

A model of the spicule giving the best coincidence of the theoretical profile of K CaII line with the observed one is that of a spinning spicule (Avery, 1970).

The line profiles resulting from rotating optically thick spicules were also calculated by Mamedov and Orudzhev (1970).

Rompolt (1972) computed a series of profiles for optically thin - but Doppler-brightened (Rompolt, 1967 a and b, 1969) - spinning filaments (spicules).

5. Facule

5.1 OBSERVATIONS

Polupan (1969) - on the basis of the observed lines in facule - came to the conclusion that the matter in facule moves along spiral trajectories. The limb observations show that the hydrogen emission lines are smeared to the red and to the violet, whereas their core part is unshifted. On the other hand, the disk observations in the $K_{2,3}$ lines exhibit the presence of vertically directed motions (St. John, 1910; Khokhlova, 1957).

Stojanova (1970) found from the analysis of the maps of the brightness distribution in the core of the H-alpha, H-beta and H_2 CaII lines, and continuum that the facular emission originates in magnetic ropes inclined at various angles to the horizontal plane. The direction of the inclination of the faculae changes with height. There is a tendency of a general inclination of the faculae to the direction of the follower of a spot group. Stojanova (1970), and Krat and Stojanova (1971) came to the conclusion - on the basis of the interpretation of the observed behaviour of H_2 and K_2 lines - that calcium faculae may be considered as twisted magnetic ropes lying in a nearly horizontal plane. The pitch of the spiral rope can be as large as 1500 - 2000 km. The rotational velocities of spiralling matter deduced from H and K lines amount to several km/s. The predominating blue shift of emissions indicates the outward flow of material in facular ropes.

The strength of the magnetic field in some parts of faculae, measured simultaneously in H-alpha and Feλ6302 A lines, appeared to be constant (Abdussamatov and Stoyanova, 1971). At the same time, the maxima of the magnetic field intensities at two levels corresponding to both lines were observed to be displaced. These results can be interpreted in terms of the spiral configurations of magnetic fields in the investigated facular region.

6. Active Regions

There is growing evidence that solar magnetic fields are not smoothly distributed over the solar surface, but are concentrated in magnetic filaments each having a diameter of the order of 1 arc second or even less. Many discrete features of that size like pores, umbral granules, penumbral filaments, spicules, fibrils, dashes, prominence filaments, and so on, are confined within the magnetic filaments.

This magnetic quantization is especially clearly seen in high space resolution magnetometer observations. For example, a pronounced magnetic filamentary structure was observed by Beckers and Schröter (1968) in an active region, and by Livingston and Harvey (1969) in the Sun's quiet areas. Recently, Howard and Stenflo (1972), and Frazier and Stenflo (1972) found that more than 90 % of the total magnetic field of the Sun is concentrated in thin filaments. These filaments are of very high field strengths in plages and at the boundaries of supergranular cells. Magnetic field strength of a single magnetic filament - evaluated observationally by Livingston and Harvey (1969) - appeared to be of the order of 500 Gauss over an area of 1 arc second cross-section.

It is evident that the foot-points of a plasma filamentary structure (or of a tube consisted of many fine structures) anchored in the photosphere may not be in the same state of rotation. As a result, a twisted magnetic tube will be produced, because magnetic field lines in the solar atmosphere are generally "frozen-in" in the plasma. Occasionally a detwisting process may take place. The observed rotation of sunspots, the rotation of their surroundings, the H-alpha chromospheric vortices, the polarization effects of sunspot magnetic fields, and the long persistence of large preceding spots for even a few months, suggest the reality and importance of twisted fields.

6.1 SUNSPOTS

The vortex configuration of the penumbra filaments of some sunspots, indicating the rotational motion, has been known for at least a hundred of years. Pictures of sunspots designed by Secchi (1875) show a strong vortex structure of the whole penumbra (5 May 1854), and of the part of the penumbra (25 September 1866). The high resolution photographs of some spots also display the eddy pattern of the penumbral filaments (e.g., Danielson, 1961 a, Figure 4).

Kuklin (1964) ascertained that the whirl-like configuration of the penumbrae filaments is not such a rare phenomenon, especially in single, unipolar spots.

Rotational mass motion in a sunspot having a strongly twisted magnetic field (Stepanov and Gopasyuk, 1962) was investigated by Kuklin and Stepanov (1963 a). It was shown that mass motion takes place in the direction of the twisted magnetic field lines. The rotation of the spot turned out to be not uniform during the 5 days; the mean velocity of rotation was of about of 180 m/s. Under the assumption that magnetic field lines are "frozen-in" into the plasma of the spot, a correspondence was established between the direction of the magnetic field lines and the filaments of the penumbrae at the photospheric level (Kuklin and Stepanov, 1963 a) on the one side, and the chromospheric H-alpha fine structure (Tsap, 1964) on the other side.

The rotation of a leader sunspot in the plage region No 10344, first 130° counterclockwise, then 142° clockwise in only 8 days was reported by Miller (1971).

Rotational mass motion in the Secchi ring of sunspots (a transitional zone at the border umbra-penumbra, somewhat brighter than penumbra) was investigated by Chistyakov (1971). The outer boundary of a Secchi ring takes part in anticyclonic motion with angular velocities of about 0.25 degree/hour (one complete revolution in 60 days), and the inner boundary - in cyclonic motion with angular velocities of about 0.75 degree/hour (one complete revolution in 20 days). The nature of such a mass rotation is not fully understandable.

Chistyakov (1964 a and b) using isodensity maps of a number of sunspots revealed that there are well defined bright features in the outer region of a bright ring surrounding the spots. These features have a characteristic scale of around 9" and a lifetime of about 2 days. The change in position of these bright features, measured in two subsequent days, led to the conclusion that the photosphere in the outer region of a bright ring is in a state of the vortex anticyclonic motion with angular velocities in between 0.75 and 2.5 degree/hour (one complete revolution in 20 and 6 days respectively).

6.2 SUNSPOT SORROUNDINGS

A. Photospheric Vortex Structure

Calamai (1934) discovered that spots forming some groups move along logarythmic spiral-like paths. The direction of spiral motion is clockwise in the northern hemisphere and anticlockwise in the southern.

Gnevysheva (1941), while investigating the proper motion of spots in sunspot groups revealed a vortex motion of some spots indicating the vortex motion of the whole group. The evaluated velocity of the vortex motion was about 300 m/s at a distance of 26 000 km from the vortex center, and about 10 - 30 m/s at a distance of 50 000 - 60 000 km. Three individual spots of a sunspot group exhibited the same direction of the vortex motion as the whole group, at a rate of one revolution in 30 days.

The existence of the vortex motion in sunspot groups was also confirmed by Brunner-Hagger (1941). The estimated time of revolution of a group - 7 days at a distance of around 30 000 km - is in good accordance with the 9 days time of revolution at the same distance derived from the vortex motion of pores located in the close vicinity of sunspots (Nikitenko, 1963).

The rotational movement of sunspots around the central spot was reported by Dezső et al. (1971), and for small high-latitude spots by Kuklin (1959, 1970).

A sequence of high resolution photographs of a complex spot, secured by Bumba and Suda (1970), shows the development of two main logarythmic spiral-like branches of small nuclei and parts of the penumbra separated from the main spot.

A scheme of the large scale flows in the solar photosphere was constructed by Starr and Fischer (1971) on the basis of the Greenwich sunspot data covering the years 1905-1954. The authors came to the conclusion that active regions and sunspot groups are generally located in an area of anticyclonic circulation.

B. Chromospheric Vortex Structure

The H-alpha vortex topology of fibrils and chromospheric filaments seen on some occasions in the vicinity of sunspots indicates the presence of large scale rotation in active regions. The H-alpha vortices were investigated extensively by Hale (1908, 1919, 1925) at the beginning of our century. Richardson (1941) - on the basis of Hale's and his own observations - concluded that under perfect visibility conditions about one-third of all spots with areas greater than 200 millionth of the visible hemisphere might be expected to show H-alpha vortices. About 60 % of the observed forms appear to be open vortices; closely wound vortices are observed but on rare occasions.

Nowadays, it is generally accepted that the H-alpha fine structure follows magnetic field lines (Tsap, 1964; Smith, 1968; Deubner and Göring, 1970 a and b; Foukal, 1971 a and b; Prata, 1971; Zirin, 1972). So, the observed H-alpha vortex structure reflects the rotation of the magnetic field of a sunspot situated in the center of a vortex.

6.3 ARCH FILAMENT SYSTEMS

The very first indication of an active region arising is the appearance of a region of unusual H-alpha brightness (Waldmeier, 1937),and the emergence within it of a system of dark loops parallely oriented (Weart and Zirin, 1969). The loops - named after Bruzek (1967, 1969) Arch Filament Systems or AFSs - continue to emerge for a day or so. Initially the AFSs are slanted with regard to the local line of solar meridian, sometimes by less than 45°. Next, the loops tend to become more organized into an east-west bipolar configuration during the course of a day. In some cases, the major part of rotation occurs as a single "jerk" lasting less than two hours. The tilt of AFSs orientation may change even by 20°in an hour - which is too fast to be caused by Coriolis or convective forces.

According to Weart (1972) the simplest field configuration which would give this effect is a twisted flux tube. In such a tube the projected inclination of the field lines changes with depth; the lines situated deeper emerge later on, and are not so steeply inclined to the equator. Weart (1970 a) has ascertained that most newly forming AFSs may be classified in one of two distinct groups: with a "correct" initial tilt relative to the equator (preceding polarity nearer the equator), and with an "incorrect" one. Both types of arches rotate during the first day of appearance, but in opposite directions, as if they represented a kind of flux tube twisted with opposite handedness. The new AFSs with a "correct" tilt are much more likely to grow up over the next five days than the "incorrect" ones. The observed twist seems to be related to the known asymmetry of sunspot groups. As will be documented in this paper in the section "Dynamo Action", supergranular convection currents can twist the individual arch filaments - the long upper filament in Weart's (1972)

Figure 3 seems to possess a rather clear helical structure.

On the other hand, Frazier (1972) argues that the observed rotation of the axis of an AFS in the local horizontal plane is the effect of the emergence of successive loops.

6.4 MAGNETIC FIELDS

According to Severny (1959 b) the observed transversal components of the magnetic field in spot penumbrae, the vortices around spots, and the shape and orientation of the closed neutral lines around unipolar spots favour the concept of the spiral-like force-free field of some spots.

The photoelectric polarization measurements of some sunspots revealed the vortex structure of their magnetic fields (Stepanov and Severny, 1962; Severny, 1965 c; Deubner and Göhring, 1970 a and b). The field direction was always in good agreement with that of the overlying chromospheric structures. A magnetic field region exhibiting a pronounced vortex structure is clearly seen in a Zeeman spectroheliogram taken by Vrabec (1971) on 29 September 1969.

The magnetic field measurements also supply evidence that small scale magnetic tubes in sunspots and their surroundings are strongly twisted (Severny, 1972).

Magnetic measurements secured at the Crimean Astrophysical Observatory simultaneously at two levels corresponding to λ6103 and λ5250, revealed the existence of the twisted fields somewhere in an active region of the photosphere (Severny, 1968). In some places the directions of the transverse field differ by as much as 90° at a height difference of only 160 km. Also polarization measurements in the λ5250 line indicate that the rotation of the transversal components of the magnetic field is pronounced in the region of strong fields near spot umbrae, where it reaches sometimes 90° in a time of about 2 hours (Severny, 1964). This seems to provide evidence of the presence of the twisted magnetic tubes in some sunspots and in some parts of active regions. u

The above conclusions were confirmed by the recordings of the transverse field in three lines of different intensity: λ5302, λ5250 and λ4808 (Severny, 1965 b). The measurements show an appreciable rotation of the transverse vector from one line to another. The rotation with time appears to be considerably smaller than rotation with depth, which sometimes attains 80° at a depth difference of 100 km.

Kuklin and Stepanov (1963 b) carried out an evaluation of the amount of rotation of the magnetic field of the same leader as investigated previously (Kuklin and Stepanov, 1963 a), but observed on 6 September 1961. The magnetic field showed a twisting clockwise rotational motion with a velocity of 300 - 400 m/s. The magnetic field at the peripheral part of the spot made a complete turn in 3.7 days, while the field observed at the border region umbra-penumbra- in 1.3 days. On 7 and 8 September a detwisting anticlockwise rotational motion took place.

Recordings of the magnetic field at two different photospheric levels (FeI λ4808 and CaI λ6103 . the height difference of 170 km) made by Kotov (1970 a and b) show the presence of a strong transversal field within the umbra, and large (up to 90°) changes in the orientation of the transversal component with depth in certain parts of the spot. The clockwise twist of the field lines is stronger at the lower level, pointing to the increase of twisting with depth. The same sense of twisting is observed in the H-alpha chromospheric structure photographed simultaneously with magnetic measurements. The magnetic data permitted the calculation of the vertical and horizontal electric currents in the investigated spot. Their spatial configuration appeared to be in the form of a spiral current filament emerging from the deeper layers. The total electric current contained in the current filament was of the order of $6x10^{12}$ A. In Kotov's opinion the magnetic field in the investigated spot seems to be not of a force-free character, because the electric currents were directed mainly perpendicularly to the direction of the transversal field.

Magnetic observations of a sunspot group carried by Abdussamatov (1970) by means of the photographic method and a Wollaston prism are in favour of the hypothesis suggesting that the sunspots are composed of a number of twisted magnetic tubes (see also Abdussamatov and Krat, 1969).

Title and Andelin (1971) using the spectra-spectroheliography technique found that the transverse magnetic field changes direction by 90° within 1 - 2 arc seconds in some normal round spots at the boundary between the umbra and the penumbra. Moreover, the transverse field in complex spots may change direction by 90° in 0.5 arc second or less.

Gokhale and Zwaan (1972) represent the opinion that the magnetic field in a large pore is more strongly twisted than in a complete spot of the same magnetic flux. The ratio of umbral area to total area of a spot may be larger in the more strongly twisted magnetic structure.

6.5 THEORY

Some models of the magnetic field configuration of spots involve the twisted magnetic field.

Bumba (1962 b), on the basis of the observed polarization effects of sunspot magnetic fields (Bumba, 1962 a and b), proposed a model of the magnetic structure in sunspot umbra, in which the field lines are inside a tube of force proceeding from the umbra, twisting into spirals having a pitch angle steeply increasing with height. At the photospheric level the lines of force are twisted to a horizontally oriented ring, while high in the corona they are nearly vertical.

Stepanov and Gopasyuk (1962) also suggested a model of strongly twisted magnetic tubes for the follower of the group, in order to account for the behaviour of the total vector of the magnetic field observed during the 8 days in a spot group (see also Stepanov, 1965).

Twisted magnetic fields in the force-free models of sunspots were considered by a number of authors. Schatzman (1961, 1965), Molodensky (1966), Nakagawa et al. (1971), and Nakagawa and Raadu (1972) showed that the observed H-alpha vortices could be well interpreted in terms of the configuration of lines of force of an axisymmetric force-free chromospheric magnetic field in the vicinity of an isolated sunspot. Subsequently, Raadu and Nakagawa (1971), and Nakagawa and Raadu)1972) demonstrated that the same good agreement may be obtained between the observed H-alpha vortices and a force-free magnetic field near bipolar sunspots.On the basis of their sunspot magnetic field model they obtained a good correspondence between the observed and predicted orientation of prominences formed in association with sunspots.

Force-free models of sunspots were also considered by Kuklin (1964, 1966).

Merkulenko (1971) - on the basis of Kotov's (1970 a and b)observations - proposed a model of the sunspot with the twisted magnetic field being force-free only in the region of the umbra. It was shown that the gas pressure difference between a sunspot and the photosphere corresponds best of all to the transparent Michard's (1953) model. In order to understand the forces supporting the gas in the transparent model, Merkulenko admits the existence of a system of twisted magnetic tubes within a spot. Mogilevsky (1971) tries to explain a number of peculiarities observed in solar active regions, by a statistical model of the solar magnetoplasma consisting of a complex of small-scale current vortex plasma elements (subgranules).

Yun (1971) considered a magnetostatic sunspot model with a twisted field. It appeared that the internal structure of sunspots is affected only to a small degree by the presence of the azimuthal component of the sunspot magnetic field. The azimuthal component of the magnetic field can be ignored in the calculations of sunspot models with horizontal magnetostatic equilibrium.

Weart (1970 b) calculated the energy needed to twist a magnetic flux tube by the supergranular convection. If, according to Babcock's (1961) theory of the solar cycle, a subsurface latitudinal field exists, then supergranular convection necessarily creates pairs of twists in it. The calculations were made under the assumptions of uniform field, no change of length, and a spiral of uniform pitch throughout the tube. It was found that for a wide variety of assumptions (like the efficiency of twisting the field by the convective energy, the value of the accepted magnetic field strength) flux tubes of field strength of around 100 Gauss - with one twist and with maximum diameters in the range 1000 - 2000 km - are energetically reasonable. Tubes with smaller diameters can be created easily.

7. Coronal Structure

7.1 OBSERVATIONS

Clearly twisted coronal streamers are rare phenomena. One such streamer was recorded on a corona eclipse photograph of 22 September 1968 (Nesmjanovich, 1970). The photograph shows that the eastern streamer is of spiral form. The pitch of the streamer is much larger than its width and increases with height. Thin filaments in the twisted streamer grow in width with height; on the other hand, the streamer as a whole widens only slightly - at least in its lower part (Nesmjanovich et al., 1971). Four hours before the eclipse, flares of importance 2 took place in the active region underlying the streamer.

7.2 THEORY

According to Merkulenko (1969) the structure of the field in dark coronal arcs ought to be twisted. A magnetic loop with the ends fixed on the plane can be in equilibrium if the strength of the toroidal component of the magnetic field is equal to 0.25 of the poloidal component strength, and the magnetic force is balanced by hydrostatic pressure.

8. Radio - range

8.1 OBSERVATIONS

Observations of bi-polar type I storm centers completed by the

Culgoora radioheliograph operating at 80 MHz show that the bipolar centers are oriented in the opposite way, as one should expect for emission in the ordinary mode and for the simplest magnetic field geometry. McLean and Sheridan (1972) interpret this as evidence of a twist of large-scale magnetic tubes.

Radio emission at millimeter wavelengths indirectly seems to indicate that its occasionally observed enhancement, about one day prior to a flare of importance 2 or 3 (Mayfield et al., 1970), is generated that the maximum of 10 % enhancement during the two days preceding the 3b flare of 27 September 1969 coincided with the central region of the vortex field (see also Vrabec, 1971), where the two polarities were contiguous.

On the basis of radio (Riddle, 1970) and optical observations (Cain, 1969; McCabe and Fisher, 1970) of a spray propagation through the corona, Riddle (1970) inferred that the radiating source was - at the distance 2 to 5.25 Sun's radius from the centre of the Sun - in the form of a smoke ring with the twisted magnetic field within it.

9. Dynamo Action

9.1 OBSERVATIONAL MODELS

Babcock's (1961) model of the origin of solar magnetic fields implies formation of the twisted magnetic tubes in the active regions. Lines of force of an initial axisymmetric dipolar field are at first stretched in longitude and wrapped in the Sun's surface layers. The irregular magnetic flux strands are then twisted by the faster rotating shallow layers in low latitudes. As a result, magnetic ropes are formed which in turn are brought to the surface by magnetic buoyancy.

Also the model proposed by Leighton (1964; 1969) suggests that twisted magnetic tubes may be produced as an initially untwisted fluxtube is rolled along by a radial gradient of the Sun's differential rotation. A rapidly rotating solar interior is here postulated. The observed predominance and longer persistence of preceding spots is probably caused by the stabilizing action of the more tightly twisted magnetic lines of force in these spots than in the following spots. Such twisted magnetic tubes offer more resistance against the process of fragmentation induced by the supergranulation currents. In most cases the differential rotation, acting on the field of a preceding spot, will tend to twist it in the direction of the observed chromospheric vortex structure, thus increasing its twist and enhancing the stability.

9.2 THEORETICAL MODELS

It has been known for several decades (Cowling, 1934, 1953, 1957; Alfvén, 1950 a) that a turbulent conducting fluid interacts strongly with the magnetic fields in the fluid, twisting and stretching it into complicated patterns of intense field, depending upon the initial magnetic field configuration, and the velocity field. This phenomenon is considered as the starting point for solar dynamo theory.

Rotational mass motions as well as the rotation and twisting of emerging magnetic flux tubes are expected according to the dynamo theory of the solar cycle developed mainly by Parker (1955 a and b, 1957, 1970 a and b, 1971 a and b - where references of other contributors are given) and by Steenbeck, Krause and Rädler (1966) in a series of papers (Krause and Steenbeck, 1967; Krause, 1968, 1969 a and b; Rädler, 1968 a and b, 1969 a and b; Steenbeck and Krause, 1969).

The dynamo theory explains the formation of new poloidal magnetic field components from toroidal components by cyclonic (vortex) motions of convective cells (Parker, 1955 b). The cyclonic motions are produced by the combined action of the nonuniform Sun's rotation and the Coriolis forces. At the time of eruption of a magnetic tube, the upward-moving plasma expands laterally, and Coriolis forces constrain it to rotate more slowly than its surroundings. This leads to twisting the magnetic loop frozen-in into the emerging plasma. A new, reverse poloidal field develops as a result of an adequate twisting and coalescing of a large number of loops.

Steenbeck et al. (1966) emphasize the possibility of explaining the origin of solar magnetic fields - even in the absence of differential rotation - by one effect only, by the dynamo action of small-scale helical motions with a preferred turning.

A dynamo involving helical motions has been also demonstrated by Lortz (1968).

The dynamo theory predicts in addition to the kinking (twisting) of magnetic loops also the twisting of magnetic lines in the magnetic flux--tubes.

Another mechanism of creation of flux-ropes - by the interaction of turbulent eddies (photospheric granules) with a large-scale weak magnetic field - has been demonstrated by Parker (1963 a). At first, the eddies break up a uniform magnetic field initially extending straight across the region of turbulence into the flux-ropes. Next, each flux-rope is lenghtened and widened by the turbulent velocity into a convoluted sheet. The various loops and swirls in each given sheet ought to be soon uncorrelated with each other.

Weiss (1964) showed that turbulent convection can concentrate the magnetic flux into ropes which resemble observed bipolar magnetic regions and sunspots. As the observations indicate these ropes consist of many discrete magnetic filaments.

Parker (1963 b) computed the magnetic field distribution for a variety of given velocity fields in photospheric and subphotospheric layers. He used the well-known hydromagnetic equations relating the interaction of the velocity field of a conducting fluid to the magnetic field. Also in this case the magnetic lines of force of an initially uniform field in the circular fluid motion are twisted into a vortex. Consequently, the resulting density of the magnetic field considerably increases by the fluid motion.

10. Final Remarks

The writer realizes that some observational arguments, presented here as well as the theoretical ones, may not be up to date, or could be found fault with. However, for the sake of their historic or scientific significance they have been included in this review. In some cases the counterarguments have not been discussed here. The presented review makes no claim for completeness.

Acknowledgements

The author wishes to thank his colleagues at the Astronomical Observatory of the Wrocław University, especially Doc. Dr. T. Jarzebowski and Dr. J. Paciorek for their critical reading of the first version of this manuscript.

R e f e r e n c e s

Abdussamatov,H.I.: 1970, *IAU Symp.*43, *231.*
Abdussamatov,H.I., Krat,V.A.: 1969, *Solar Phys.* 9, *420.*
Abdussamatov,H.I., Stoyanova,M.N.: 1971, *Soln. Dannye* No. 10, *72.*
Agrawal,G.S.: 1969, *J. Phys. Soc. Japan* 26, *1519.*
Alfvén,H.: 1950a, *Cosmical Electrodynamics* (Clarendon)
Alfvén,H.: 1950b, *Tellus* 2, *74.*
Alfvén,H.: 1968, *Nobel Symp.* 9, *189.*
Alfvén,H., Carlqvist,P.: 1967, *Solar Phys.* 1, *220.*
Ambrož,P.: 1970, *personal communication.*
Anzer,U.: 1968a, *Solar Phys.* 3, *298.*
Anzer,U.: 1968b, *Solar Phys.* 4, *101.*
Anzer,U., Tandberg-Hanssen,E.: 1970, *Solar Phys.* 11, *61.*
Athay,R.G., Bessey,R.J.: 1964, *Astrophys.J.* 140, *1174.*
Avery,L.W.: 1970, *Solar Phys.* 13, *301.*
Babcock,H.W.: 1961, *Astrophys. J.* 133, *572.*
Beckers,J.M.: 1964, *Thesis* (Utrecht) *A.F.Cambr.Res.Lab.Environ. Res. Paper, No.* 49.
Beckers,J.M.: 1966, in K.O.Kiepenheuer (ed.) *'The Fine Structure of the Solar Atmosphere'*, (Wiesbaden) *82.*
Beckers,J.M.: 1968, *Solar Phys.*3, *396.*
Beckers,J.M., Noyes,R.W., Pasachoff,J.M.: 1966 *Astron J.*71, *155.*
Beckers,J.M., Schőter,E.H.: 1968, *Solar Phys.* 4, *142.*
Berge,G.: 1959, *HAO Solar Research Memo., No.* 129.
Billings,D.: 1957, *Publ. Astron. Soc. Pacific* 69, *407.*
Bostick,W.H.: 1966, in *Pubbl. IV. Cent. di Galilei* (Firenze) Vol.II. *Tomo 2, 218.*
Brunner-Hagger,W.: 1941, *Astron. Nachr.* 272, *153.*
Bruzek,A.: 1967, *Solar Phys.* 2, *451.*
Bruzek,A.: 1969, *Solar Phys.* 8, *129.*
Bruzek,A.: 1972, *Solar Phys.* 26, *94.*
Bumba,V.: 1962a, *Bull. Astron. Inst. Czech.*13, *42.*
Bumba,V.: 1962b, *Bull. Astron. Inst. Czech.*13, *48.*
Bumba,V., Suda,J.: 1970, *IAU Symp.* 43, *201.*
Cain,S.: 1969, *Sky Telesc.* 37, *289.*
Calamai,G.: 1934, *Oss. Mem.Oss.Astr.* Fasc.52, *41.*
Carlqvist,P.: 1968, *Nobel Symp.* 9, *193.*
Carlqvist,P.: 1969, *Solar Phys.* 7, *377.*
Chistyakov,V.F.: 1964a, *Thesis, Vladivostok.*
Chistyakov,V.F.: 1964b, *Soln. Dannye No.* 2, *56.*
Chistyakov,V.F.: 1971, *Issledovanja po Geomagnetizmu, Aeronomii i Fizike Solnca* 2, *60.*
Cowling,T.G.: 1934, *Monthly Notices R.A.S.* 94, *39.*
Cowling,T.G.: 1953, in G.P. Kuiper (ed.) *'The Sun'*, (Chicago) *532.*
Cowling,T.G.: 1957, *'Magnetohydrodynamics'* (Interscience Publ.)
Danielson,R.E.: 1961a, *Astrophys. J.* 134, *275.*
Danielson,R.E.: 1961b, *Astrophys. J.* 134, *289.*
De Jager,C.: 1968, *Nobel Symp.* 9, *209.*
De Jager,C.: 1969, in C. de Jager and Z. Svestka (ed.) *'Solar Flares and Space Research'*, (North-Holland Publ.) *1.*
Deubner,F.L., Gőhring,R.: 1970a, *Solar Phys.* 13, *118.*
Deubner,F.L., Gőhring,R.: 1970b, *IAU Symp.* 43, *190.*

Dezső,L., Gyertyános,G., Kálmán,B., Kovács,A.: 1971, *Soln. Dannye No.* 7, *77.* , *and in this Volume.*
Dizer,M.: 1968, *Solar Phys.* 4, *99.*
Dungey,J.W., Loughhead,R.E.: 1954, *Australian J. Phys.* 7, *5.*
Dunn,R.B.: 1972, *Mercury, May/June, cover photograph.*
Ellison,M.A.: 1947, *J.Br. Astron. Ass.*57, *229.*
Engvold,O., Livingston,W.: 1971, *Solar Phys.* 20, *375.*
Foukal,P.: 1971a, *Solar Phys.* 19, *59.*
Foukal,P.: 1971b, *Solar Phys.* 20, *298.*
Frazier,E.N.: 1972, *Solar Phys.* 26, *130.*
Frazier,E.N., Stenflo,J.O.: 1972, *Solar Phys.* 27, *330.*
Giovanelli,R.G., Michard,R., Mouradian,Z.: 1965, *Ann.Astrophys.* 28, *871,*
Gnevysheva,R.S.: 1941, *Astr. Zhurn. Akad Nauk SSSR* 18, *27.*
Gokhale,M.H., Zwaan,C.: 1972, *Solar Phys.*26, *52.*
Gold,T.: 1968, *Nobel Symp.* 9, *205.*
Gold,T., Hoyle,F.: 1960, *Monthly Notices R.A.S.* 120, *89.*
Hagen,J.P., Neidig,D.F. Jr.: 1970, *Astrophys. J.* 161, *751.*
Hale,G.E.: 1908, *Astrophys. J.* 28, *100.*
Hale,G.E.: 1925, *Proc. Nat. Acad. Sci.* 11, *691.*
Hale,G.E., Ellerman,F., Nicholson,S.B., Jay,A.H.: 1919, *Astrophys. J.* 49, *153.*
Harvey,J.W.: 1969, *Thesis, University of Colorado.*
Haugen,E.: 1967, *Solar Phys.*2, *227.* 6
Howard,R., Stenflo,J.: 1972, *Solar Phys.* 22, *402.*
Jefferies,J.T.: 1967, *IAU Symp.*28, *467.*
Kawaguchi,I., Oda,N., Mizuno,S.: 1972, *Solar Phys.*22, *140.*
Khokhlova,V.L.: 1957, *Izv. Krym. Astr. Obs.* 17, *177.*
Kiepenheuer,K.O.: 1953, in G.P. Kuiper (ed.) *'The Sun'*, (Chicago) *322.*
Kiepenheuer,K.O.: 1968, *Nobel Symp.*9, *123.*
Kippenhahn,R., Schlüter,A.: 1957, *Z.Astrophys.* 43, *36.*
Kleczek,J.: 1963, *Bull. Astron. Inst. Czech.* 14, *86.*
Kleczek,J.: 1968, *IAU Symp.*35, *280.*
Kotov,V.A.: 1970a, *IAU Symp.* 43, *212.*
Kotov,V.A.: 1970b, *Izv. Krym. Astr. Obs.* 41-42 *67.*
Koval,A.N., Stepanjan,N.N.: 1972, *Soln. Dannye No.* 1, *83.*
Krat,V.A.: 1968, *Nobel Symp.*9, *89.*
Krat,V.A., Stojanova,M.N.: 1971, *Solar Phys.* 20, *57.*
Krause,F.: 1968, *Z. angew. Math. Mech.* 48, *333.*
Krause,F.: 1969a, *Acta Universitatis Wratislaviensis* (Mat.Fiz.Astr.)8 *157.*
Krause,F.(1969b, *Monatsber. Deutsch. Acad. Wiss.* 11, *188.*
Krause,F., Steenbeck,M.: 1967, *Z. Naturforschung* 22a, *671.*
Kuklin,G.V.: 1959, *Thesis, Irkutsk University.*
Kuklin,G.V.: 1964, *Soln. Dannye No.* 7, *45.*
Kuklin,G.V.: 1966, *Pubbl. IV. Cent. di Galilei* (Firenze) Vol.II. *Tomo 4. 216.*
Kuklin,G.V.: 1970, *Issledovanja po Geomagnetizmu,Aeronomii i Fizike Solnca* 10, *161.*
Kuklin,G.V., Stepanov,V.E.: 1963a, *Soln. Dannye No.*1, *55.*
Kuklin,G.V., Stepanov,V.E.: 1963b, *Soln. Dannye No.*2, *45.*
Kuperus,M.: 1971, a review paper presented at the Colloquium on "Physics of Prominences (see *Solar Phys.*24, *3*).
Kurochka,E., Kurochka,L., Stembcovskaya,T.: 1971, *Soln. Dannye No.*4, *87.*

Leighton,R.B.: 1964, *Astrophys. J.* 140, *1547.*
Leighton,R.B.: 1969, *Astrophys. J.* 156, *1.*
Lindberg,L., Witalis,E., Jacobsen,C.: 1960, *Nature* 185, *452.*
Livingston,W., Harvey,J.: 1969, *Solar Phys.*10, *294.*
Livshitz,M.A.: 1966, *Astr. Zhurn. Akad. Nauk SSSR* 43, *718.*
Lortz,D.: 1968, *Phys. Fluids* 11, *913.*
Lundquist,S.: 1951, *Phys. Rev.*83, *307.*
Machado,M.E.: 1971, *Bull. Astron. Inst. Czech.* 22, *117.*
Machado,M.E., Gallegos,H.G.: 1972, *Solar Phys.* 23, *340.*
Mamedov,S.G., Orudzhev,E.Sh.: 1969, *Solar Phys.* 6, *41.*
Mamedov,S.G., Orudzhev,E.Sh.: 1970, *Soln. Dannye No.*11, *106.*
Martres,M.J., Soru-Escaut,I.: 1971, *Solar Phys.* 21, *137.*
Martres,M.J., Soru-Escaut,I., Rayrole,J.: 1971, *IAU Symp.* 43, *435.*
Mayfield,E.B.: 1971, *IAU Symp.* 43, *376.*
Mayfield,E.B., Higman,J., Samson,C.: 1970, *Solar Phys*13, *372.*
McCabe,M.K., Fisher,R.R.: 1970, *Solar Phys.*14, *212.*
McIntosh,P.S.: 1969, *Report UAG-5* (Boulder) *14.*
McIntosh,P.S.: 1970, *Report UAG-8* (Boudler) *22.*
McLean,D.J., Sheridan,K.V.: 1972, *Solar Phys.* 26, *176.*
Menzel,D.H., Smith,E.P., De Mastus,H., Schnable,G., Lavrènce,R.: 1956, *Astron.J.* 61, *186.*
Menzel,D.H., Wolbach,J.G.: 1960, *Sky Telesc.* 20, p.*254.*
Merkulenko,V.E.: 1968a, *Soln.Dannye No.*3, *92.*
Merkulenko,V.E.: 1968b, *Soln. Dannye No.*8, *73.*
Merkulenko,V.E.: 1969, *Soln. Dannye No.* 8, *81.*
Merkulenko,V.E.: 1971, *Issledovanja po Geomagnetizmu, Aeronomii i Fizike Solnca* 20, *125.*
Michard,R.: 1953, *Ann. Astrophys.* 16, *217.*
Michard,R.: 1954, *Observatory* 74, *209.*
Miller R.A.: 1971, *Solar Phys.* 16, *373.*
Mogilevsky,E.I.: 1971, *IAU Symp.* 43, *480.*
Molodensky,M.M.: 1966, *Astr. Zhurn. SSSR* 43, *727.*
Nakagawa,Y., Raadu,M.A.: 1972, *Solar Phys.*25, *127.*
Nakagawa,Y., Raadu,M.A., Billings,D.E., McNamara,D.: 1971, *Solar Phys.* 19, *72.*
Nesmjanovich,A.T.: 1970, *Astron. Vestnik*4, *123.*
Nesmjanovich,A.T., Dzjubenko,N.I., Chomenko,Yu.A., Popov,O.S.: 1971, *Astron. Cirk. Izdav. Bjuro Astron. Soob.*(Kazan)*No.*657, *1.*
Nikitenko,L.A.: 1963, *Soln. Dannye No*7, *60.*
Nikolsky,G.M.: 1970, *Solar Phys.*12, *379.*
Nikolsky,G.M., Sazanov,A.A.: 1966, *Astron. Zhurn. SSSR* 43, *928.*
Noyes,R.W.: 1967, *IAU Symp.* 28, *467.*
Ogir,M.B.: 1971, *Izv. Krym. Astr. Obs.* 43, *157.*
Öhman,Y.: 1951, *Astrophys. J.* 114, *367.*
Öhman,Y.: 1968a, *Nobel Symp.* 9, p.*14.*
Öhman,Y.: 1968b, *IAU Symp.* 35, *240.*
Öhman,Y.: 1968c, in L. Perek (ed.) *'Highlights of Astronomy'*, (Reidel) *533.*
Öhman,Y.: 1969, *Solar Phys.* 9, *427.*
Öhman,Y.: 1970, *Scientia* 105, *1.*
Öhman,Y.: 1972, *Solar Phys.* 23, *134.*
Öhman,Y., Hosinsky,G., Kusoffsky,U.: 1968, *Nobel Symp.* 9, *95.*
Öhman,Y., Stiber,G., Kusoffsky,U.: 1967, *Solar Phys.* 1, *60.*

Palus,P.: 1972, *Bull. Astron. Inst. Czech.* 23, *60.*
Parker,E.N.: 1955a, *Astrophys. J.*121, *491.*
Parker,E.N.: 1955b, *Astrophys. J.*122, *293.*
Parker,E.N.: 1957, *Proc. Nat. Acad. Sci.* 43, *8.*
Parker,E.N.: 1963a, *Astrophys. J.*138, *226.*
Parker,E.N.: 1963b, *Astrophys. J.*138, *552.*
Parker,E.N.: 1970a, *Ann. Rev. Astron. Astrophys.*8, *1.*
Parker,E.N.: 1970b, *Astrophys. J.*162, *665.*
Parker,E.N.: 1971a, *Astrophys. J.*163, *279.*
Parker,E.N.: 1971b, *Astrophys. J.*164, *491.*
Pasachoff,J.M.: 1968, *IAU Symp.* 35,*245.*
Pasachoff,J.M., Noyes,R.M., Beckers,J.M.: 1968, *Solar Phys.*5, *131.*
Pettit,E.: 1925, *Publ. Yerkes Obs.* 3, *Part 4, 205.*
Pettit,E.: 1932, *Astrophys. J.* 76, *9.*
Pettit,E.: 1941, *Publ. Astr. Soc. Pacific* 53, *289.*
Pettit,E.: 1943, *Astrophys. J.* 98, *6.*
Pettit,E.: 1946a, *Publ. Astr. Soc. Pacific* 58, *150.*
Pettit,E.: 1946b, *Publ. Astr. Soc. Pacific* 58, *310.*
Pettit,E.: 1950, *Publ. Astr. Soc. Pacific* 62, *144.*
Pettit,E., McMath,R.R.: 1937, *Astrophys. J.* 85, *279,* Plate XIV.
Pneuman,G.W.: 1971, *Solar Phys.* 19,*16.*
Polupan,P.N.: 1969, *Visnik Kijev, Univ.* 11, *ser. astron., 27.*
Prata,S.W.: 1971, *Solar Phys.* 20, *310.*
Prokofjeva,I.A.: 1957, *Soln. Dannye No.*4, *132.*
Raadu,M.A.: 1972, *Solar Phys.* 22,*425.*
Raadu,M.A., Nakagawa,Y.: 1971, *Solar Phys.*20,*64.*
Rädler,K.H.: 1968a, *Z. Naturforschung* 23a, *1841.*
Rädler,K.H.: 1968b, *Z. Naturforschung* 23a, *1851.*
Rädler,K.H.: 1969a, *Monatsber.Deutsch. Acad. Wiss.* 11, *194.*
Rädler,K.H.: 1969b, *Monatsber. Deutsch. Acad. Wiss.* 11, *272.*
Richardson,R.S.: 1940, *Publ. Astr. Soc. Pacific* 52,*326.*
Richardson,R.S.: 1941, *Astrophys.J.*93, *24.*
Riddle,A.C.: 1970, *Solar Phys.* 13, *448.*
Roberts,W.O.: 1964, *Sky Telesc.* 5, *11.*
Rodionov,V.V.: 1968, *Vestnik Moskovskovo Univ.* Fiz. Astr. 4, *33.*
Rompolt,B.: 1967a, *Acta Astron.* 17, *329.*
Rompolt,B.: 1967b, *Acta Universitatis Wratislaviensis No.*75, *Contr. Wroclaw Obs. No.*15.
Rompolt,B.: 1969, *Acta Universitatis Wratislaviensis No.*77, *117, Contr. Wroclaw Obs. No.*17.
Rompolt,B.: 1971a, this Volume.
Rompolt,B.: 1971b, to be published in *Acta Univ. Wratislaviensis*
Rompolt,B.: 1971c, to be published in *Solar Phys.*
Rompolt,B.: 1972, to be published in *Contr. Astron. Obs. Skalnate Pleso.*
Rompolt,B., Kozar,T., Szumiejko,E.: 1969, *Geod. Geoph. Veröff.* (Berlin) R.II, H.13, *55.*
Rybanský,M.: 1971, *Bull. Astr. Inst. Czech.* 22, *380.*
Sakurai,K.: 1967, *Report Ionosphere Space Res. Japan* 21, *113.*
Sawyer,C., Smith,S.F.: 1970, *Report UAG-9,* (Boulder) *9.*
Schatzman,E.: 1961, *Ann. Astrophys.* 24, *251.*
Schatzman,E.: 1965, *IAU Symp.* 22, *337.*
Secchi,A.: 1875, 'Le Soleil', 2-nd ed., (Gauthier Villars, Paris).

Severny,A.B.: 1957, *Izv. Krym. Astr. Obs.* 17, *129.*
Severny,A.B.: 1959a, *Izv. Krym. Astr. Obs.* 21, *131.*
Severny,A.B.: 1959b, *Astr. Zhurn. SSSR* 36, *208.*
Severny,A.B.: 1964, *Izv. Krym. Astr. Obs.* 31, *126.*
Severny,A.B.: 1965a, in *Astrophys. Space Sci. Library* Vol. 2, *221.*
Severny,A.B.: 1965b, *Izv. Krym. Astr. Obs.* 33, *3.*
Severny,A.B.: 1968a, *Nobel Symp.* 9, *71.*
Severny,A.B.: 1968b, *Nobel Symp.* 9, p.*209.*
Severny,A.B.: 1969a, *IQSY Annals* 3, *11.*
Severny,A.B.: 1969b, in C. de Jager, Z. Švestka (ed.) *'Solar Flares and Space Research'*, (Norht-Holland Publ. Comp.) *38.*
Severny,A.B.: 1972, in *Astrophys. Space Sci.Library* Vol. 29 *Part 1, 38.*
Severny,A.B., Khokhlova,V.L.: 1953, *Izv. Krym. Astr.Obs.*10, *9.*
Shpitalnaja,A.A.: 1964, *Izv. GAO* (Pulkovo) 177, *60.*
Smith,S.F.: 1968, *IAU Symp.*35, *267.*
Solovjev,A.A.: 1971a, *Soln. Dannye No.*5, *86.*
Solovjev,A.A.: 1971b, *Soln. Dannye No.*10, *93.*
Solovjev,A.A.: 1971c, *Soln. Dannye No.*11, *90.*
Solovjev,A.A.: 1972, *Soln. Dannye No.*2 *94.*
Starr,V.P., Fischer,H.J.E.: 1971, *Pure and App. Geophys.* 92, *219.*
Steenbeck,M., Krause,F.: 1969, *Astron. Nachr.* 291, 49
Steenbeck,M., Krause,F., Rädler,K.H.: 1966, *Z. Naturforschung* 21a, *369, 1285.*
Stepanov,V.E.: 1965, *IAU Symp.* 22, *267.*
Stepanov,V.E., Gopasyuk,S.I.: 1962, *Izv. Krym.Astr. Obs.* 28, *194.*
Stepanov,V.E., Severny,A.B.: 1962, *Izv. Krym. Astr. Obs.* 28, *166.*
St.John,Ch.E.: 1910, *Astrophys.J.*32, *36.*
Stojanova,M.N.: 1970, *Solar Phys.* 15, *349.*
Švestka,Z.: 1951, *Bull. Astron. Inst. Czech.* 2, *165.*
Švestka,Z.: 1964, *Contr. Wroclaw Astron.Obs. No.*14, *41.*
Švestka,Z.: 1965, *Adv. Astron. Astrophys.* 3, *204.*
Takakura,T.: 1971a, *Solar Phys.* 19, *186.*
Takakura,T.: 1971b, *IAU Symp.* 43, *390.*
Takakura,T., Kai,K.: 1966, *Publ. Astr. Soc. Japan* 18, *57.*
Title,A.M., Andelin,J.P.Jr.: 1971, *IAU Symp.* 43, *298.*
Tsap,T.T.: 1964, *Izv. Krim. Astr. Obs.* 31, *200.*
Valniček,B.: 1968, *IAU Symp.* 35, *282.*
Vrabec,D.: 1971, *IAU Symp.* 43, *337.*
Waldmeier,M.: 1937, *Z. Astrophys.* 14,*91.*
Warwick,J.W.: 1957, *Astrophys. J.* 125, *811.*
Weart,S.R.: 1970a, *Astrophys. J.* 162, *987.*
Weart,S.R.: 1970b, *Solar Phys.* 14, *274.*
Weart,S.R.: 1972, *Astrophys. J.* 177, *271.*
Weart,S.R., Zirin,H.: 1969, *Publ. Astr. Soc. Pacific* 81,*270.*
Weiss,N.O.: 1964, *Monthly Notices R.A.S.* 128, *225.*
Young,C.A.: 1881, 'The Sun', (1-st ed.) *208*,Fig.59.
Yun,H.S.: 1971, *Solar Phys.*16, *398.*
Zirin,H.: 1966, "The Solar Atmosphere", (Blaisdell Publ. Co.)
Zirin,H.: 1968, *Nobel Symp.* 9, *131.*
Zirin,H.: 1972, *Solar Phys.* 22, *34.*
Zöllner,F.: 1870, *Astron. Nachr.* 76, *225.*

LIST OF THE OFTEN QUOTED SYMPOSIUM VOLUMES:

Symposium		Editor	Topics
IAU No.22	*(Rottach-Egern)*	R.Lüst	Stellar and Solar Magnetic Fields
IAU No.28	*(Nice)*	R.N.Thomas	Aerodynamic Phenomena in Stellar Atmospheres
IAU No.35	*(Budapest)*	K.O:Kiepenheuer	Structure and Development of Solar Active Regions
IAU No.43	*(Paris)*	R.Howard	Solar Magnetic Fields
NOBEL No.9	*(Anacapri)*	Y.Öhman	Mass Motions in Solar Flares and Related Phenomena

PUBLICATIONS OF DEBRECEN HELIOPHYSICAL OBSERVATORY
Vol. 2 No. 11 1971

A B S T R A C T   O F   P A P E R S

PUBLISHED ELSEWHERE

INFLUENCE AND ELIMINATION OF INSTRUMENTAL POLARIZATION CONCERNING MAGNETOGRAPHIC MEASUREMENTS

F. W. JÄGER

Central Institute for Solar-Terrestrial Physics, GDR Acad.Sci.,
Solar Observatory, Einstein-Tower, Potsdam

Abstract:

Magnetographic measurements may be severely disturbed by instrumental polarization mainly due to oblique reflections at the plane mirrors, which are in use in most solar telescopes. For the investigation of those effects, which up to now have been taken into account only in a very unsatisfying manner, a detailed discussion of the so-called Mueller matrix of the optical system in question has been performed. The matrix elements representing the instrumental polarization enter into the magnetographic signals in a complicated way. The most severe complication arises from the fact that the signal due to the automatic Doppler compensation becomes zero only for an asymmetric position of the line with respect to the two exit slits.

For the elimination of the instrumental polarization in principle two possibilities exist: the computation method and the compensation method. The former means that by an additional program the disturbing effects are calculated and the signal corrected; the latter that by an additional optical arrangement the disturbances in the signals are compensated. As a rigorous application of one or other of the two methods will be very troublesome, i.e. impracticable, a partial elimination of the disturbing effects by a combined method leading to a good approximation comes out to be most convenient. In a numerical example it is shown that by a compensator consisting of a phase plate and a glass plate and by additional computation the disturbing effects amounting to more than 25 per cent in the resulting magnetic parameters can be largely eliminated.

THE BUTTERFLY DIAGRAM OF TYPE IV BURST-ACTIVE CENTRES ON THE SUN

A. KRÜGER, B. TRINKKELLER
Central Institute for Solar-Terrestrial Physics,GDR Acad.Sci., Berlin

Abstract:

A study of the butterfly diagrams of type IV bursts and type IV burst-active centres together with statistical tests using the Poisson distribution show that

a) the occurrence of type IV bursts during the solar cycle differs significantly from a random distribution in time even after normalization by division of a suitable measure of solar activity;

b) the temporal occurrence of type IV burst-active centres is almost randomly distributed if the periods of the solar minimum are excluded from the consideration.

ON THE SUPERGRANULATION INTENSITY FIELD IN INTEGRATED LIGHT

A. K U B I Č E L A

Astronomical Observatory, Belgrade

Abstract:

By the photographical addition of information from several successive photographs of the photosphere at $\lambda_{eff} = 5200 \pm 500$ A a very high contrast picture has been obtained, where the granular intensity field has been averaged and the supergranulation pattern to some extent revealed. A nearly simultaneous Ca+ K_{232} spectroheliogram was a position reference. The cells with bright boundaries and dark centers (in a negative) as well as the opposite type of cells, though the last ones not very abundant near the center of the solar disk, have been observed. Even a couple of intermediate type of cells could be noticed. Calibrating one of the final photographs by the means of the known limb darkening, a photometry has been made and intensity variations across supergranular cells up to 1.5 % have been found.

X-RAY EMISSIONS AND THE LAG IN THE D-LAYER

B. VALNÍČEK

Astronomical Institute of the Czechoslovak Acad. Sci.,Observatory Ondřejov

Abstract:

The comparison of various phenomena in the ionosphere with direct observations of X-radiation on board the Interkosmos 1 satellite during October 1969 indicates that the value of the lag Δt varies over quite a wide range. The determining factor is the total radiation flux, which causes a certain degree of saturation of the D-layer. At the time of a quiet, or little active Sun, after the irradiation of the D-layer level (after sunrise) first of all the ion concentration increases. At this time Δt is of the order of 2 minutes, and the ionosphere reacts sensitively to the variations of the X-ray flux. After equilibrium has been reached Δt, increases and attains a value of 6-12 minutes, which is preserved even during low solar activity.

If the activity increases, the change in the spectral composition of the X-radiation, in which the proportion of the hard component increases, becomes effective. This in turn leads to a decrease in Δt to the values found by Křivský (1964), of the order of 2-4 minutes. Under exceptional conditions, when the most active processes are in evidence, e.g., a proton flare, the D-layer reacts by displaying a minimum Δt. The electron concentration of the D-layer varies in a similar way.

If one considers Nestorov's data (1970), who determined a lag Δt of 20 minutes for October 22, 1969, one arrives at an increase of N by a factor of 2.4 for the flare of October 22, considering a recombination coefficient of $3.3 \cdot 10^{-7}$. As regards the flare of October 20, under the same assumptions one arrives at $N = 6.1\ N_0$. The proton flare with $\Delta t=0.5$ mins (Švestka 1969), then yields $N = 38\ N_0$.

It is interesting that Donnelly (1970), who studied the relations between SFD and EUV (Extreme Ultra Violet), found a similar thing. He found that the average time of incidence of SFD's, which are due to the effects

of EUV in the E- and F-layers, was 2.1 mins; however, the minimum value was 10 secs and the maximum more than 10 minutes!

The comparison of the result, at which Krivský arrived by analysing optical observations, with the measurements of the primary phenomenon, directly measured X-radiation, enlightens some of the more general principles of the mechanisms in the D-layer. Neverthelees, the data treated, as well as the conclusions drawn, cannot be considered to be definite. The fundamental drawback here is the small time resolution of the X-photometer used, the short period of observation, and insufficient data on the spectral distribution. It is anticipated that the application of amplitude analysis, tested with the Interkosmos 4 satellite, will yield better results. In the latter case a spectrum of continuous radiation of events from 5 to 100 keV and a time resolution of 12 secs were available. However, the experiment calls for good synchronization with ground-based observations.

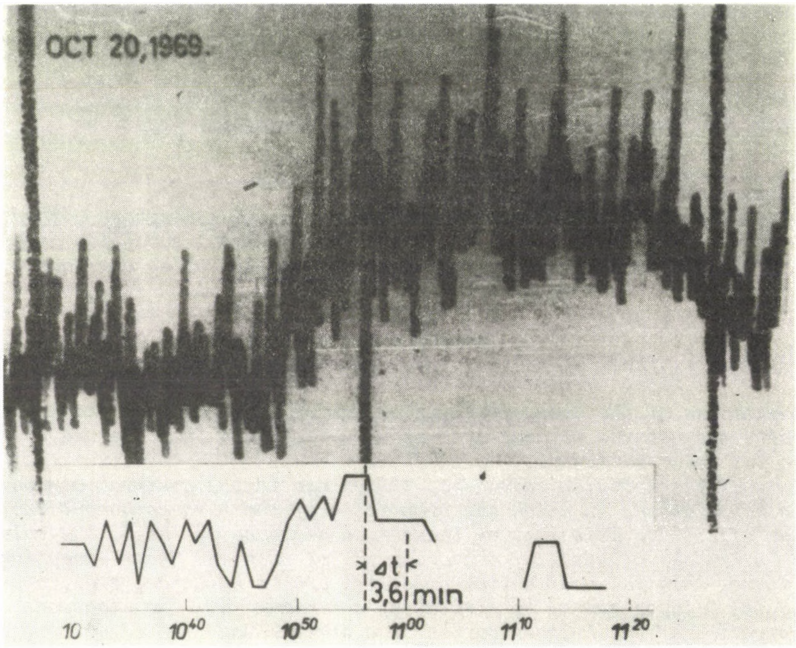

Atmospherics record from Ondřejov in comparison with the record of the Intercosmos 1 X-ray detector (Bewindow, range 1 - 6 A). Δt = 3.6 mins. Flare of October 20, 1969.

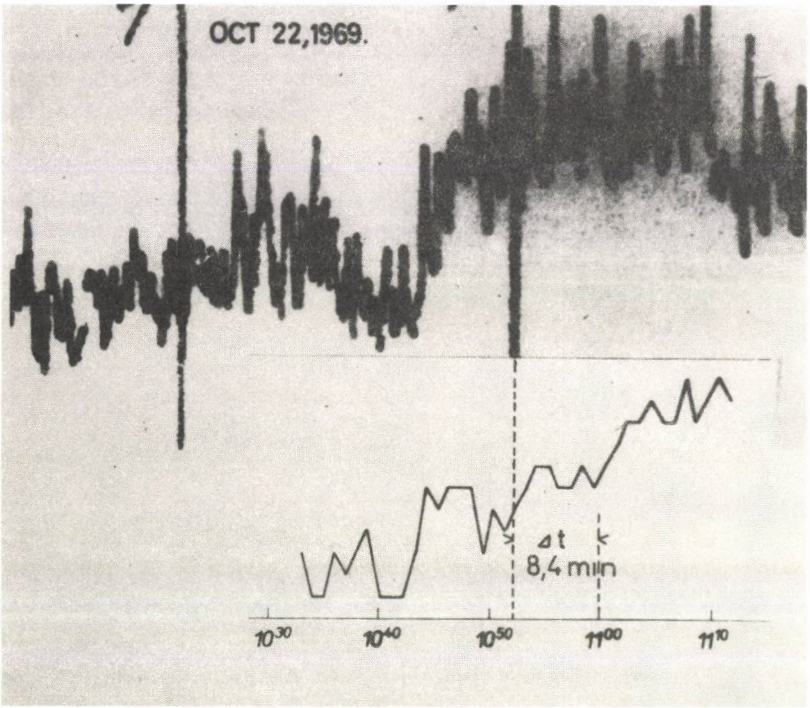

Atmospherics record from Ondřejov, associated with the flare of October 22, 1969, in comparison with the X-ray record. (Other features the same as on the preceding page.)

R e f e r e n c e s

Donelly, R.F.: 1970,*ESSA Tech.Report 169-SDL, 14.*
Křivský, L.: 1964,*Bull.Astr.Inst.Czech.*13,*59.*
Nestorov, G.: 1970,*Compt.Rend.Acad.Bulgarie*,23,*No.10.*
Švestka, Z.: 1969,*Solar Phys.*,10,*3.*

Felelös kiado: Dezső Loránt

789833 MTA KESZ Sokszorosító. F. v.: dr. Héczey Lászlóné